Stability of Proteins in the Presence of Anionic Additives

Dissertation

Zur Erlangung des Doktorgrades der Naturwissenschaften (Dr. rer. nat.)
der Fakultät Chemie und Pharmazie
der Universität Regensburg

vorgelegt von
Johannes Mehringer
aus Regensburg
2021

The experimental work for this thesis was conducted between Mai 2018 and July 2021 in Regensburg at the institute of physical and theoretical chemistry (department of chemistry, UR) and the institute of developmental biology (department of biology, UR). Further work was done at the laboratories (material physics: surfaces & interfaces) of the BASF SE research facility in Ludwigshafen, Germany.

Official Registration:	12.10.2021
Defense:	16.12.2021
Ph.D. Supervisor:	Prof. Dr. Werner Kunz
Adjudicators:	Prof. Dr. Werner Kunz
	Prof. Dr. Rainer Müller
	Prof. Dr. Joachim Wegener
Chair:	Prof. Dr. Axel Dürkop

Acknowledgments

First and foremost, I would like to express my sincere gratitude to my professor Dr. Werner Kunz for having offered me the opportunity to do my doctoral thesis at his institute. Without his scientific advice and ample help in correcting and proof-reading (those pesky commas) various manuscripts, this work would not have been possible. I would also like to thank my colleagues that coauthored and contributed to the scientific papers that we were able to publish in the last three years, namely Evamaria Hofmann, Tuan-Minh Do, Matthias Kellermeier, Didier Touraud and Prof. Dr. Horinek. Part of the experimental work was also performed by various interns and bachelorstudents (Moritz Koeglmeier, Dominik Kreutzer, Patrick Maue, Patrick Denk, Bastian Rödig and Selina Reigl) whom I owe a massive thanks! The same is true for Suganya Sadagopalan, who has performed countless experiments on my behalf over the past few years.

As this work was the result of a very productive industry cooperation, I would like to express my sincere gratitude toward by colleagues at the BASF, namely Sebastian Koltzenburg, Lisa Wagner, Arek Boron, Sonja Kübelbeck, Grit Baier, Karthik Rathinam and especially Matthias Kellermeier, who I had many fruitful discussions with. I appreciated their help and their warm hospitality during my visits in Ludwigshafen.

Part of this thesis was done in cooperation with the department of developmental biology. Therefore, I would like to thank Prof. Dr. Schneuwly and his staff for letting me perform my experiments at their institute and for always helping me in this somewhat unfamiliar environment. I especially like to express my gratitude to Svenja Oestreich, Laura Gizler and Gudrun Karch, whom I must have asked a thousand questions. Of course, a special thanks goes to my coworker Juan Navarro for having taken on this project with me and his constant help and advice even after his relocation to Spain.

Obviously, I would also like to thank all my colleagues at my department for creating this wonderful and productive atmosphere. In particular, I would like to thank Didier Touraud for countless fruitful conversations and for bearing with me on this journey. A special thanks goes to my office colleagues Evamaria Hofmann, Dominik Zahnweh and Sebastian Krickl. Without you, the past few years would not have been such a joy.

Lastly, I would like to express my sincere gratitude toward my family, close friends and in particular my girlfriend Lea for their constant support and understanding. This would not have been possible without you.

Johannes Mehringer

Abstract

In this dissertation the effects of anionic additives on the stability of proteins have been investigated. For this, distinct yet related issues were examined ranging from general observations to in-depth examinations. The range of topics accounted for different forms of protein stability (e.g. functional versus colloidal). The first chapter reiterates experimentally the role specific ion effects play for protein stability and outlines the limitations therewithin. In the second chapter, the balance between headgroup ionicity and tail hydrophobicity was investigated for amphiphilic, hydrotrope-type molecules. Here it was found, that a compromise between Hofmeister effects and surface activity dominates the effect of ionic additives on solubilization characteristics and protein stability. In the third chapter, a proposed hydrotropism for ATP was investigated. By performing a variety of comparative experiments, it was found that ATP does not exhibit hydrotropic properties, but influences the solubility and stability of proteins via specific ion effects and adenine-specific interactions. In the fourth chapter, phosphorylated resveratrol was investigated as a potential aggregation suppressor and was found to possess stabilizing properties for chicken egg white, amyloid beta and human insulin. Further in-vivo studies using drosophila Alzheimer´s disease models revealed signs of a neuroprotective property for the investigated compound. In the fifth chapter, the goal was to find a suitable replacement of the anti-spotting agent HEDP in automatic dishwasher formulations. Here, several experiments on the colloidal stability of suspended protein particles allowed the identification of promising alternatives. In the last chapter, the effect of ionic additives on the activity and conformational stability of functional proteins (lysozyme, proteases, phytase) was investigated. Individual trends could be recognized while a cohesive theory could not be established due to the complex nature of interconnected phenomena.

"Every comprehensive theory passes first through a classical stage, when only those facts are recognized which conform to it exactly, and then through a stage of complications, when the exceptions begin to come forward. […] In the end there are often more exceptions than normal instances."

—Ludwik Fleck, *Genesis and Development of a Scientific Fact*

Table of Contents

CHAPTER 0: PROLOGUE

0.1 Introduction

Proteins were first considered their own class of compounds in the eighteenth century during a time when the science of matter slowly transitioned from alchemy to chemistry.[1] It took well over a hundred years until their structure was correctly (and independently) identified by Franz Hofmeister and Emil Fischer in 1902 as a heteropolymer consisting of various amino acids, joined by peptide bonds.[2] A further 24 years later, enzymes, which up to this point were considered a different compound class of unknown composition, were found to be proteins as well.[3] This very influential work by James B. Sumner was later rewarded with the Nobel prize in chemistry.[4]

It is no surprise that early investigations into proteins focused on aggregation/coagulation behavior and solubility experiments[1], as the methods were limited and little was known about the function and composition of polypeptides. This includes the Hofmeister series (1888), a now famous ordering of ions according to their specific ion effects.[5] Even though the series can be easily and reproducibly recognized in a variety of experiments, its underlying mechanisms, though mostly understood, remain a source of rumination for researchers to this day.[6] With the beginning of the twentieth century, coagulation experiments became more sophisticated (e.g. Handovsky and Pauli, 1908[7]) and the role of enzymes started to become more clear with pioneering works of Michaelis and Menten in 1913.[8] Still, it took until the 1950s for the unrevealing of the (ternary) protein structure using x-ray crystallography. A scientific breakthrough, that was again rewarded with a Nobel prize.[9] In the years to follow, the understanding of protein structure and stability increased rapidly and a variety of publications drew a more or less accurate picture that is still relevant today. A fine example are the publications by Lumry, Eyring, Tanford and coworkers in the 1950s[10–12], von Hippel, Wong and Schleich throughout the 1960s[13–15] and those of Arakawa and Timasheff in the 1980s.[16–19]

Today, protein science is a vast field of research, as dysfunctional or misfolded proteins are often at the heart of many pathological conditions. Prominent members include Creutzfeld-Jakob,

Alzheimer´s, Huntington´s and Parkinson´s disease.[20–22] For such conformational diseases, the stability of proteins remains a key factor and the target of various biomedical endeavors.[23]

While it would traditionally be considered a staple of biochemistry, the mechanisms influencing the stability of proteins have deep roots in physical science. As such, contemporary household names in physical chemistry such as Collins, Cremer and others have frequently published on protein stability and other biochemical issues.[24–27] It is at this intersection of biology and physical chemistry that this work seeks to contribute to the ever-growing body of knowledge.

0.2 Fundamentals

0.2.1 Hofmeister Series

In a now famous publication dating back to 1888, the physiologist Franz Hofmeister described a very distinctive trend among ions in their capacity to salt-in or salt-out dissolved proteins. This is to say they increased the solubility or lead to the precipitation of egg white solutions.[5,28] Eventually, this led to the establishment of a series for cations and anions according to their salting-in and salting out character which bears his name. Over the years, it became apparent that this series has an impact on a variety of physiochemical aspects transcending the solubility of polypeptides. It also affects the surface tension and viscosity of solutions, ion-hydration and pairing, the solubility of hydrophobes and the conformational stability of proteins. As such, the consequences of these *specific ion effects* are manifold and appear in, one way or another, almost every discipline of chemistry such as formulation, synthesis, nano-technology, chromatography and biochemistry.

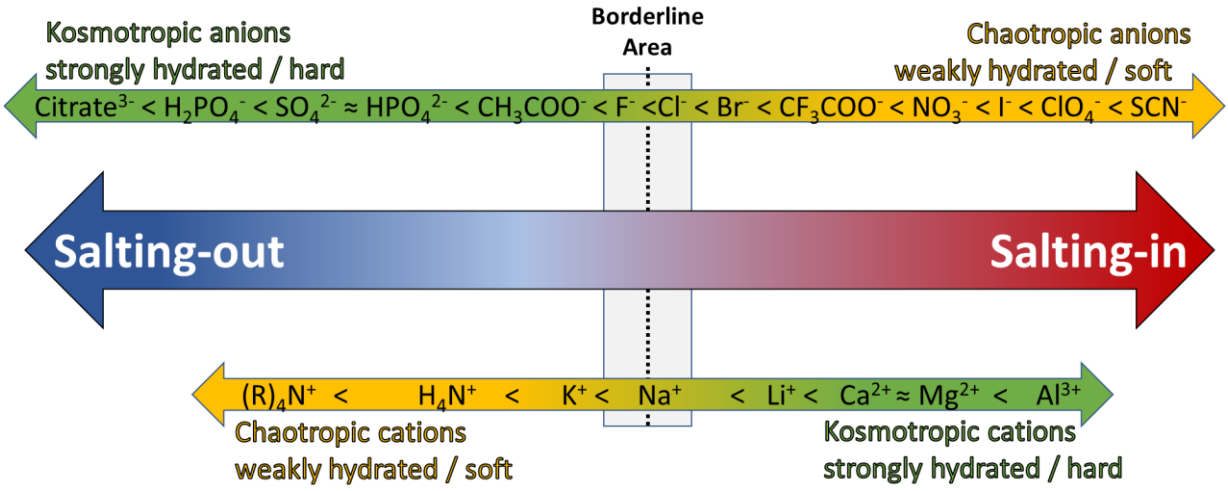

Figure 1 Hofmeister series depicting salting-out and salting-in ions according to their position. Anions and cations are additionally labelled according to their kosmotropic or chaotropic character.

There exists a separate series for anions and cations ranging from salting-out to salting-in as can be seen in Figure 1. Here anions range from strongly hydrated and hard (meaning high charge density) to weakly hydrated and soft (low charge density), which coincides with salting-out on one side and increasingly salting-in on the other side. Alternatively, these characteristics are also

labelled “kosmotropic” and “chaotropic”. According to a definition by Collins, this behavior broadly aligns to kosmotropes having a stronger interaction with water than water with itself. For chaotropes, the opposite is to be expected, with a lower interaction with water respectively.[29] Interestingly, for cations, the association with salting-in/out and chaotropic/kosmotropic behaviour is inverted. Here chaotropic cations are salting-out and kosmotropic anions are salting in. In general, the impact of specific ion effects is usually stronger with anions than it is with cations, which can be attributed to a higher surface charge density for equal ionic radii.[30] Depending on what system is being observed, one will occasionally encounter a reversed Hofmeister series, meaning the sequence of ions with which an effect scales is identical, but the order is inverted.[25,31] As opposed to popular believe, Hofmeister effects can already appear at low salt concentrations (< 10 mM).[32] The molecular mechanism behind these specific ion effects is not fully understood[6,33], but it amounts to a collection of distinctive but different modes of action which are merely summarized under the well-known umbrella term “Hofmeister effects”. The key role plays the degree of hydration for ions, which is connected to their propensities to enrich or deplete in solution surface layers.[34–36] These might be air-solution or solute-solution interfaces, where the modulation of hydration shells is of prime importance.[25,37]

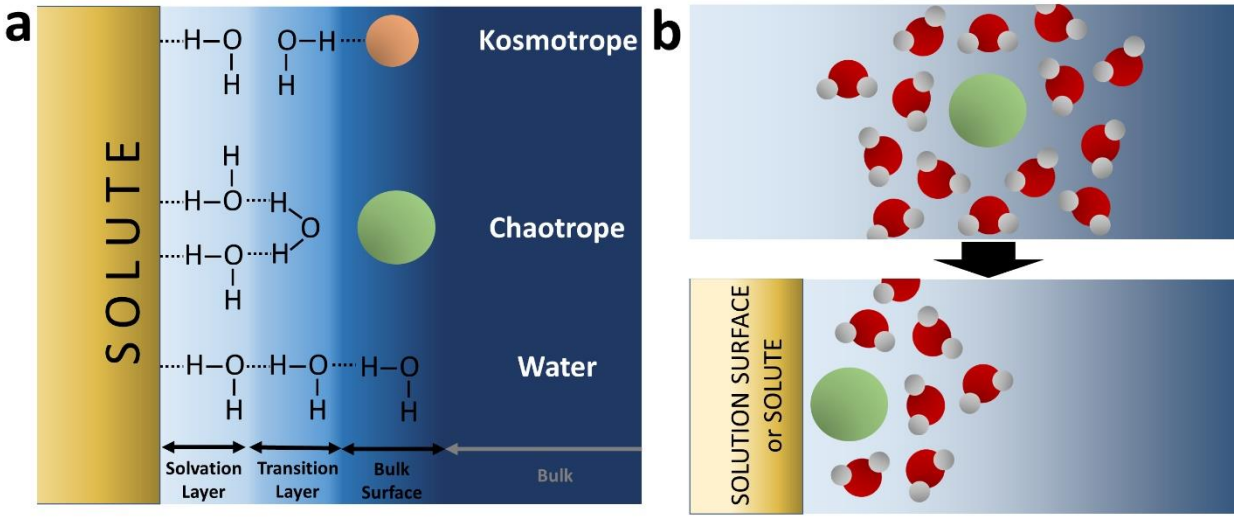

Figure 2 Schematic representation for the mechanism of the Hofmeister effect. **a:** depicts the effect of kosmotropic or chaotropic ions on the surface hydration layers of solutes. Figure adapted from Collins.[29] **b:** depicts the preferential adsorption of weakly hydrated ions (e.g. chaotropes) to surfaces of solutes or solutions. Figure adapted from Pegram and Record.[35]

A simple representation of these effects is shown in Figure 2. In scheme a, three different layers are depicted between the surface of a solute (e.g. hydrophobe or protein) and the bulk solvent (water). Whereas the first layer interacts directly with the solute (solvation layer), the bulk surface is dominated by the properties of the bulk phase. Due to volume exclusion effects, ions are usually restricted to sit in this layer but not closer to the surface of the solute.[38,39] Water molecules in the transition layer can potentially interact with either of the neighbouring layers. This is the case if the bulk surface is also occupied with a water molecule. For kosmotropic ions however, their strong hydration will turn the water molecules toward them and away from the solvation layer ("preferential hydration"), effectively reducing the solvation of the solute (i.e. "salting-out"). For chaotropic ions, interactions with water are (by definition) weaker than water-water interactions. Therefore, water molecules in the transition layer will preferentially interact with the solvation layer and increase the solvation of solutes (i.e. "salting-in").[29] Due to the weak hydration layer around chaotropes, another effect will frequently overcompensate the volume exclusion effect: driven by a (partial) release of their hydration layer, chaotropic ions can adsorb to the solute surface ("preferential adsorption") and this way increase the charge of a solute (see Figure 2 b).[24,32,35,38,40] This in turn will increase the solvation of the solute (i.e. "salting-in").[6] One interesting example of this is the recently reported case, where chaotropes could turn non-ionic surfactants effectively into ionic surfactants by preferential adsorption to neutral lamella structures.[41]

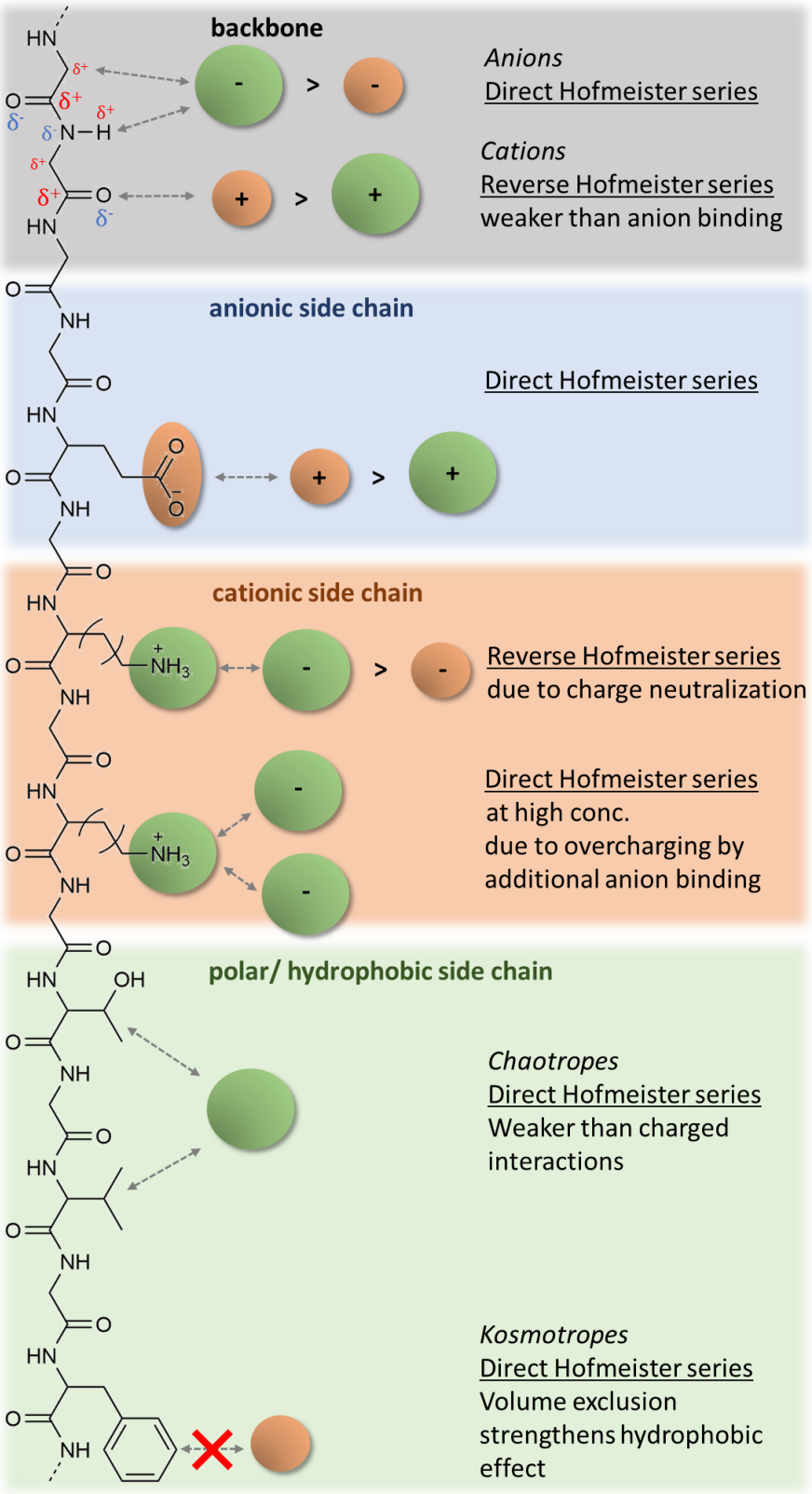

Figure 3 Schematic overview depicting the various interactions of kosmotropic or chaotropic ions with protein subunits. Chaotropic or kosmotropic ions are depicted as green or orange spheres.

Proteins are complex macromolecules that consist of (positively or negatively) charged, hydrophobic or polar side chains, held together by a backbone, that in itself carries partial charges and is highly polar (cf. Figure 3). Hence, the resulting protein surface is a diverse landscape of hydrophobic and hydrophilic areas, that present multiple interaction sites for dissolved ions.[31] These interactions are principally ion specific and their mechanistical underpinnings rest on the previously mentioned ion properties (hydration, charge density, specific adsorption, volume exclusion, etc.). Figure 3 aims to provide a comprehensive overview of possible ion-protein interactions on a very basic level. Firstly, a rather strong effect is reported for ion-backbone interactions. Here, weakly hydrated anions will have attractive interactions with the partially positively charged amine proton and alpha-carbon (incl. hybrid binding), leading to a direct Hofmeister series, as chaotropic ions will "salt-in" the protein backbone leading to increased solubilization but also denaturation. For cations, attractive interactions were measured between the partially negatively charged carbonyl oxygen and hard, highly charged kosmotropes. This implies a reversed Hofmeister ordering, though the effect of (in particular monovalent) cations on protein-backbone binding is genuinely much weaker than it is for anions.[26] Negatively charged protein side chains generally feature a carboxylic headgroup that can be characterized as hard (or kosmotropic) in nature. In line with the law of matching water affinities, kosmotropic cations will yield the best interaction energies, again giving a direct Hofmeister series.[24] For (rather soft) cationic protein side chains, the effects are more complex. Here, a reverse Hofmeister series is observed at lower and a direct at higher ion concentrations. This counterintuitive observation is the result of effective charge neutralization due to the good match (of water affinities) between the positive side chain and negative anion, if both are of the chaotropic variety. As a result, the neutralized charges will drastically reduce the stabilization of (positively charged) proteins and cause a salting-out effect as opposed to the salting-in effect expected for chaotropic anions. At higher ion concentrations, additional anion binding will lead to an overcharging effect (net negative), leading again to a salting-in behavior. As this anion binding is especially effective for weakly hydrated anions, a direct Hofmeister series will establish itself at higher ion concentrations.[24,26] Along similar lines, anion binding to polar or hydrophobic protein moieties will also lead to a salting-in behavior that is particularly prominent with

chaotropic compounds (yielding a direct Hofmeister series).[6] Kosmotropes, on the other hand, exert a volume exclusion effect that is particularly effective against hydrophobic side chains, forcing them out of solution and into the protein interior ("salting-out").[26,29]

These mechanisms have profound effects on solute-solubility, surface tension and the stability of proteins. The latter case is particularly interesting as it involves all the subtle mechanisms subsumed under the umbrella term "Hofmeister effects", such as the specific screening of charges and the breakage of intermolecular salt-bridges. As these aspects are of paramount importance to this work, their consequences on protein stability will be discussed in much greater detail in section 0.2.3.

0.2.2 Hydrotropy

The term "hydrotrope" was first used by Carl Neuberg back in 1916 to describe compounds that increase the solubility of hydrophobes in water.[42,43] While the compounds he used and the observations he made are still relevant today, the underlying molecular mechanisms for the solubilisation remained elusive for Neuberg. Today, the core concept of "hydrotropy" is well established: in principle, hydrotropic compounds are water or oil soluble, but do not form defined structures (such as micelles) on their own in their respective solvents. Only upon addition of a third component (e.g. hydrophobe to aqueous hydrotrope solution) will a distinctive structuring occur. This is connected to an increase in solubility for the otherwise sparingly soluble hydrophobic compound. The underlying mechanism can be visualized by a gathering of hydrotrope molecules around the hydrophobic compounds (see Figure 4).[44,45] As hydrotrope molecules will also start to accumulate at the air/water interface, the surface tension of hydrotrope solutions with higher concentrations will decrease significantly.[46]

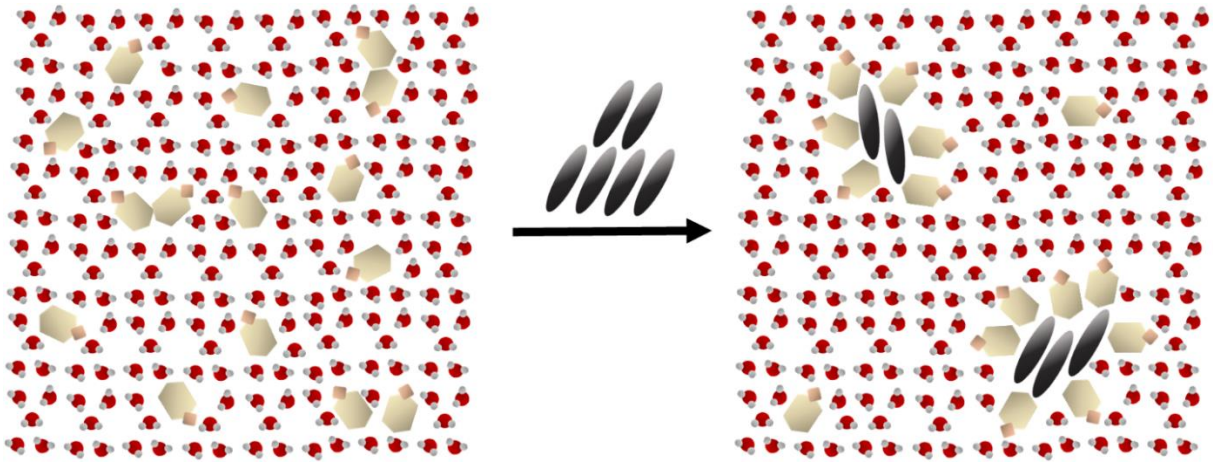

Figure 4 Schematic drawing of hydrotropic action. In aqueous solution, hydrotrope type molecules do not form defined aggregates (left) but will cluster around a sparingly soluble hydrophobe and increase its solubility (right). Figure adapted from Kunz et al.[44]

Typically, hydrotropes are amphiphilic and small organic molecules with a charged ionic headgroup (e.g. sodium xylene sulfonate) but non-ionic compounds exist as well (e.g. nicotinamide).[47] Hydrotropes can solubilize large quantities of hydrophobic substances, that would otherwise form liquid crystals or become insoluble. The often small and bulky structure of hydrotropes will break up the rigid liquid crystal structure as opposed to many surfactants, which would get incorporated or form liquid crystals themselves.[48] As the organic, hydrophobic volume increases, hydrotropes will become more similar to surfactants in nature up to the point where self-aggregation becomes possible. Therefore, the transition from hydrotropes to surfactants is considered fluent.[49,50]

Many ubiquitous compounds in living organisms or products made thereof are amphiphilic in nature and could at least in part be classified as hydrotropes.[42] This includes many polyphenols, sugars, secondary metabolites, amino acids and other compounds known as phytochemicals.[51,52] Prominent compound classes are derivatives of the benzoate, cinnamate, stilbene, flavonoid or anthocyanin family. These compounds are an important constituent of the cellular milieu and contribute strongly to the crowded environment in the cell matrix with grave effects on protein solubility and function.[53–56] Therefore, the concept of hydrotropy was deemed a relevant aspect in the discussion on protein stability and the effects on a molecular scale are discussed further in the next section among specific ion effects.

0.2.3 Stability of proteins

0.2.3.1 Structure and function of proteins

In living organisms, proteins play a vital part and have diverse roles as storage or structural elements and as functional entities (enzymes). These are best understood as macromolecular nano-machines that perform certain chemical tasks, such as ester cleavage reactions, with great specificity and usually high turn-over rates. Energetically, these reactions are either catalysed (without "external fuel") or facilitated by consuming or generating energy (cf. *anabolism* and *catabolism*) in the form of biochemical cofactors, such as NADPH/$NADP^+$.

In order to achieve their purpose, proteins assume a predetermined conformation that can be divided into *primary*, *secondary*, *tertiary* and *quaternary structures*. The *primary structure* refers to the highly specific sequence of amino acids innate to each enzyme and polypeptide which is hard-coded into the DNA. The specific order of these amino acids then allows a *secondary structure* to establish itself. By forming intramolecular contacts between carbonyl oxygens and amino-groups further up or down the backbone, the entire string can start to locally coil up into well-defined structures such as helices or beta-sheets (flat structures). These higher-molecular subunits then start to fold into structures of their own, again owed to favourable intramolecular interactions. This is referred to as the *tertiary structure* and can already represent the final (and catalytically active) form of a functional enzyme. A direct consequence of tertiary enzyme structure is the strict spatial arrangement as well as the strategic placement of functional groups supplied by amino acids. This will form the *active site*, which enables catalytic activity while ensuring high substrate selectivity. In some cases, an assembly of several non-covalently bound yet fully folded proteins is necessary to form the actual target structure, which would then be termed the *quaternary structure*. These very specific protein assemblies are often found in molecular machines, that perform complex tasks such as DNA replication, transcription or biosynthesis.[57]

The intramolecular contacts that hold the secondary structure together are dominated by hydrogen bonds bridging the various peptide moieties (i.e. backbone) within the same chain. The tertiary (and quaternary) structures are then the result of hydrogen bonds, salt-bridges,

disulphide bonds, hydrophobic and cation-π interactions between the residues.[58–63] It should also be mentioned that proteins frequently undergo post-translational modifications. Here, additional changes are made to a protein after its general structure is assembled from the DNA template. This can include the removal of parts of the peptide chain, phosphorylation, glycosylation (addition of sugar chains), oxidation and several other modifications.[22,64]

A great deal of biochemical reactions are performed by single-domain proteins that have a well-defined ternary structure also referred to as the native state. This is to discriminate from other, non-native states, that usually feature heavy structural distortions (“denaturation”) that render the enzyme incapable of performing its task (“inactive”). Some of these misalignments have their root cause in deviating secondary structure features such as helix-to-sheet transitions. Generally, protein folding events are subject to rather subtle energetic differences having grave implications on protein stability and, therefore, activity and solubility. Hence, a comprehensive energy-diagram will be introduced in the following section.

0.2.3.2 Energy landscape of proteins in solution

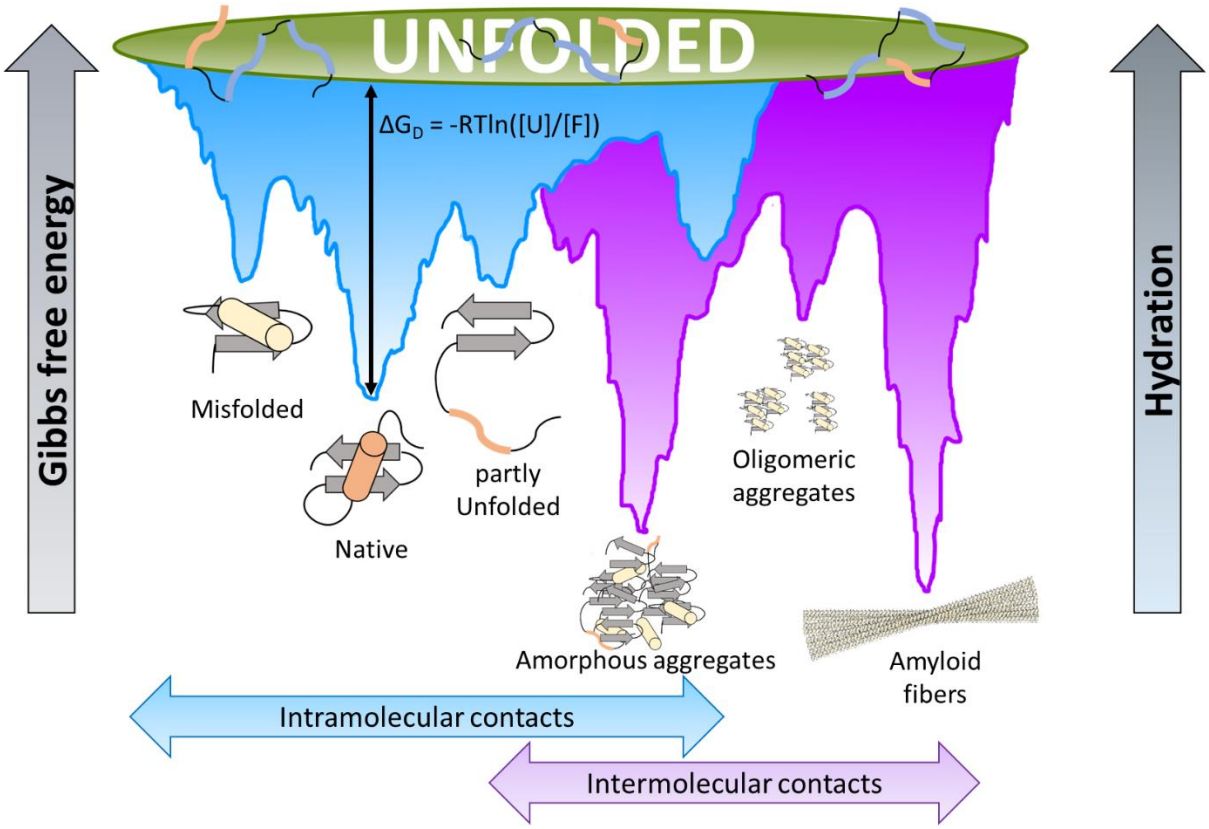

Figure 5 Energy landscape diagram of proteins in solution depicting the conformational space. Adapted from literature.[65,66]

Generally, the various folding conformers of polypeptides correspond to discrete energy states. Therefore, certain low energy states experience a strong thermodynamic preference resulting in strongly populated minima. This is best envisaged as a conformational space where every point corresponds to a very specific conformation of a protein (including secondary, tertiary and if applicable quaternary structure). Local minima, then, represent a distinct form such as the native state. Points very close to this state will be also very similar in structure, but occupy a slightly higher energetic state. Therefore, all conformer species within the vicinity of the local minimum will be funnelled into the energetically lowest form by subtle structural rearrangements.[67] In reality, any "discrete" state, including the native state, is a canonical collection of structurally very similar states, that are also very close in energy. The swift transition between these sub-states is often referred to as "transient protein breathing" and does not compromise the functional integrity of enzymes.[53,68] The potential energy diagram typically

features a variety of local minima, that correspond to intramolecular contacts ("folding") and intermolecular contacts ("aggregation") relying on the interaction of multiple proteins. This will open up what is called an *energy landscape diagram*, encompassing the various processes of folding and aggregation (see Figure 5). The depth of an energy well can be interpreted as the stability of the conformation at its bottom. It is also directly connected to the population balance between thusly folded and partially unfolded states further up the energetic funnel. This way, conformers can transition between local minima and transfer from misfolded or partially unfolded to native (and back).[69] Both, the depth of the well and the threshold between local minima can be modulated by use of additives and cosolutes (e.g. chaperones) that directly or indirectly affect protein folding.[70] This will be discussed in greater detail in the next section. The same is true for intermolecular contacts that lead to various forms of protein aggregation, which will be the subject of section 0.2.3.4. The fully unfolded state is generally the energetically most unfavourable one, as it is bereft of all intermolecular amino acid contacts requiring total hydration of the entire polypeptide string regardless of local hydrophilicity.[66]

Besides misfolded or partially unfolded states, various forms of aggregation pose a significant threat to enzyme activity. Many aggregation pathways are irreversible and form insoluble precipitates. This can be interpreted as an energetic funnel with a hole at the bottom draining these aggregated conformers from the ensemble. Aggregation can genuinely take many forms, such as the formation of oligomers consisting of several proteins exhibiting a decisive structure (e.g. misfolded). These non-native protein assemblies can potentially "ripen" to even larger aggregates such as amyloid-type fibres, which exhibit a certain degree of long-range order. On the contrary, misfolded or partially unfolded proteins can also undergo amorphous aggregation yielding large connected networks of proteinaceous matter, that do not resemble any short- or long-range order. In principle, the crystallisation of proteins from supersaturated solutions (e.g. via salting-out additives such as ammonium sulfate) could be considered as a special case of aggregation, though it is typically fully reversible as the proteins remain in their native configuration.[71,72]

0.2.3.3 Functional and conformational stability

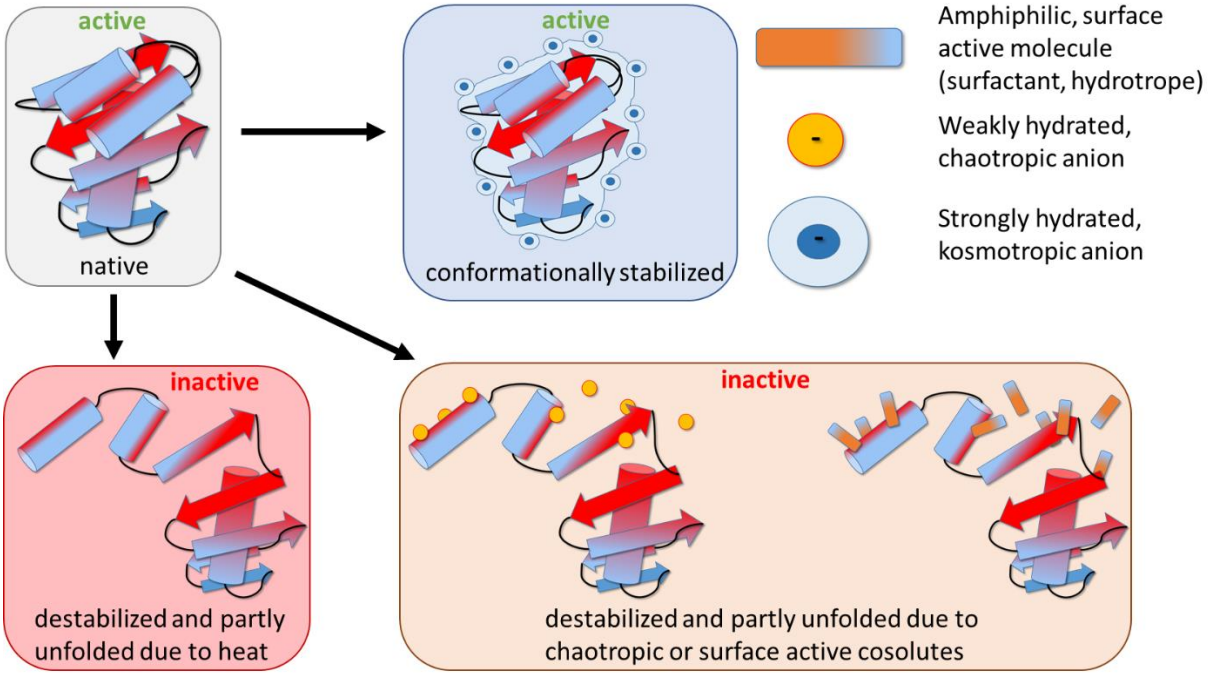

Figure 6 Scheme depicting the influence of additives or thermal stress on the functionality and conformational stability of proteins

Conformational and functional stability are inherently connected, as the former is the prerequisite of the latter, i.e. there is no protein activity without conformational stability. Hence, it is paramount for functional enzymes to retain the native state by stabilizing against unfolding of the peptide chain. As can be seen in Figure 6, different chemical or thermal conditions can affect the conformational state of a dissolved protein. Increasing the solution temperature will supply energy to the protein molecule enabling it to eventually overcome the intramolecular forces, that hold the ternary structure together. As the protein *melting temperature* (T_d) is approached, enthalpic and entropic contributions will drive the unfolding events leading to enzyme inactivity and frequently subsequent aggregation (see next section). The strength of these intramolecular forces can be altered by use of co-solutes, which in turn directly affects T_d. Kosmotropic additives (such as strongly hydrated anions) will increase the stability of proteins and raise the denaturation temperature. The mechanistic underpinnings for this are the volume exclusion and preferential hydration effects of kosmotropic additives (cf. Figure 2 a & Figure 3). As a consequence, this will strengthen the hydrophobic effect and increase the energy threshold

necessary for unfolding events. Additives such as chaotropes or surface-active molecules (hydrotropes, surfactants), on the other hand, will weaken the intra-molecular forces and lower T_d down to the point where denaturation (and loss of enzyme activity) sets in already at ambient temperatures. The mechanistic background for this was laid out in the previous sections (cf. Figure 2 & Figure 3). In short, preferential adsorption to both, the backbone and most side chains, will effectively increase their solubility (i.e. "salting-in") and facilitate the deterioration of the tertiary and at high concentrations even the secondary structure. It becomes apparent that surface-active molecules act similar to chaotropic agents, as both can easily adsorb to weakly or uncharged surfaces.[73] This work focusses on ionic additives, though non-ionic kosmotropes (e.g. sucrose, TMAO) and chaotropes (e.g. urea) do exist and are frequently encountered in nature as "osmolytes".[32,72]

0.2.3.4 Colloidal stability

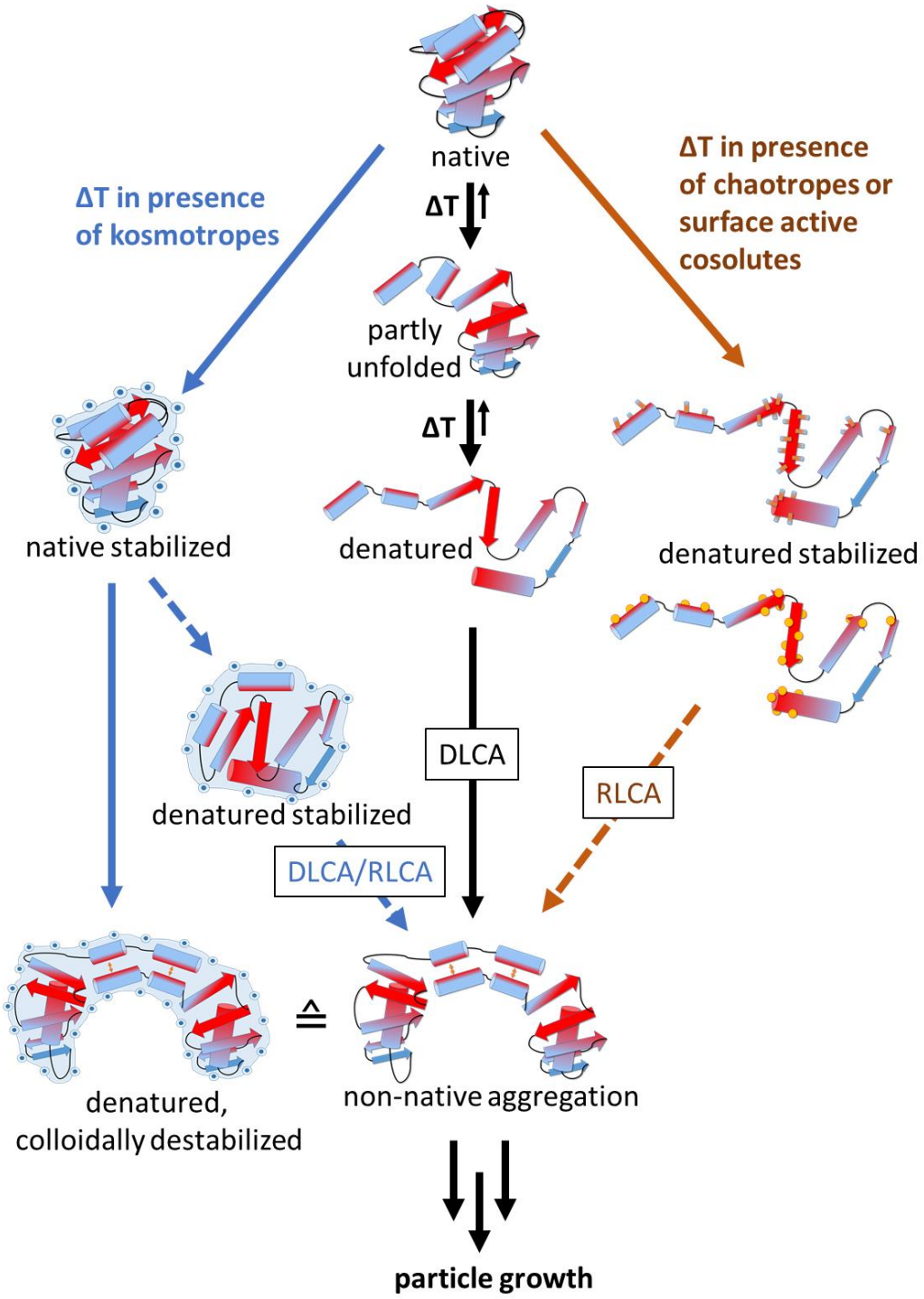

Figure 7 Scheme depicting the different pathways for colloidal protein stability after applying thermal stress with kosmotropes, chaotropes, surface active cosolutes or no additives present. Different aggregation regimes are denoted as diffusion limited cluster aggregation (DLCA) or reaction limited cluster aggregation (RLCA). Dotted arrows indicate pathways affected by potentially hindering circumstances.

As mentioned previously, unfolding and denaturation is often closely followed by aggregation. Genuinely, native proteins or fully unfolded polypeptides (without secondary structure) are less aggregation prone, as they either burry their hydrophobic moieties on the inside or have them scattered along the chain leaving no sizable hydrophobic patches to interact with.[71] The association of proteinaceous particles via intermolecular contacts into larger structures is often energetically favourable, leading to deep energetic wells (cf. Figure 5). Protein aggregation as a special form of colloidal aggregation is genuinely limited either by diffusion (diffusion-limited cluster aggregation; DLCA) or reaction (reaction-limited cluster aggregation; RLCA). The former implies that any contact between aggregating particles will result in (irreversible) binding and therefore growth. RLCA, on the other hand, means that not every particle collision will result in a permanent connection.[74] The attractive forces leading to particle-particle binding can be electrostatic or hydrophobic (or both) in nature and are counter-balanced by repulsive forces, mostly exerted by significant particle surface charges. If these surface charges are high enough, the repulsion will become so strong that a binding-incidence upon a particle collision will become less likely (cf. DLVO theory) and the aggregation is under RLCA control. This can be achieved through extreme pH values leading to highly charged proteins or by preferential adsorption of anionic chaotropes (see Figure 7).[75,76] A similar result will be achieved in the presence of surface-active additives or non-ionic chaotropes (e.g. urea), as these will also bind to hydrophobic patches and effectively compete against intermolecular contacts.[72,77]

For kosmotropic agents, the mechanism is less straight forward. Principally, a protection against (partial) unfolding of proteins by strengthening the native state will indirectly reduce aggregation tendencies.[76,78] Once the protein is denatured, the salting-out properties of kosmotropes can still force the partially unfolded protein to assume a compact state, thus decreasing the chance of favourable protein-protein interactions that would lead to aggregation (Figure 7).[79] In other cases, aggregation is actually increased by kosmotropes, as their salting-out effect can also facilitate intermolecular protein-protein interactions as a way to minimize the exposure of hydrophobic patches toward the solvent (cf. similarities between folding and aggregation).[80,81]

0.2.4 Methodology

The following section aims to provide a comprehensive overview of the principal methods applied in this work. Depending on what is being monitored, various techniques need to be used.

0.2.4.1 Methods to measure conformational stability

In order to measure the conformational stability of proteins in solution, chiefly two methods were employed: Differential Scanning Calorimetry (DSC) and various enzyme activity assays. Both techniques allow the monitoring of the native state and its reaction toward changes in the solvent environment (temperature, additives, etc.). DSC measures the energy (more precisely: the energy difference) that is necessary to linearly heat up a sample versus an inert reference. Changes inside the sample, that either release or consume energy, will be recorded as exothermic or endothermic peaks in the diagram. Protein denaturation and unfolding is typically an endothermic effect resulting in a rather broad peak. Its tip corresponds with the half-point of the denaturation (exactly half of the proteins are denatured at this stage) and yields the protein melting temperature (T_d). Assuming that the protein started out in its native conformation, this will allow to measure the relative stability of this state in the specific solution environment.

Functional enzymes that catalyse a specific reaction, can also be checked for their native structure by measuring their activity. This is, because only those protein fractions that are within the native protein ensemble will be able to perform their task, while denatured or aggregated proteins will lose their activity. Typically, an enzyme assay will consist of a suitable protein-substrate combination that allows the tracking of the reaction progress. This can be achieved either by measuring the remaining substrate concentration or by detecting the degradation products. Enzyme activity is typically given as the amount of converted substrate (in moles) per unit of time. Relative enzyme activity, however, is often easier to measure and more convenient. Here, the results are normalised to a specific enzyme solution (condition, concentration, etc) and enhancing or inhibiting effects can be easily recorded and quantified.

Circular dichroism (CD) is a frequently used method to monitor changes in protein conformation. This photometric technique measures the absorption of circularly polarized light. The different absorbance of left- or right-handed light by chiral molecules such as polypeptides, contains

information on the secondary and tertiary structure of proteins. This is because changes in conformation will have effects on the chirality and hence the molar extinction coefficients for left- or right-handed light. As CD is typically done in the UV-region of the electromagnetic spectrum, additives that have a large extinction coefficient in this range (e.g. unsaturated ring structures as encountered in chapters 3 and 4) will lead to an overwhelming non-specific absorption already at low (millimolar) concentrations. Therefore, the solution will effectively become “opaque” in this spectral range, rendering the method invalid.

0.2.4.2 Methods to measure colloidal stability and aggregation

Colloidal stability and aggregation are inherently connected, as was described in the previous sections. Some methods, such as turbidimetry, fluorescence and dynamic light scattering (DLS) allow direct tracking of protein aggregation processes, while other methods such as zeta potential measurements and quartz chip microscales (QCM) will yield valuable information on specifically colloidal stability.

Turbidimetry, the method of measuring the transmittance of a sample, is a versatile way to study aggregation. As the particles grow, they will reach a size threshold (submicron regime) where visible light will start to scatter, rendering the sample increasingly turbid. Therefore, the extent of the reduction in transmittance (i.e. the optical density) is an indicator for the extent of protein aggregation. The reason for this aggregation could be (thermal) denaturation, precipitation due to salting-out additives or colloidal destabilisation by charge reduction (cf. DLVO). Turbidimetry typically does not discriminate between the type of aggregation, making supplemental techniques necessary. As such, fluorescence measurements utilizing aggregation specific dyes (e.g. thioflavine T) can provide insight. Here, the change in fluorescence (both, quantum yield as well as emission/excitation shifts) can track aggregation processes yielding specific morphologies (e.g. fibres). Using DLS, the particle growth can be measured directly: By recording the time resolved correlation of the scattering intensity fluctuations, the particle size of the scatterer can be calculated. While this method is superior to turbidimetry in measuring particle growth (as it provides quantitative data), it is much more susceptible to disturbances and has significantly higher requirements regarding sample preparation. This is because even minute amounts of

especially micron-sized impurities (e.g. dust particles) will dominate the signal and lead to invalid readings.

One of the principal drivers of colloidal stability is the surface charge of dispersed particles. This value can be directly obtained using zeta-potential measurements. The zeta-potential is defined as the electric charge at the slipping plane (meaning the surface of the charged cloud that is "attached" to a particle). Charge screening effects can be measured with this method just as well as the influence of pH on the net surface charge of dissolved proteins. Lastly, the adsorption of charged (protein) particles to surfaces is a sign of suboptimal colloidal stability and can be measured using a QCM. This device utilizes quartz chips, that, supplied with an electrical voltage, resonate at a frequency that is proportional to its mass. As particles adsorb and increase the mass, the resonance frequency will decrease accordingly. Conveniently, quartz chips can be coated with a variety of different materials (e.g. gold or glass) allowing for various experimental settings.

0.2.4.3 In-vivo experiments

As proteins are an integral part of biochemistry and living organisms, in-vivo (meaning in living cells) experiments are the logical successor to in-vitro (meaning "in beaker") measurements. Due to their complexity, they could be considered the pinnacle of protein research and require a whole host of highly specific methods. Analytically, this includes quantitative polymerase chain reaction (qPCR), western blot, locomotion and histology. As in-vivo systems, cell cultures or entire live animals (such as *drosophila melanogaster* in this work) can be used.

In order to measure how much of a specific protein has been commissioned by the organism, qPCR allows to quantitatively measure the amount of free mRNA coding for this protein. This way, one can investigate if the protein is expressed (meaning synthesized) at all and check if its expression is potentially suppressed (or stimulated) via intracellular pathways. To measure the actual amount of expressed protein, complex procedures of protein extraction, separation (by electrophoresis) and quantitative recognition (using specific antibodies) are deployed in a method called *Western Blotting*. Additionally (or alternatively), wholemount immunostaining can be used to investigate histological samples. Here, parts of the organism (e.g. the brain) are

dissected and stained using highly specific antibodies. Subsequent analysis using confocal laser microscopy can yield information on various parameters such as protein localisation, quantity and aggregation state (morphology). The data gathered in the methods above can then be cross-correlated with macroscopic and behavioural aspects of the examined organisms. For animals, this includes locomotor data, meaning parameters that relate to motion and physical fitness (e.g. climbing speed).

0.3 Goal of this research

This thesis was originally inspired by the interesting observation that ATP appears to increase the solubility of various proteins and thusly contribute to the stability of the crowded cellular milieu.[82,83] Patel et al. postulated a hydrotrope-type action for ATP, which sparked a variety of intriguing questions concerning charged and amphiphilic compounds. It became quickly apparent that the "stability of proteins" was a semantically diverse issue subsuming a variety of very different processes and mechanisms (as laid out in the previous sections). The goal was to understand each process and gain insight into how to control individual aspects (e.g. functional stability, colloidal stability). As everything is connected, this effort is obviously not straight forward. I started out with the original topic on ATP and tried to disassemble its effects on proteins in order to establish property-effect relationships (chapter 3). This led to a more generalized investigation into the fine balance of surface-activity and specific ion effects that is key in understanding the behaviour of amphiphilic compounds in the biological context (chapter 2). Having understood this, my focus turned towards applying and testing these principles on a variety of subjects such as biochemical (chapter 4) and industrial (chapters 5 and 6) issues. The former led to a cooperation with the department of biology (UR), underscoring this work´s bridging character between physical chemistry and biology. The latter was enabled through an industry cooperation with the BASF SE, which gave me the opportunity to work on topics that are relevant for the private sector.

The overarching theme of this thesis is the quest for protein stability in all its aspects. The goal was to understand the subtle connections between the individual processes involving protein chemistry, and to modulate them using ionic additives. The relevance of this topic is given by the ubiquitous nature of proteins in science, technology and life itself.

CHAPTER 1: PROTEINS AND SPECIFIC ION EFFECTS

1.1 Introduction

In his original publication, Franz Hofmeister noted distinct effects of inorganic ions on the solubility of aqueous egg whites.[5] Some caused precipitation, while others facilitated a solubilised state even in high concentrations. It was later found that this effect encompassed much more than just the solubility of proteins, but also extended to the stability and indirectly the activity of enzymes. Since then, the basic and augmented ideas of his theory have been used to explain a variety of processes in protein chemistry. This chapter seeks to outline and underscore these principles with experimental data, while at the same time revealing the limitations of a simple and unified concept.

1.2 Experimental

1.2.1 Chemicals

Trishydroxymethylaminomethane (TRIS, 99.8 %), sodium sulfate (99 %), citric acid monohydrate (98 %), sodium chloride (99.5 %), tetrasodium diphosphate decahydrate (SDP, ≥99.0%), sodium dihydrogen phosphate (SMP, ≥99.0%), sodium triphosphate (STP, ≥98.0%) and sodium acetate were all sourced from Merck. Ammonium chloride (99.5 %), sodium benzoate (99.5 %), sodium xylene sulfonate (≥ 90%), sodium thiocyanate (≥98.0%) and BSA (>98%, fraction V) were purchased from Sigma Aldrich. Crude chicken egg white (CCEW) was prepared from fresh eggs bought at local supermarkets. All chemicals were used without further purification, and all solutions were prepared with millipore water (MilliQ, $\rho \geq 18$ MΩcm).

1.2.2 Methods

Turbidity and Zeta Potential measurements – Solutions were prepared in MilliQ with 1-3 wt% of protein and the pH was continuously adjusted using HCl or NaOH to achieve a range of acidic to basic conditions at room temperature. For each suitable pH increment, a small quantity of protein solution (< 1 mL) was retrieved to measure the transmission at 488 nm using a Hitachi U-1000 photometer against a blank sample (water only). Similarly, samples were taken to

measure the Zeta Potential using DTS1070 cuvettes in a Malvern Zetasizer. Measurements were done in triplicate and the results averaged. Error bars mean ± SD (N=3).

Protein aggregation – Additive solutions were prepared in 50 mM TRIS Buffer at various concentrations and the pH was adjusted to 7.4. Then, addition from a suitably diluted protein stock solution in 50 mM TRIS adjusted to pH 7.4 led to 1 wt% for BSA or 0.7 wt% (for CCEW) protein content in all samples. The samples were heated up slowly in a water bath, and small quantities of solution (< 800 µL) were retrieved at suitable temperature increments and measured for transmission at 488 nm on a Hitachi U-1000 photometer. Measurements were done at least in duplicate and the results averaged. Error bars mean ± SD (N=2-3).

Differential scanning calorimetry – Protein solution samples with various additives were prepared as described above and the pH was set to 7.4. Then the denaturation curve was measured using a Setaram micro DSC III. The denaturation peak temperature was determined using the proprietary software *Setsoft 2000*. Protein concentrations used were 1 wt% for BSA and about 4.4 wt% (total protein) for CCEW samples.

1.3 Results and Discussion

1.3.1 Chicken egg white

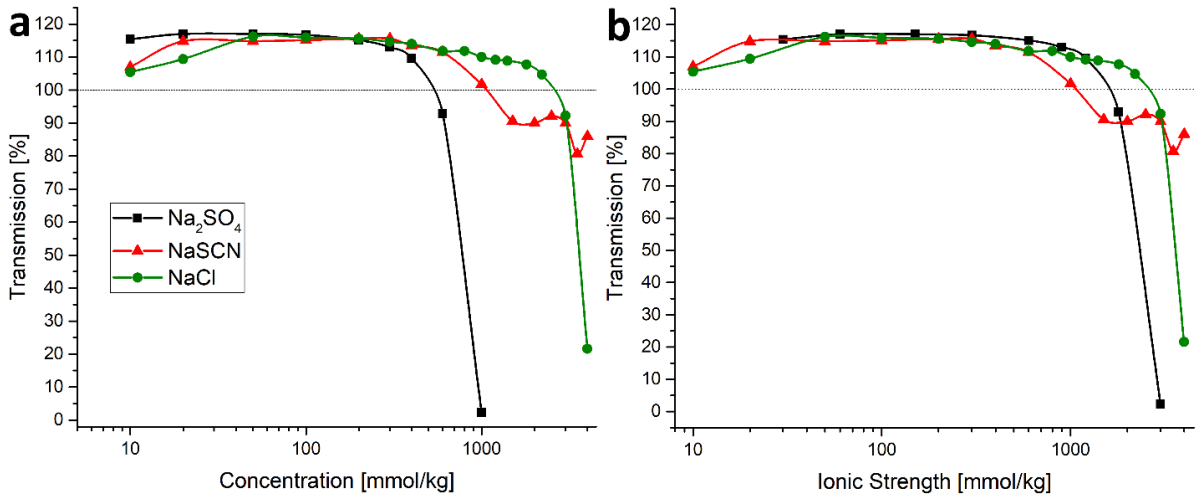

Figure 8 Solubility of crude chicken egg white (CCEW; 1.8 wt%) with increasing concentrations of various inorganic salts ordered according to the concentration (**a**) or ionic strength (**b**).

The solubility of proteins is directly influenced by the presence of dissolved ions. This was the key point of Hofmeisters original discovery and the ion specificity of this effect can be easily seen in Figure 8, where the proteins in CCEW will precipitate upon the addition of larger quantities of inorganic salt. The order, with which (in this case) anions will cause this "salting-out" is given in the previously mentioned Hofmeister series (cf. Figure 1). It can be seen that kosmotropic compounds such as sulfate have a more strongly precipitating effect than the more "neutral" chloride. Thiocyanate, on the other hand, is strongly chaotropic and will facilitate the solubilization of proteins ("salting-in"). Therefore, no "salting-out" behavior is observed even up to very high concentrations (Figure 8 a). Specific ion effects are generally more recognizable if the ionic strength is considered as well. Therefore, data plotted against the ionic strength will reveal ion specificity more comprehensively (see Figure 8 b). It also becomes apparent that in most cases, the solubility of proteins is only compromised with relatively high, molar concentration of salts, even in environments with high protein load (in this case 1.8 wt%). Below these concentrations, however, ions already influence proteins to a significant effect, in

particular concerning the colloidal and functional stability. This then will be the main focus of this work and its key aspects will be discussed in the following.

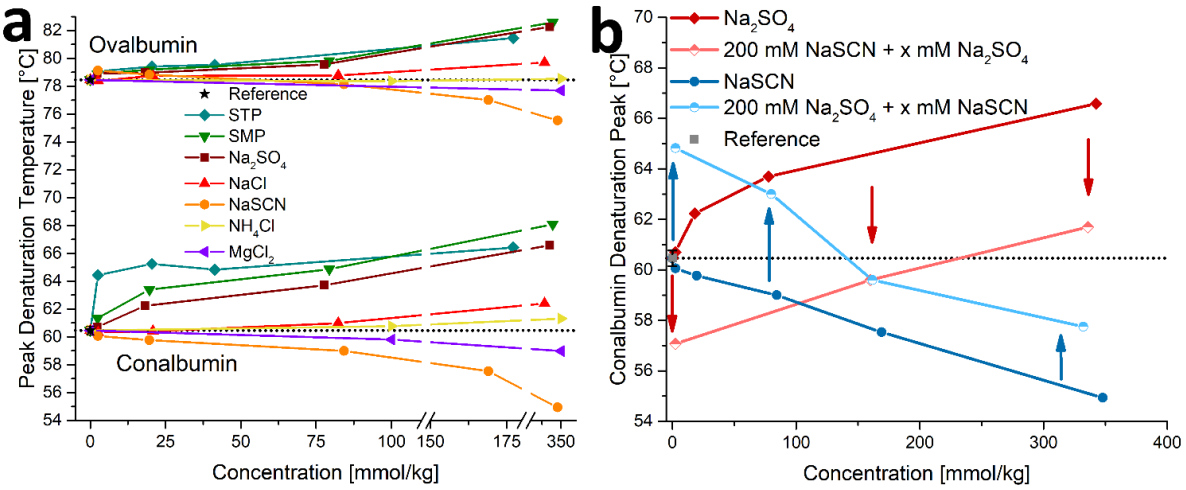

Figure 9 DSC data for CCEW. **a:** Peak denaturation temperature for conalbumin and ovalbumin in CCEW with various ionic additives. Error bars for reference measurements (buffer only) mean ±SD (N=3). **b:** Peak denaturation temperatures for conalbumin in the presence of sodium sulfate and sodium thiocyanate showing approximately additive behaviour.

Crude chicken egg white (CCEW), as isolated from chicken eggs, consists of a protein mixture containing chiefly conalbumin, lysozyme and ovalbumin. Heating will result in a fractionized denaturation of these proteins, as their denaturation ranges are spread out over almost 40°C of temperature, starting with conalbumin at around 55°C and ending with ovalbumin at around 94°C.[84,85] Using a differential scanning calorimeter (DSC), the exo- or endothermic unfolding of the peptide chains can be tracked. Increasing or decreasing the denaturation temperature of proteins by the use of additives directly relates to enzyme stability, respectively affecting its long term storage longevity and catalytic activity.[84,86] By using the two CCEW constituents conalbumin and ovalbumin as model proteins, the effect of inorganic salts on the denaturation peak temperature can be examined (see Figure 9 a). Here, a classical Hofmeister ordering can be observed, both for anions and cations. As such, salting-out ions like the (anionic) kosmotropic phosphate, sulfate and triphosphate as well as the (cationic) chaotropic ammonium will lead to an increase of denaturation temperature. Likewise, salting-in ions like the chaotropic (anionic) thiocyanate and the kosmotropic (cationic) magnesium ion will lead to a reduction in denaturation temperature. The same is observed for hydrotropic compounds such as benzoate and sodium xylene sulfonate (SXS). These compounds will also reduce the stability of proteins

due to their intrinsic salting-in character (data not shown), which is in line with the denaturing properties of the even more solubilizing surfactants. There genuinely is a balance between the specific ion effects of ionic headgroups and the salting-in character of amphiphilic compounds that dictates the overall stabilizing or destabilizing effect on proteins (more on this in chapter 2). Moreover, the specific ion effects responsible for the Hofmeister ordering of ions are additive in nature.[13,32,87,88] This means that salting-out effects of one ion species can be outbalanced by the addition of another salting-in species and vice-versa. One example of this effect can be seen in Figure 9 b, where the addition of a fixed amount of thiocyanate (200 mM) will lower the denaturation temperature of conalbumin. Increasing additions of sulfate will then lead to a corresponding increase in protein stability (red curves). The same trend can also be seen in the opposite case with the initial stabilization due to sulfate addition and an increase in destabilization with thiocyanate additions (blue curves). The additivity of cosolute effects transcends ionic compounds and also includes nonionics.[13] This effect also extends to subsequent processes such as aggregation.[89]

As both, conalbumin and ovalbumin have their isoelectric points (IEP) below the physiological pH (where the experiments were carried out), their negative surface charge facilitates a classical behavior according to the general Hofmeister effects (e.g. direct series).[90]

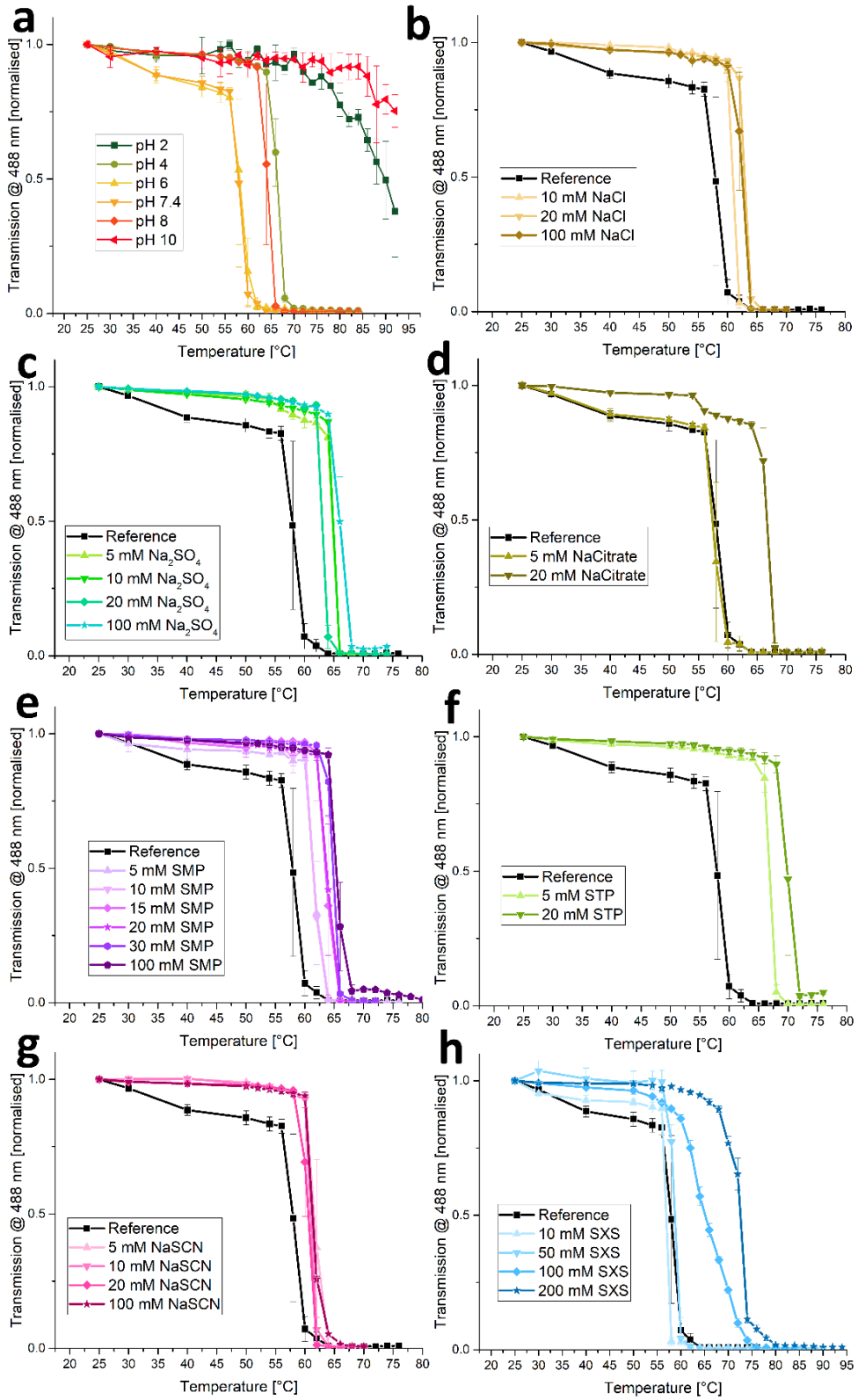

Figure 10 Aggregation data for CCEW with various additives. Aggregation of CCEW in relation to the pH (**a**) or the presence of NaCl (**b**), Na_2SO_4 (**c**), Na Citrate (**d**), SMP (**e**), STP (**f**), NaSCN (**g**) or SXS (**h**) in 50 mM TRIS (pH 7.4). **a-h:** Error bars mean ±SD (N=2).

The denaturation of proteins is usually closely followed by aggregation often leading to turbid or opaque samples. As proteins unfold (thermally), they expose hydrophobic patches (formerly buried inside the protein) toward the solvent enabling protein-protein contacts which then leads to association, forming disordered aggregates.[76] For CCEW, this process is pH dependent (see Figure 10 a). At very high and low pH conditions, the aggregation yields a rather transparent solution potentially owed to the formation of homogeneous protein filaments that only weakly scatter light.[91,92] In these extreme pH conditions, proteins will also often carry high surface charges and the subsequent electrostatic repulsion will effectively retard thermal aggregation (cf. section 0.2.3.4).[76] In moderate (and physiological) pH conditions ranging from 4-8, complete turbidity with a rather steep onset will be observed. Besides pH, the presence of additives greatly affects the aggregation behaviour of proteins as well. As can be seen in Figure 10 b-f, compounds that increased the conalbumin denaturation stability (cf. Figure 9 a), also shift the aggregation point to higher temperatures. This is, in part, due to denaturation being the prerequisite of aggregation and a shift of one will lead to a corresponding shift of the other. As can be seen in Figure 10 g & h, however, the additives thiocyanate and SXS can also shift the aggregation point despite having a destabilizing effect on the ternary protein structure. This can be explained by considering the mechanism of reaction-limited cluster aggregation (RLCA), which dominates in systems with relatively high protein loads (cf. also Figure 7).[93,94] Here, salting-out ions will force proteins to assume a compact state that exposes as little hydrophobic patches to the solvent as possible, slowing down aggregation.[79] For salting-in ions and in particularly for surface active hydrotropes (and by extension surfactants), their interaction with hydrophobic protein moieties (preferential binding) will compete with hydrophobic protein-protein interactions, resulting also in a reduced aggregation. For hydrotropes, this effect becomes relevant only at higher concentrations (see Figure 10 h).

In general, CCEW serves a good model for more complex protein systems, as it represents a mixture of different enzymes, high protein load as well as featuring cheap and abundant availability. As the following data for bovine serum albumin (BSA) will show, however, protein behaviour can significantly deviate from the archetypical (i.e. “classical Hofmeister”) trends observed for conalbumin and ovalbumin.

1.3.2 BSA

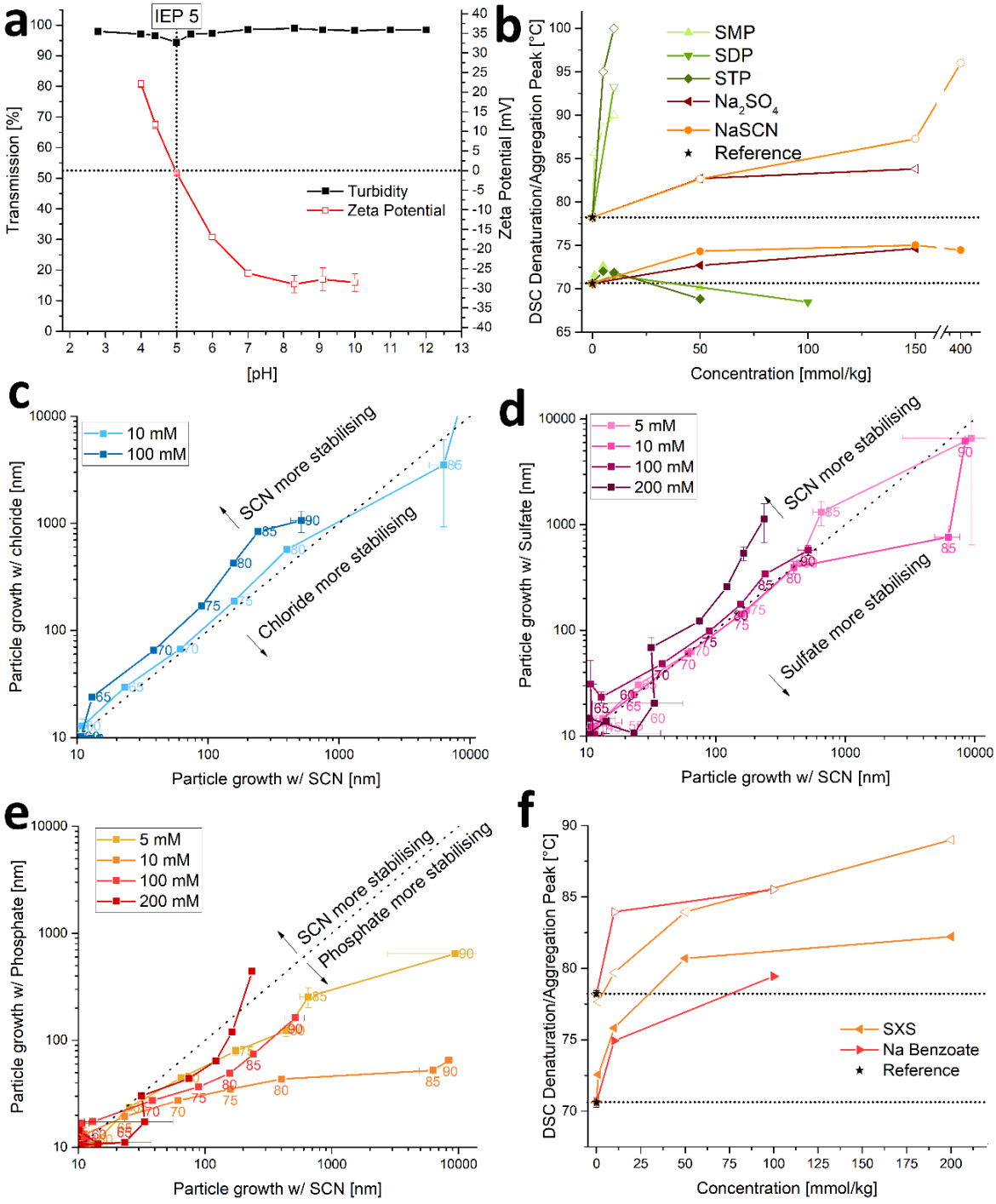

Figure 11 BSA stability data. **a:** transmission and Zeta potential as a function of pH for BSA. Error bars mean ±SD (N=3) **b:** denaturation and aggregation peak of BSA with various ionic additives. Error bar of reference measurements (buffer only) means ±SD (N=3). **c-e:** Comparative particle aggregation of BSA as measured by DLS during heating (corresponding temperatures given as numbers) with chloride (**c**), sulfate (**d**) and SMP (**e**) compared to thiocyanate each. Error bars mean ±SD (N=2). **f:** denaturation and aggregation peak of BSA with two hydrotropic additives. Error bar of reference measurements (buffer only) mean ±SD (N=3).

BSA has an isoelectric point of around 5, where its lack of surface charge leads to lose and reversible particle aggregation, causing a dip in the transmission (Figure 11 a). Despite its negative surface charge at pH 7.4, the effect of anions on the denaturation temperature is not as clear cut as it was for the egg white albumins (see Figure 11 b). Sulfate and Thiocyanate both lead to an increased stability against unfolding, but inorganic phosphates (SMP, SDP and STP) will slightly decrease the stability at moderate concentrations. It was shown in a previous study that the Hofmeister series was reversed for BSA at lower salt concentrations (>0.2M) and direct at high salt concentrations.[88] Therefore, thiocyanate will only become denaturing at much higher concentrations. The second peak at higher temperatures is exothermic and correlates with aggregation, as samples with this peak will have jellified and those without will remain less viscous and more clear.[95] Here, inorganic phosphates shift the aggregation peak outside the temperature window of the DSC (>95°C) already at low concentrations (>20 mM), while sulfate and thiocyanate only raise the exothermic peak by a few degrees. This shows that for BSA, phosphates have little effect on the protein stability, but a much greater influence on the aggregation process. This can be analysed further by measuring the particle growth during aggregation directly with DLS. Here, a direct comparison of thiocyanate with chloride (Figure 11 c), sulfate (Figure 11 d) and phosphate (Figure 11 e) trace the effect on aggregation. Thiocyanate is not only more stabilizing than chloride[88], but it also hinders aggregation slightly better at moderate concentrations (100 mM). The results for sulfate versus thiocyanate measurements show strong similarities which mirrors their behaviour for the DSC data. Phosphate on the other hand can effectively reduce aggregation, as was already apparent for the aggregation peak in the DSC (cf. Figure 11 b). Therefore, the effect of ions on the ternary stability and aggregation of BSA is very ambivalent, with multiple effects overlaying each other (concentration regimes, ion specificity, aggregation mechanisms) making a simple interpretation along the Hofmeister effects rather difficult.

For surface-active molecules (such as SDS), it was found in the past that BSA will be unfolded due hydrophobic interactions.[96] For shorter amphiphilic molecules (e.g. hydrotropes) it was found, however, that the denaturation temperature actually increased (Figure 11 f). Simultaneously, the aggregation peak is also shifted upward at higher hydrotrope concentrations. It was reported

in the past that hydrotrope-type compounds such as ethanol can bind to BSA[97] and this ligand binding can strengthen the ternary structure.[98,99] In this sense, BSA again deviates from what was observed for CCEW albumins and exhibits a complex interplay of specific and non-specific binding with multiple ramifications on protein stability.

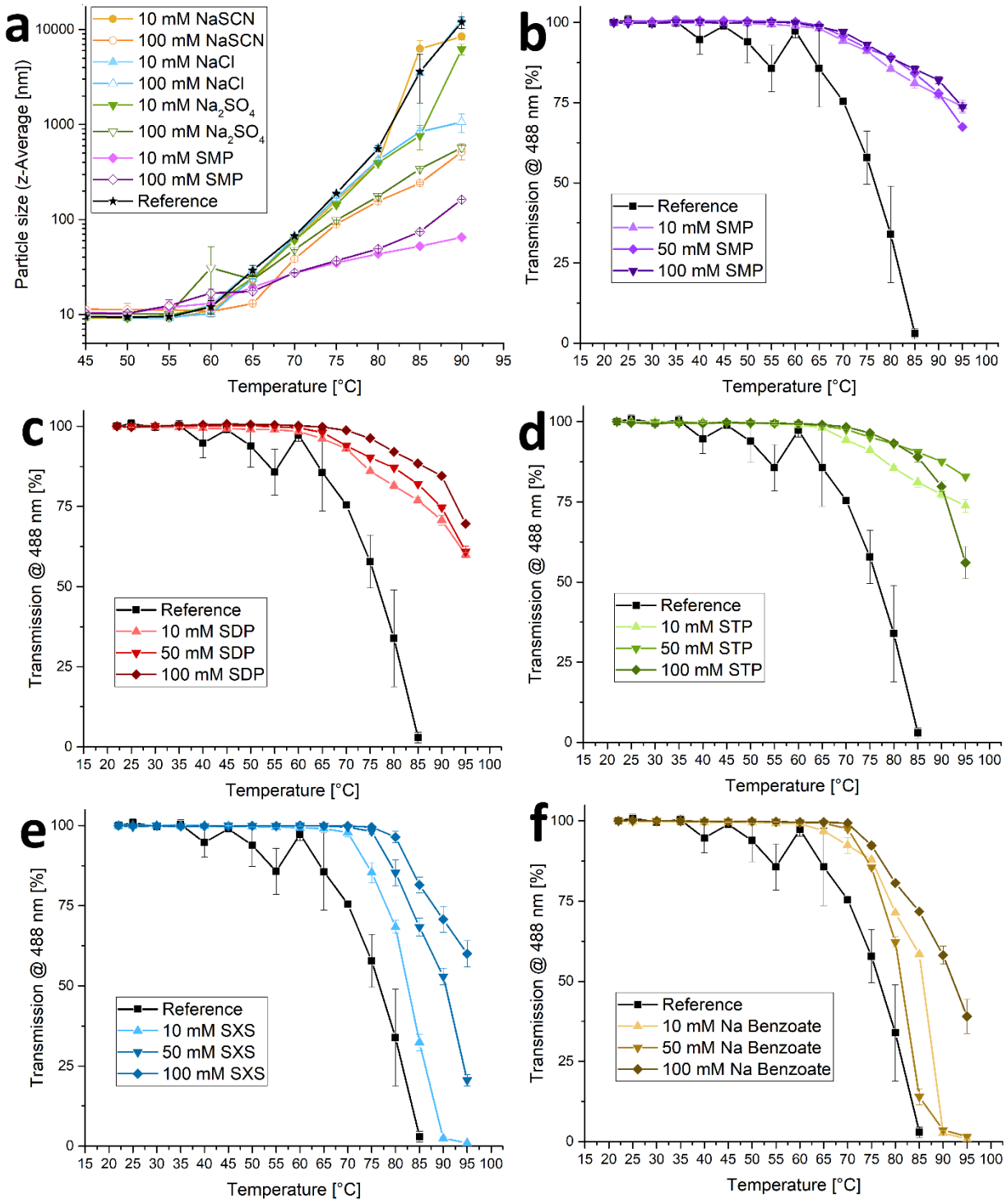

Figure 12 BSA aggregation data. **a:** BSA aggregation as measured by DLS with various ionic additives. **b-f:** Aggregation of BSA in the presence of SMP (**b**), SDP (**c**), STP (**d**), SXS (**e**) and Na Benzoate (**f**) in 50 mM TRIS (pH 7.4). **a-f:** Error bars mean ±SD (N=2).

Concerning the aggregation of BSA, measuring the particle size by DLS revealed that small salt concentrations (10 mM of NaCl, Na_2SO_4 or NaSCN) had little effect (Figure 12 a), while higher concentrations (100 mM) showed some reduction in particle size for sulfate and thiocyanate (cf. also Figure 11 b & d). The resulting onset of turbidity was, however, only slightly shifted upward by these salts (even up to 400 mM), similar to what was seen for CCEW (data not shown; cf. Figure 10). As seen in Figure 11 e, phosphate has the most severe effect on curbing aggregation, which also translated into a significant reduction of turbidity for aggregated samples (Figure 12 b). The same was observed for longer phosphate homologues such as pyrophosphate (SDP; Figure 12 c), triphosphate (STP; Figure 12 d) and etidronate (HEDP; data not shown). Despite the fact that phosphates have little effect on the denaturation temperature, their strong upshifting effect on the aggregation peak suggests that they keep BSA in a configuration that is not prone to aggregate. This effect was not observed for the similarly charged (and structured) sulfate, indicating potential binding sites on BSA specific to phosphates.[100] For hydrotropes, a significant reduction in resulting turbidity was recorded as well (Figure 12 e & f). This can, in part, be explained by their upshifting effect on the denaturation and aggregation peaks (cf. Figure 11 f). Additionally, it can be assumed that hydrotrope molecules will competitively bind to exposed hydrophobic patches of (partially) unfolded BSA molecules reducing the chances of protein-protein aggregation. This is in line with what was observed for CCEW (cf. Figure 10 h) and typically requires larger hydrotrope concentrations to be effective (≥100 mM).

1.4 Conclusion

The general idea of Hofmeister effects on proteins, summarised in section 0.2.1, holds true for simple, globular and negatively charged proteins such as conalbumin. This concerns both, conformational and colloidal stability including aggregation phenomena. Such a simplistic approach, however, can quickly clash with reality as the experiments with the equally globular and negatively charged BSA showed: here, grave deviations from the "rules" were observed as "kosmotropic" and "chaotropic" behaviours appear to lose their universal meaning. Secondary aspects such as specific binding sites, special protein characteristics and the amphiphilicity of compounds will start to overlay (and dominate) specific ion effects. As the complexity of proteins and the systems they appear in expands, so will the mechanistic background for their stability increase. Hence, the analysis of processes in protein chemistry should always involve but not be limited to the discussion of Hofmeister effects.

CHAPTER 2: THE BALANCE OF SPECIFIC ION EFFECTS AND HYDROPHOBICITY

2.1 Introduction

In colloidal chemistry, it is of particular interest to consider not only the effects of free ions, but also of the charged headgroups of amphiphilic molecules. In 2009, Vlachy et al. proposed the ordering of anionic headgroups of surfactants.[101] Their interactions with counterions were interpreted in terms of *Collins' concept of matching water affinities*[29], see Figure 13. In this classification, the carboxylate headgroup is considered as the "hardest" (kosmotropic) one with the highest charge density and strongest hydration, whereas the sulfate and sulfonate headgroups are "softer" (chaotropic) and less hydrated.

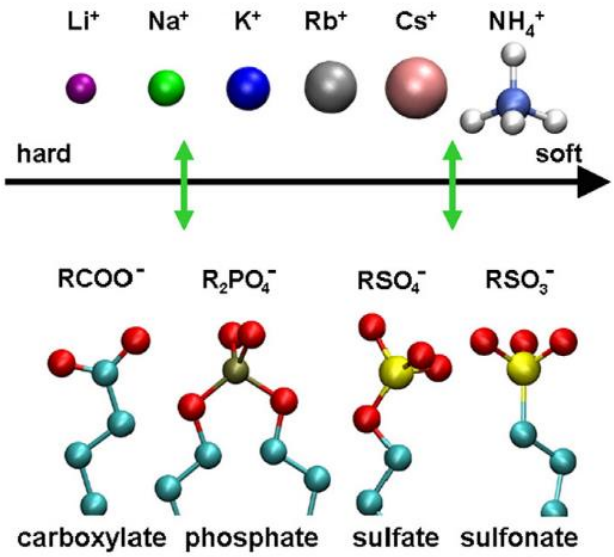

Figure 13 Ordering of headgroups according to the Hofmeister series. Source: Vlachy et al. Adv.Coll. Int. Sci. 2009. Reprinted with permission from Elsevier.

The so established charged headgroup series was well received and could explain a variety of effects, such as counter-ion binding affinities in molecular brushes[102], mixed surfactant systems[103] and microheterogeneous catalysis.[104] In addition, similar Hofmeister-type series have been put forward for cationic headgroups.[105,106] A few papers also have dealt with the influence

of different headgroups on the hydrophilic/hydrophobic balance of ionic amphiphiles. One such finding was the apparent correlation of chain melting temperatures and headgroup hydration (greater hydration enthalpy correlates with lower T_m).[107,108] In another publication by Hammer et al., it was shown that anionic surfactants show a dependence of the retention time in liquid chromatography on both the chain length and the type of ionic headgroup (i.e. the hydration), depending on the polarity of the mobile phase.[109] In a work by Shao and Jiang, the properties of a zwitterionic compound to be resistant to non-specific protein adsorption was calculated to be dependent on the degree of hydration, which in turn allowed for a Hofmeister-type ordering of ionic headgroups (both, cationic and anionic).[110] Lastly, in a recent paper by Sultana et al.[111], it is shown, how the increasing chain length of a carboxylate leads to a change from kosmotropic behaviour to one dominated by its hydrophobicity.

Hydrotropes are also amphiphilic molecules that facilitate the solubilization of nonpolar (or only slightly polar), mostly hydrophobic molecules in water. However, the limited size of hydrotropes does not allow them to build up well-defined structures such as micelles or liquid crystals (cf. section 0.2.2 for more details).[44] Many of the commonly used hydrotropes are also charged, i.e. SXS or short-chain carboxylates. Because of the shorter hydrocarbon chains compared to true, classic surfactants, it is clear that here, the charged headgroup is of even higher importance. Again, the headgroup can be soft and as such facilitate “salting-in” behaviour. In this case, the hydrotropic power of the molecule can be further strengthened. By contrast, if the headgroup is strongly “kosmotropic” (of high charge density), it may be so “salting-out” that the whole molecule is no longer a hydrotrope at all. This complete reversal of the solubilising power of a molecule due to the change of the headgroup is not possible in the case of true surfactants. In the case of hydrotropes, however, it is of significant importance. Surprisingly, to the best of my knowledge, this very significant dependence of the solubilization power of a hydrotrope on its headgroup identity, has never been studied in detail before, despite its general relevance for a multitude of applications.

This chapter has been published in the Journal of Physical Chemistry and Chemical Physics (J. Mehringer, E. Hofmann, D. Touraud, S. Koltzenburg, M. Kellermeier and W. Kunz, *Phys. Chem. Chem. Phys.*, 2021, *23*, 1381-1391). This study was conducted with the help of Evamaria Hofmann, who performed the COSMO-RS calculations on my behalf.

2.2 Experimental

2.2.1 Chemicals

Additives – Sodium benzoate (≥99.5%), sodium benzene sulfonate (97%), sodium benzene phosphate (≥95%), phenyl phosphonic acid (98%), diphenyl phosphate (99%), sodium xylene sulfonate, trichloroacetic acid (≥99.0%), tridecanoic acid (≥98%), sodium monodecyl phosphate, ethyl malonic acid (97%), butyl malonic acid (99%), dextrane sulfonate sodium salt (SA#: 75027), Poly(N-isopropylacrylamide) (PNIPAM) (Mwt. 7000), and Disperse Red 13 (95%) were all purchased from Sigma-Aldrich. Sodium dodecyl sulfate (≥99%), sodium acetate-trihydrate (p.a.), sodium butyrate (≥98%), sodium chloride (99.5%) and malonic acid (≥99%) were acquired from Merck. Heparin sodium salt, 3,4-Dimethyl benzoic acid (>99%), sodium hexanoate (>99%), sodium methyl sulfate (≥98%) and sodium pentyl sulfonate were purchased from TCI. Decanoic acid (99%) and sodium pentyl sulfate (99%) were acquired from Alfa Aesar and sodium octyl sulfate from Lancaster. Sodium pentyl phosphate was synthesized from pentanol (≥ 99%), phosphor pentoxide (99%) and crystalline phosphoric acid (≥99.999%) all from Sigma-Aldrich according to a method by Tracey et al.[112] *Proteins* – Egg White was prepared from fresh chicken eggs bought in local supermarkets. Phytase was supplied as a 25 wt% stock solution directly by BASF. *Solvents* – Tris(hydroxymethyl)aminomethane (TRIS) Buffer salt (>99.8%) was purchased from Merk. Di(propylene glycol) propyl ether (DPnP, ≥98.5%) was obtained from Sigma-Aldrich. The pH was adjusted using HCl (1 N, VWR Chemicals) and NaOH (1 N, Roth). Deionized water (Millipore quality) with a resistivity of 18 MΩ·cm was used.

2.2.2 Methods

Disperse Red 13 – Sample solutions were prepared in their respective concentrations in MilliQ. Then 2 mL of each solution were added to 10 mg of Disperse Red 13 (2-[4-(2-Chloro-4-nitrophenylazo)-*N*-ethylphenylamino]ethanol) and stirred in the dark for 2 h. After that, the solutions were filtered by means of a 200 nm syringe filter and measured for absorbance at 503 nm using a Perkin Elmer Lambda 19 Spectrophotometer. Samples exceeding 1.5 absorbance were diluted accordingly. All measurements were done in duplicates and the results averaged. Error bars mean ±SD.

Pendant Drop – Sample solutions were prepared in their respective concentrations in MilliQ. The surface tensions were determined using a Sinterface pendant drop Tensiometer. Each measurement was recorded, until it reached an almost constant value. In any case, the value after 300 s was chosen for comparability's sake. All measurements were done at least in duplicates and the results averaged. Error bars mean ±SD.

Differential Scanning Calorimetry (DSC) – DSC measurements were carried out using a Setaram micro DSC III. Protein samples of phytase and crude chicken egg white (CCEW) in TRIS Buffer pH 7.4 (50 mM) were scanned at a heating rate of 1 K/min from 25-90°C. Sample sizes were around 800 mg. Denaturation peak temperatures and onsets were determined using the Setsoft 2000 program by Setaram. Error bars meaning ±SD (N=3) are provided for reference measurements without additive and serve as a guide for the methodical precision.

Determination of the lowest critical solubilization temperature (LCST) of DPnP/H_20 mixtures with additives – This experiment is based on previous works by Grundl et al. and Bauduin et al. and detailed procedures can be found there.[113,114] Additives were dissolved in a DPnP/water mixture (55 wt%) and the samples were cooled down to 0°C. The sample tubes were then slowly heated under constant agitation and the cloud point was recorded by visual observation. No hysteresis was observed and samples could be chilled/heated repeatedly with constant results. The error is estimated to be < ±0.2 K, based on repeated measurements.

PNIPAM – Aqueous solutions containing 1 wt% PNIPAM (Mwt: 7000) were prepared with varying contents of additives and the LCST was determined during heating the samples in a water bath

by visual observation of the cloud point. Then the slope α [°C/mmol] of the temperature-concentration dependence was calculated from a fit to the linear part in the concentration ranges up to 100 mM of additive concentration.

COSMO-RS Calculations – The *COSMOthermX*[115] software (version 19.0.4 by COSMOlogic), which is based on COSMO-RS theory[116–118], was applied to compute both hydrogen-bonding and van der Waals enthalpies of 100 mmol/kg salt dissolved in water. The salt consisted of a simple or twice negatively charged anion and sodium cations as counterions. All calculations have been performed on TZVPD-FINE level. When considering the σ-profiles of the molecules, the contributions of the individual conformers were weighted by their weight factor given in the mixture. The water molecule and the sodium ion were taken from the *COSMObase TZVPD-FINE 19.0* database. The conformational analysis of the anions has been performed using the COSMOconfX software (version 4.3 by COSMOlogic) and the TURBOMOLE program (version TmoleX 3.4 by COSMOlogic). Geometry optimizations have been performed with DFT/COSMO calculations on TZVPD-FINE level.

2.3 Results and Discussion

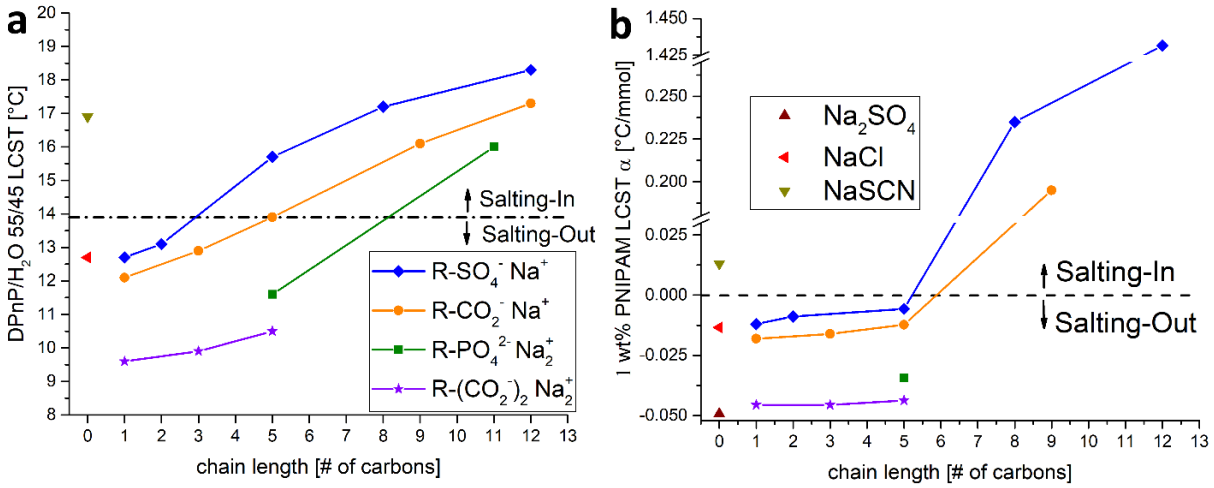

Figure 14 **a:** LCST for different headgroups with varying chain length at 10 mmol/kg in DPnP/water 55:45 w/w. **b:** Slope α of linear fit to LCST of a 1wt% PNIPAM (Mwt: 7000 Da). Slope was calculated for concentration ranges 0-100 mM of additives. Inorganic salts were added for comparison.

While it does not allow a precise discrimination between surfactants, hydrotropes and chaotropic anions (in literature sometimes referred to as hydrophobic or hydrotropic ions), the change in the lowest critical solubilization temperature (LCST) of the simple DPnP/water mixture can be used as a versatile indicator for general salting-in or salting-out properties of various additives.[113,119] An increase of the LCST upon addition of a third component means that this compound is salting-in, i.e. increasing the miscibility of DPnP and water, whereas a decrease of the LCST indicates a salting-out behaviour.

Using this system, we could measure the properties of amphiphilic compounds with different headgroups as a function of the chain-length of the hydrophobic tail (see Figure 14 a). It becomes apparent that the ionic nature of all examined headgroups (sulfate, carboxylate and phosphate) dominates the character of the compound if the tail is short enough. As the "Hofmeister neutral" counterion Na^+ does not form strong ion pairs with any of these headgroups, they are strongly hydrated and the entire molecules are not chaotropic (or partially hydrophobic) enough to behave as a hydrotrope. Once the hydrophobic part becomes long enough, however, the molecules become hydrotropes at medium chain length (i.e. around 5 carbons) and transition to true surfactants with even longer chains (e.g. SDS with 12 carbons).

The same principal behaviour was also observed for the LCST of PNIPAM (see Figure 14 b), a thermo-responsive polymer that is often used as a protein model.[26] It must be noted, that in this case longer chains (i.e. larger hydrophobic parts) are necessary to switch the behaviour from salting-out to salting-in. This corresponds to previous findings that for PNIPAM, ions need to be quite strongly chaotropic to induce a salting-in effect, with chloride, bromide and even nitrate failing to do so (cf. inorganic ions plotted in Figure 14 for reference). This is because the preferential adsorption effect (cf. section 0.2.1) could not overcompensate the increase in surface tension.[120] It becomes apparent that compounds need to be (closer to) surfactants to exhibit a salting-in behaviour for PNIPAM. It was found that SXS, a very strong hydrotrope, remains very weakly "salting-out" in character up to 1 M, while SDS is "salting-in" already below its cmc (data not shown).

From the results in Figure 14, it is also apparent that short chain sulfates have a similar salting-out tendency as the chloride ion, which is often referred to as a "borderline-ion", that can act as either a chaotrope or kosmotrope, depending on the circumstances.[121,122] This implies that short alkyl sulfates might also exhibit "borderline-ion" behaviour.

The general trend for both, the order of the headgroups as well as the effect of the chain length is identical for DPnP/water and PNIPAM experiments: Longer chain lengths and softer headgroups lead to better solubilizing efficiencies. The former is not surprising as it has been known for a long time that the efficiency of surfactants scales with the chain length[123,124]. The latter essentially reproduces the headgroup order first derived from *Collins law of matching water affinities* by Vlachy et al.[101]

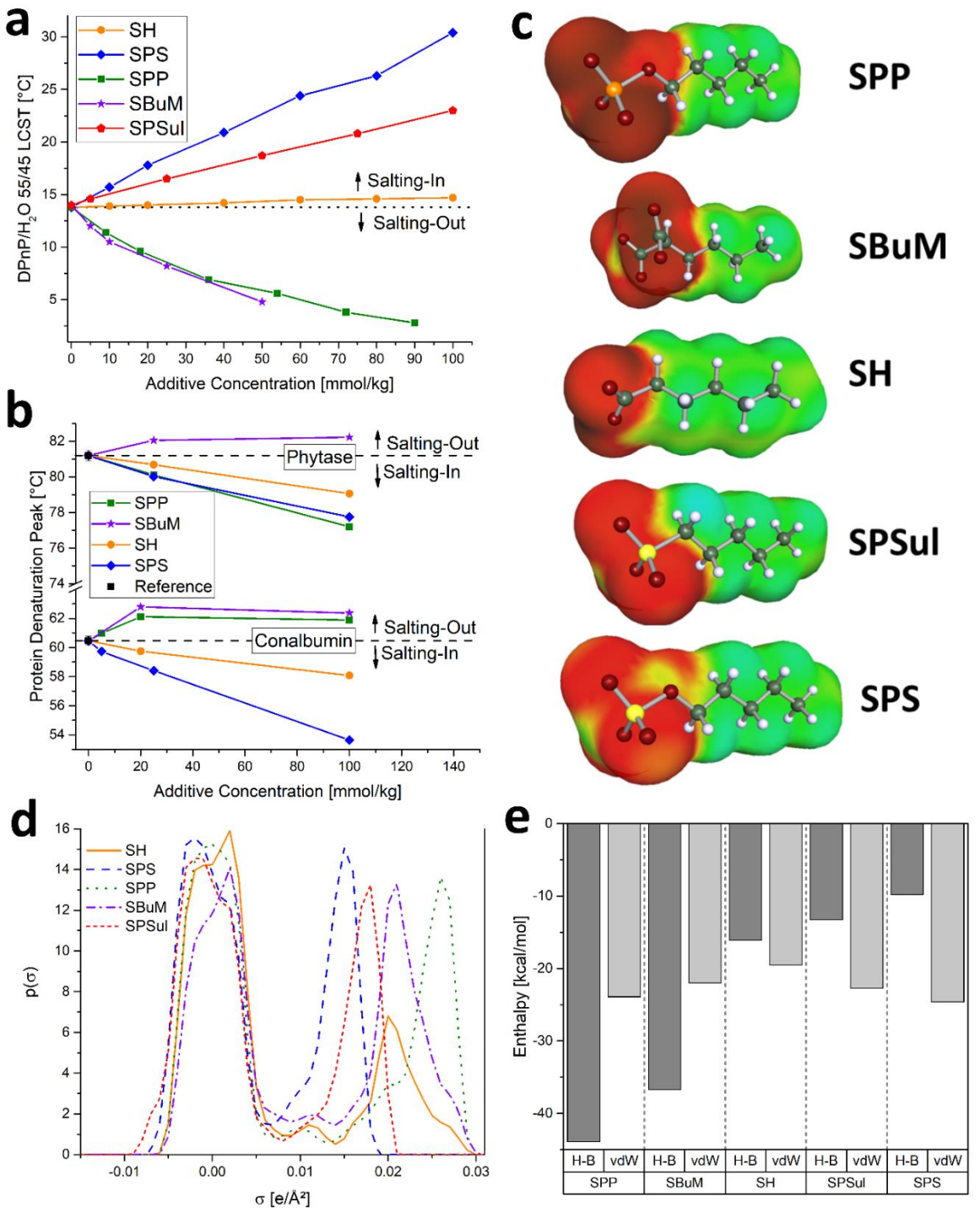

Figure 15 **a:** LCST of DPnP/water (55/45) mixtures with varying content of additive. Sodium hexanoate (SH), sodium pentyl sulfate (SPS), sodium pentyl phosphate (SPP), disodium butyl malonate (SBuM) and sodium pentyl sulfonate (SPSul). **b:** Change in denaturation temperature for conalbumin and phytase in 50 mM TRIS at pH 7.4 with varying additive concentrations, as determined by DSC. **c:** Predicted additive structures with superimposed screening charge density σ (C0 conformers only). **d:** Averaged σ-profiles for all additives from **c**. **e:** Predicted hydrogen-bonding (H-B) and van der Waals (vdW) enthalpies for all additives from **c**.

The relative importance of headgroup ionicity and hydrophobicity will become very obvious, when examining the generic hydrotrope structure consisting of a pentyl chain and a charged head. As it can be seen in Figure 15 a, sodium pentyl sulfate (SPS) and sulfonate (SPSul) are strongly salting-in for DPnP/water mixtures, while sodium pentyl phosphate (SPP) and sodium butyl malonate (SBuM) are strongly salting-out, certainly, because the headgroups are double charged. Sodium hexanoate (SH) is very weakly salting-in, which is a compromise between the nature of its headgroup (carboxylates are salting-out) and its function as a surface-active hydrotrope (salting-in). This fine balance can be tipped in favor of total salting-out, by adding another carboxy-group to the head (see SBuM). Now the compound is on a par with SPP, due to the double charge. We may call this a "Debye" effect, because it is more a purely Coulomb, rather than a specific (Hofmeister) effect. It should be noted that the LCST rises or falls nearly linearly with the concentration of the additive. Apart from the DPnP/water system, this behaviour was also observed for the solubilization of disperse red (DR) (data not shown), a very hydrophobic and virtually insoluble dye. Here, the SPS and SH can solubilize the dye molecules in considerable quantities once a sufficient amount of the hydrotrope (typically >500 mM) is reached. Much like in the DPnP/water system, SPS was effective at a lower concentration than SH. On the contrary, SPP and SBuM did not solubilize DR at all (data not shown).

As seen in previous sections, the consequences of hydrotropy and Hofmeister/Debye effects are also apparent in other contexts, e.g. on the stability of proteins, quantifiable by the peak denaturation temperature. In Figure 15 b, the thermal stability of conalbumin (in CCEW) and phytase is given as a function of the additive concentration. The addition of SPS and SH led to a weakening of the hydrophobic effect within the protein (a major contributor to native protein stability[67]), due to their hydrotropic properties. This is reflected by a decrease of the denaturation temperature. Again, the alkyl sulfate is a stronger hydrotrope/denaturant than the alkyl carboxylate. On the other hand, the addition of SBuM led to an increase of denaturation temperatures, indicating a stabilization of the ternary protein structure. The same is observed for the SPP, with the exception of phytase. Here, SPP is also weakening the protein structure, which might be due to a specific interaction of phosphates with phytase, as this protein is designed to cleave phosphate ester bonds (cf. section 6.3.4). In general, however, kosmotropes

(such as carboxylates and phosphates) tend to stabilize proteins by strengthening the hydrophobic effect, due to partial dehydration of protein subunits (cf. also sections 0.2.1 & 0.2.3.3).[29] On occasion, a reversal of the Hofmeister effect can be observed[31], such as for positively charged proteins, but in the present case, both proteins are negatively charged at pH 7.4 (cf. sections 1.3.1 & 6.3.4).

In order to analyze these diverse effects further, theoretical calculations based on COSMO-RS were carried out for all of these compounds in water. Figure 15 c shows their structures with the superimposed screening charge density σ. The reduction in charge density at the headgroup going from phosphates to sulfates can be seen easily (red depicts areas of high charge density, green of low charge density) and are further quantified by their σ-profiles in Figure 15 d. Here, the drift in headgroup charge density is clearly visible (at positive sigma values), while the hydrophobic contribution of the tail remains relatively unchanged (area at low/zero sigma). In energetic terms, Figure 15 e lists the enthalpic contributions of hydrogen bonding (H-B) with solvent (i.e. water) molecules and van der Waals interactions (vdW). Again, the vdW forces remain largely unperturbed, and the differences observed in our systems for various headgroups are mostly due to the effects on hydrogen bonding with water. As is expected for more kosmotropic ions, high H-B enthalpies (i.e. strong hydration) are reported for phosphate and carboxylate, while sulfate and sulfonate exhibit much weaker HB enthalpies (i.e. weaker hydration). Therefore, our theoretical calculations support the claim that the proficiency of a headgroup to bind water directly impacts the effect and efficiency of an amphiphilic compound in terms of solubilization and protein stabilization.

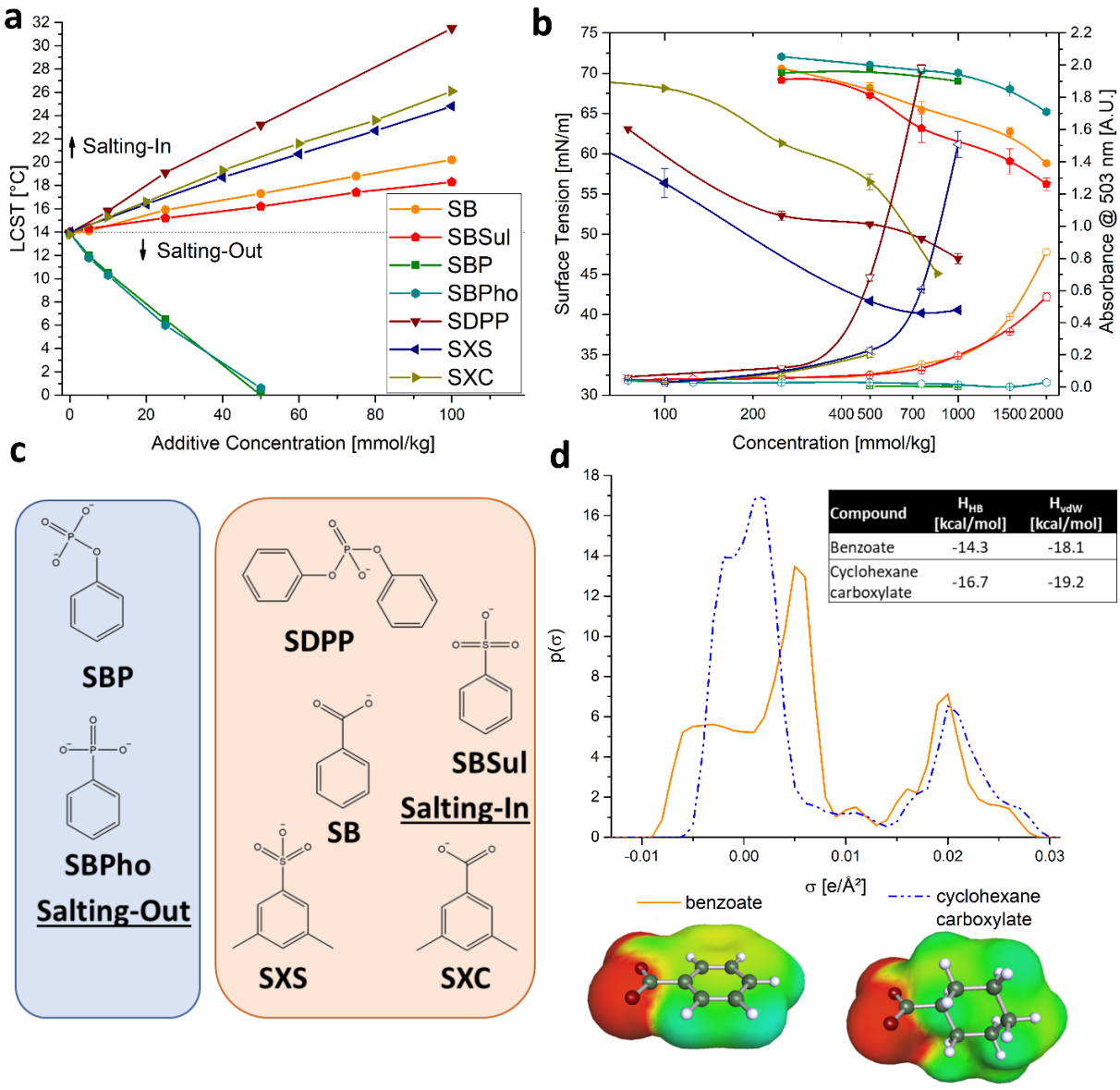

Figure 16 **a:** LCST of DPnP/water (55/45) mixtures with varying content of additive. **b:** Surface tension (filled symbols) and disperse red solubilization (hollow symbols) for various additives. Error bars mean ±SD. **a & b:** Sodium benzoate (SB), sodium benzyl sulfonate (SBSul), sodium benzyl phosphate (SBP), sodium benzyl phosphonate, sodium diphenyl phosphate (SDPP), sodium xylene sulfonate (SXS) and sodium xylene carboxylate (SXC). **c:** Molecular structure of compounds in **a** and **b** depicted in ionic form. **d:** Averaged σ-profiles of benzoate and cyclohexane-carboxylate. The molecular structures of their C0 conformer is superimposed by the predicted screening charge-density σ. Insert: Theoretically determined enthalpies of H-bonding (H-B) and van der Waals forces (vdW) for both compounds.

By expanding the experiments to the relatively simple structures consisting of benzyl moieties with ionic headgroups as shown in Figure 16, we could investigate further aspects that play a key role in the fine balance between salting-in and salting-out characteristics of hydrotrope-type compounds. For this, experiments were carried out using the DPnP/water system as well as surface tension and DR solubilization measurements. Looking at Figure 16 a & b, it can be noted that sodium benzyl phosphate (SBP) and sodium benzyl phosphonate (SBPho) behave very much alike: both are salting-out, do not solubilize DR and show very little effect on the surface tension, suggesting little difference between phosphonate and phosphate groups, regarding their ionic nature. This mirrors the large similarities between sulfate and sulfonate groups (cf. Figure 15). Sodium benzoate (SB), sodium benzene sulfonate (SBSul), sodium xylene carboxylate (SXC) and SXS were all found to be good salting-in agents (Figure 16 a & b), with xylene-bearing compounds being slightly more effective due to their larger hydrophobic moiety (Figure 16 c). Interestingly, sodium di-phenyl phosphate (SDPP), unlike SBP, exhibits a very strong salting-in behaviour that can be attributed to two key differences when compared to SBP (see also Figure 16 c): i) the hydrophobic content is doubled due to the additional phenyl ring and ii) the charge of the headgroup is reduced to one, making the phosphate mono-ion much more similar to a carboxylate.[24] These two structural changes tip the balance fully in favour of a salting-in behaviour, with a strong reduction in surface tension and good DR solubilization (see Figure 16 b).

What might surprise, however, is the fact that for both, the benzene and the xylene structures, the carboxylates (SB & SXC) appear to be a slightly better hydrotropes than the sulfonates (SBSul & SXS), based on their effect on DPnP and DR. This is the reverse of what was observed for linear alky-chains (see Figure 15) and can be explained by the effect of the phenyl ring on the vicinal head group. The σ-profiles from our COSMO-RS calculations (see Figure 16 d) indicate that the carboxy group will be weakened in its ionic character because some electron density of the carboxylate will be lost to the (in comparison) more electronegative phenyl ring carbons. As a consequence, the headgroup will be diminished in its intrinsic salting-out character (by becoming “less hard”), making the overall compound more salting-in (i.e. hydrotropic). It was observed in the past that benzoate appears to be a better hydrotrope than its fully saturated

(cyclic or linear) counterpart.[49,50] This was explained by a higher hydrophobicity of the aromatic compound. However, our theoretical calculations showed that the vdW interactions are actually slightly stronger for the saturated compound (see insert Figure 16 d), while the hydrogen-bonding enthalpies are lowered. Hence, it might seem reasonable that the weakening of the kosmotropic headgroup by charge redistribution will be the main contribution to this observation. This electron-withdrawing effect also occurs for SBSul (as confirmed by COSMO-RS, data not shown), but the impact on the net salting-in behaviour appears to be less pronounced.

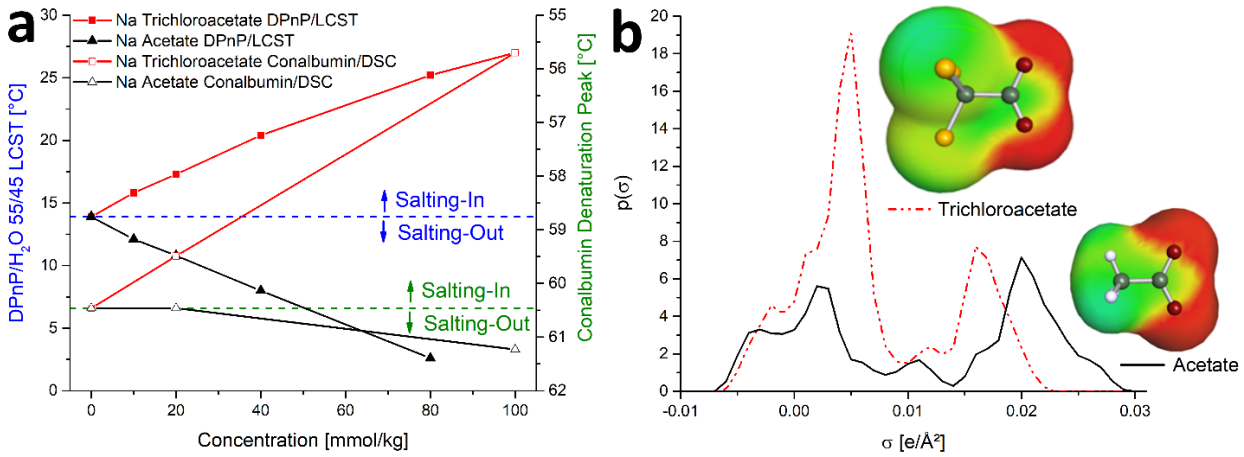

Figure 17 **a:** Left axis: LCST of DPnP/water (55/45) mixtures with varying content of sodium acetate and sodium trichloroacetate. Right axis: Denaturation peak of conalbumin in crude chicken egg white with sodium acetate and sodium trichloroacetate. Note the reverse scale for the denaturation temperature to visually match the LCST data. The dashed lines give the LCST of the binary DPnP/water system and the denaturation of conalbumin without additives respectively. **b:** Averaged σ-profiles for sodium trichloroacetate and sodium acetate. The molecular structures of their C0 conformers are superimposed by the screening charge density σ.

The same mechanism can also be observed when comparing sodium acetate with sodium trichloroacetate. The former is a known kosmotropic salting-out compound (cf. also Figure 14), while the latter is a member of the chaotropic side of the Hofmeister series (even more chaotropic than thiocyanate).[125] The corresponding effects can be seen in both, the LCST of DPnP/water and the denaturation temperature of conalbumin (see Figure 17 a). The reason, again, lies in the removal of electron-density by the three electronegative chlorine atoms away from the headgroup. For trichloroacetate this redistribution is so strong that it becomes effectively a soft, weakly hydrated ion with a lower overall charge-density at the headgroup. This can be seen in our COSMO-RS calculations (Figure 17 b), where the shift in the σ-profile is clearly

visible and the screening charge-density depicts a much larger area of low charge density (green) and a smaller area of high charge density (red).

As it has become apparent already in Figure 14, esterified sulfate groups can be considered as "borderline-ions" capable of exhibiting either chaotropic or kosmotropic properties (cf. also Figure 1). The latter (salting-out) character will prevail if the rest of the molecule they are attached to is not sufficiently hydrophobic (i.e. general lack of amphiphilicity), and/or if the number of headgroups is high (i.e. "Debye-effect"). This can be observed when examining the natural compound heparin or its chemically similar, yet artificial counterpart dextran sulfate (see Figure 18). Both polysaccharide compounds exhibit a salting-out behaviour in the DPnP/water and aqueous PNIPAM systems, which can be linked to their overall high charge density (heparin is the biological macromolecule with the highest negative charge density in nature[126]), resulting in strong hydration which is typical of kosmotropes.[24] These polymers have rather hydrophilic sugar-backbones (see Figure 18 b), that give the specific ion effects free rein over the compound's overall characteristics.

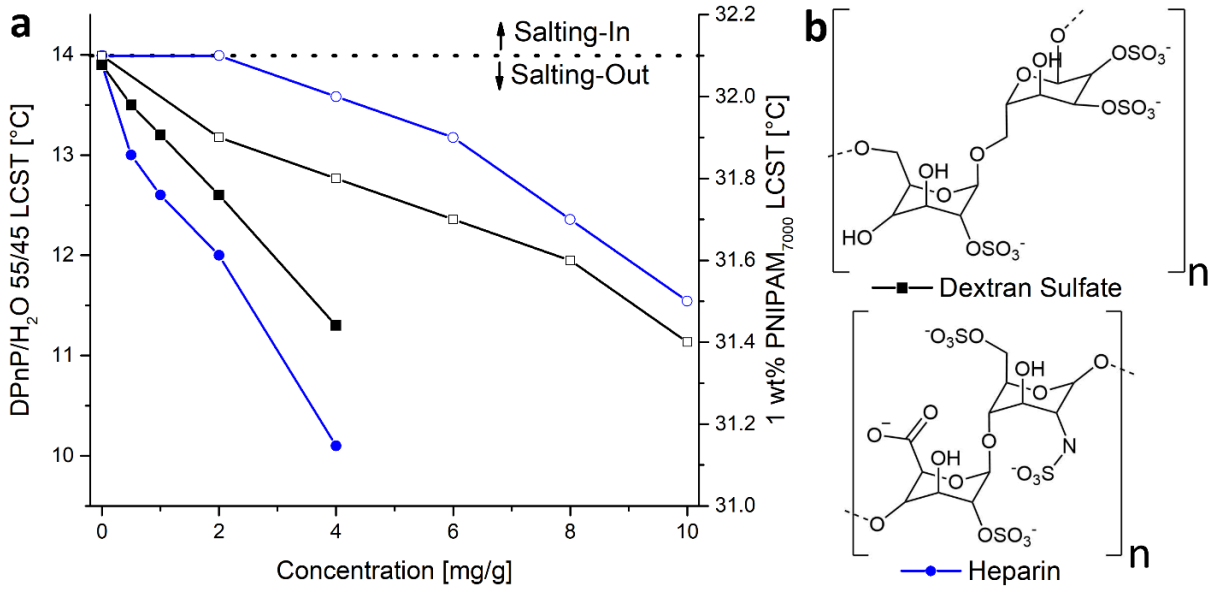

Figure 18 **a:** LCST of DPnP/water (55/45) (filled symbols) and 1 wt% $PNIPAM_{7000}$ (hollow symbols) with heparin (circle) and dextran sulfate (square) both as sodium salts. **b:** The structures of both polymeric compounds are given as their repeating units in ionic form.

In the past, sulfate (or sulfonate) groups were typically characterized as rather soft[24,101,127], however a study showed that chloride ions will replace the sulfonate group of congo red when binding to soft cationic sites on residues in alpha-synuclein.[128] Along similar lines, it was found that sulfated ion exchangers can retain cationic proteins better than carboxylated ones, though increasing sodium chloride concentration will effectively reduce the retention in both cases.[129] This implies a positioning of substituted sulfonate (and sulfate) groups somewhere to the "left" of chloride in the Hofmeister series (but still within the "borderline" region; cf. Figure 1). This is also in accordance with a study on the HPLC retention of amines by different counterions.[130] A Raman spectroscopy study on aqueous dextran sulfate found a weakening of water-water hydrogen bonds in the presence of sulfate groups which was attributed to the strong bonding of the solvent to the anionic subunits.[131] This suggests a stronger interaction of water with sulfate groups than with itself, which is a defining characteristic of kosmotropes and the reason for their strong hydration.[24] The magnitude of the effect scaled with the nature of the sulfate containing compound and was found to be sodium sulfate > sodium methyl sulfate > sodium dextran sulfate, when normalized to the number of bonding sites per mole. Additionally, it was reported that heparin and dextran sulfate exhibit a distinctively kosmotropic behaviour, such as the stabilization of inorganic precursor material form nucleation and mineralization.[132,133] Lastly, it was found that heparin could increase the thermal stability of antithrombin III similar to other kosmotropic additives.[134] This outcome at least provokes the question, whether this kosmotropic behaviour is of any importance for the biological function of glycosoaminoglycans (e.g. heparin)[135], besides its specific protein binding by electrostatics.

2.4 Conclusion

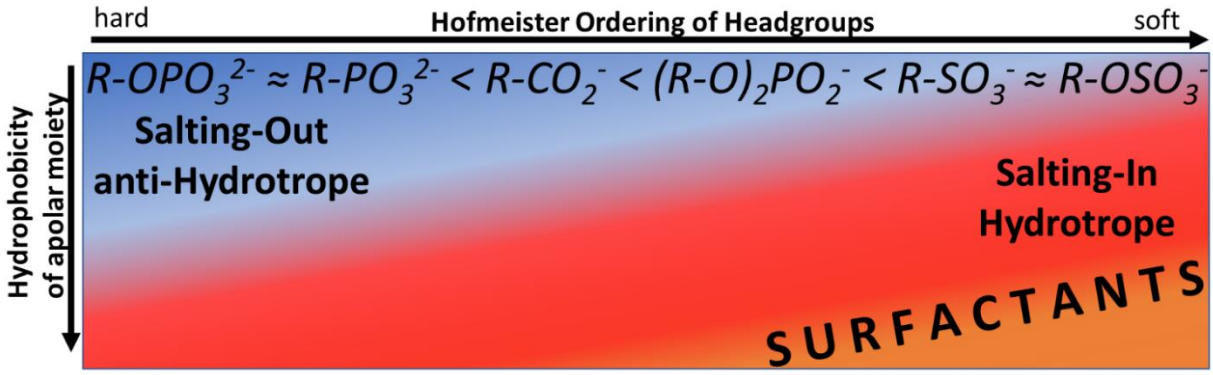

Figure 19 Expanded Hofmeister series of ionic headgroups in amphiphilic molecules listed along the abscissa and the hydrophobicity of the remaining molecule plotted along the ordinate. The resulting field is divided in salting-out and salting-in with a smooth transition zone.

As a result, we propose an expanded Hofmeister-inspired series for ionic amphiphilic compounds, that ranges from strongly salting-out (i.e. anti-hydrotropic, "hard") to weakly salting-out/"borderline" (i.e. "softer"), see Figure 19. Moreover, it becomes apparent that the characteristics of an amphiphilic compound to be salting-in or salting-out (and any shade in between) is down to the balance of the hydrophobic part of the molecule and the nature of the ionic headgroup. Therefore, a second dimension was added, termed simply "hydrophobicity". This will open up a field, where compounds with weakly salting-out headgroups (e.g. alkyl-sulfates) tend to become good hydrotropes already with relatively small hydrophobic backbones. In turn, strongly salting-out headgroups (e.g. mono alkyl-phosphates) require much bigger/more hydrophobic parts to become hydrotropic. Obviously, the balance is mostly of importance to hydrotropes, as surfactants typically have a rather large hydrophobic moiety anyway, so specific ion effects of the headgroup are merely modulating the solubilizing efficiency rather than its overall character. A similar (though one-dimensional) scheme was also put forward by Leontidis, giving a range of anions from kosmotropic over chaotropic and hydrophobic/hydrotropic all the way to surfactants.[73] The transition from hydrotropes to surfactants caused by increasing hydrophobicity of the nonpolar moiety (e.g. by chain elongation) is generally thought to be fluent, with typical characteristics (e.g. aggregation behaviour) of either type only clearly visible for extreme cases.[49,50]

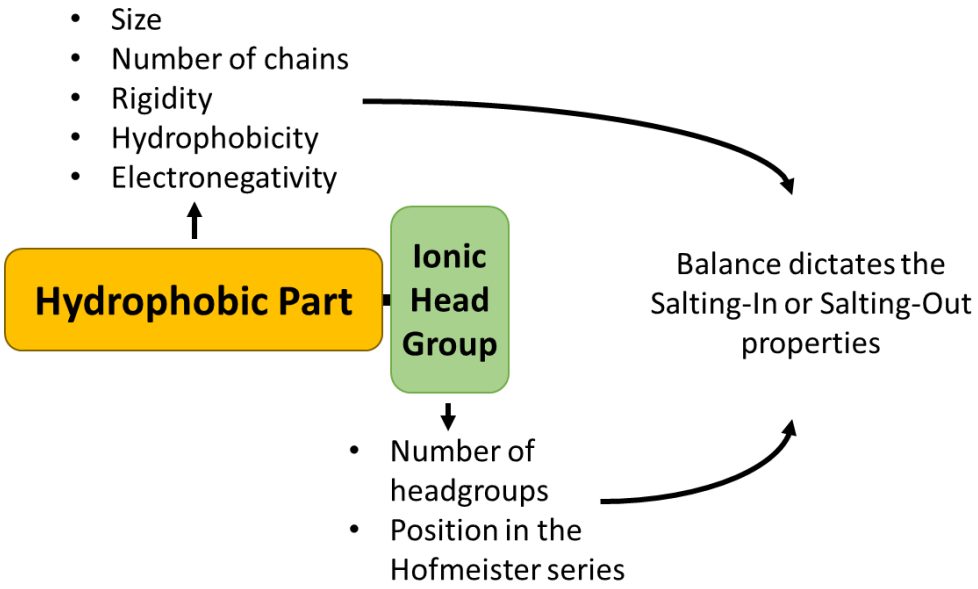

Figure 20 **:** Scheme illustrating the balance of the hydrophobic part and the ionic headgroup in amphiphilic compounds.

The deciding factors for the balance between ionic headgroups and the nature of the hydrophobic part is summarized in Figure 20. Here, it is reiterated that not only the size of the hydrophobic part is important, but also features like its structural rigidity and the propensity to withdraw electron-density from the headgroups, thus weakening their ionic character. Of course, counterions also play a crucial role. By limiting our present studies to sodium, we did not consider this aspect.

Perhaps the most interesting point is that sulfate-groups, despite being reasonably softer than carboxylates or phosphates, are in principle still hard enough to act as “borderline anions”. This has important implications for a variety of compounds either of natural or artificial origin, that carry sulfate groups, but do not have enough hydrophobic structure to counterbalance the salting-out properties, such as heparin or dextran sulfates.

CHAPTER 3: HOFMEISTER VS. NEUBERG – IS ATP REALLY A BIOLOGICAL HYDROTROPE?

3.1 Introduction

In a recent paper, Patel et al. reported on the surprising finding that ATP can significantly enhance the solubility of proteins, some of them being involved in neurodegenerative diseases such as Alzheimer's disease.[82] The authors termed ATP a "biological hydrotrope", using the word that denotes a solubilising enhancer. More than 50 years ago, Mandl and Neuberg have already published a study on the strange solubilising power of ATP at neutral and elevated pH.[136,137] They asked the question, "whether the phenomena of solubilisation are in any way connected with the functions of ATP in nature and to what extent its effect on solubility of so many substances has a definite place in the mechanism of biological reactions". In light of the newly published data, it might be speculated that, in evolution, the original role of ATP was to ensure the solubility of easily aggregating and precipitating proteins.

Neuberg has also been the scientist who coined the word "hydrotrope", now more than hundred years ago.[42,43] Today, hydrotropes are considered to be amphiphilic substances that can solubilise sparingly soluble compounds, without making defined structures such as micelles or liquid crystals in water (cf. also section 0.2.2 for a detailed definition).[45]

Also more than hundred years ago, Franz Hofmeister made an observation that various inorganic salts have specific effects on the solubility of proteins and other macromolecules.[28] He put forward a theory, ordering cations and anions according to their ability to "salt-in" or "salt-out" hydrocarbons in aqueous media, hence termed the "Hofmeister series". For anions, sulfates and phosphates can be found on the kosmotropic side (strongly hydrated, hard ions), whereas perchlorates and thiocyanates are located on the chaotropic end (weakly hydrated, soft ions) of the spectrum.[26] The observed effects on proteins can be summarized as a decrease of protein solubility ("salting-out"), but an increase of protein stability for kosmotropic anions and an increase of protein solubility ("salting-in") with a decrease in conformational stability for

chaotropic anions.[29,138–140] For a detailed description of the underlying mechanisms the reader is referred to section 0.2.1.

As ATP contains a rather large and highly charged triphosphate moiety, and it is not unlikely that the molecule as a whole could, under the right circumstances, act as salt on the strongly hydrated side of the Hofmeister series.[101] In fact, even Neuberg et al. mentioned analogies to the specific effects of inorganic triphosphate in their first publication[136], most probably referring to a later work.[141] This would, however, be in conflict with its role as a hydrotrope, as hydrotropes are considered to have "salting-in" properties, while phosphates exhibit a strong "salting-out" behaviour.[142]

In this chapter, we look into the question, whether ATP is a hydrotrope in general or whether its effect on proteins can be explained by other modes of action.

The contents of this chapter have been part of a publication in the Journal Cell Reports Physical Science (J. Mehringer, T. Do, D. Touraud, M. Hohenschutz, A. Khoshsima, D. Horinek and W. Kunz, *Cell Reports Physical Science*, 2021, *2*, 100343.).

3.2 Experimental

3.2.1 Chemicals

Additives – Sodium salicylate (≥99.5%), sodium triphosphate pentabasic (≥98.0%), sodium xylene sulfonate, adenine (≥99%), adenosine (≥99%), thioflavine T, disperse red 13 (95%), adenosine tri- (≥99%), di- (≥95%) and mono- (≥99%) phosphate as sodium salts were all purchased from Sigma-Aldrich. SDS (≥99%), NaCl (>99.5%) and sodium sulfate (>99%) were acquired form Merck. Sodium thiocyanate (≥98%) was supplied by Fluka and $MgCl_2$ (≥98,5%) by Roth.

Polypeptides – BSA (>98%, Fraction V) and amyloid β protein fragment 1-42 (≥95%) were obtained from Sigma-Aldrich. Egg white was prepared from fresh chicken eggs bought in local supermarkets.

Solvents – Octanol (≥95%) and TRIS Buffer salt (>99.8%) were purchased from Merk. Di(propylene glycol) propyl ether (≥98.5%) and PBS buffer tablets (1x) were both obtained from Sigma-Aldrich. Acetonitril (99.5%) was acquired from VWR Chemicals. The pH was adjusted using

HCl (1N, VWR Chemicals) and NaOH (1 N, Roth). Deionized water (millipore quality) with a resistivity of 18 MΩ·cm was used.

3.2.2 Methods

Disperse Red 13 – Sample solutions were prepared in their respective concentrations in MilliQ. Then 2 mL of each solution were added to 10 mg of Disperse Red 13 and stirred in the dark for 24h. After that, the solutions were filtered by means of a 200 nm Syringe filter and measured for absorbance at 503 nm using a Perkin Elmer Lambda 19 Spectrophotometer. Samples exceeding 1.5 absorbance were diluted accordingly. All measurements were done in duplicates and the results averaged.

Pendant Drop – Sample solutions were prepared in their respective concentrations in MilliQ. The surface tensions were determined using a Sinterface pendant drop Tensiometer. Each measurement was recorded, until it reached an almost constant value. In any case, the value after 300 s was chosen for comparability's sake. All measurements were done at least in duplicates and the results averaged.

DLS Temperature resolved – The protein particle growth was observed utilizing a Zetasizer by Malvern. All samples were prepared in 50 mM TRIS Buffer at pH 7.4 and filtered through a 200 nm Syringe filter directly into the quartz cuvette. All measurements were done in duplicates and the results averaged.

Turbidity – Turbidity was measured at 488 nm by means of a photometer. For temperature scans, 20 mL of the sample solution was heated in a water bath at a constant rate of 1K/min. At appropriate temperature increments, a small volume was retrieved and subjected to absorbance/transmission measurement. All measurements were done in duplicates or triplicates and the results averaged.

DSC – DSC measurements were carried out using a Setaram micro DSC III. Protein samples in 50 mM TRIS Buffer pH 7.4 were scanned at a heating rate of 1 K/min from 25-90 °C. Sample sizes were around 800 mg. Denaturation peak temperatures and onsets were determined using the Setsoft 2000 program by Setaram.

Determination of LCST of DPnP/H_2O mixture – This experiment is based on previous works by Grundl et al. and detailed procedures can be found there.[113] Additives were dissolved in a DPnP/water mixture (55 wt%) and the samples were cooled down to 0°C. The sample tubes were then slowly heated under constant agitation and the cloud point was recorded by visual observation. No hysteresis was observed and samples could be chilled/heated repeatedly with constant results.

Thio T assay – 70 µL of additive solutions in 1x PBS (pH 7.4) were mixed with 10 µL of Amyloid beta 1-42 stock solution (11 µM in 50/50 v/v acetonitrile/H_2O) and incubated at room temperature for 1 h. Then 20 µL of Thio T stock solution (75 µM) were added to the multi-well plate and the fluorescence intensity was measured (λ_{exc} = 450 nm, λ_{det} = 490 nm). The aggregation signal was normalized according to the negative (0%) and positive (100%) control. All measurements were done in triplicates and the results averaged.

DLS Amyloid – The fibrillated amyloid particles were measured utilizing a Zetasizer by Malvern. All samples were prepared in 10 mM PBS at pH 7.4. To 360 µL of additive solution was added 40 µL of a 22 µM Amyloid beta 1-42 stock solution (in 50/50 v/v acetonitrile/H_2O) directly into suitable half-micro cuvettes and subsequently pipette-mixed. After an incubation period of 1 hour at room temperature the duplicates were measured at least 3 times and the results averaged.

3.3 Results and Discussion

3.3.1 The physicochemical properties of ATP

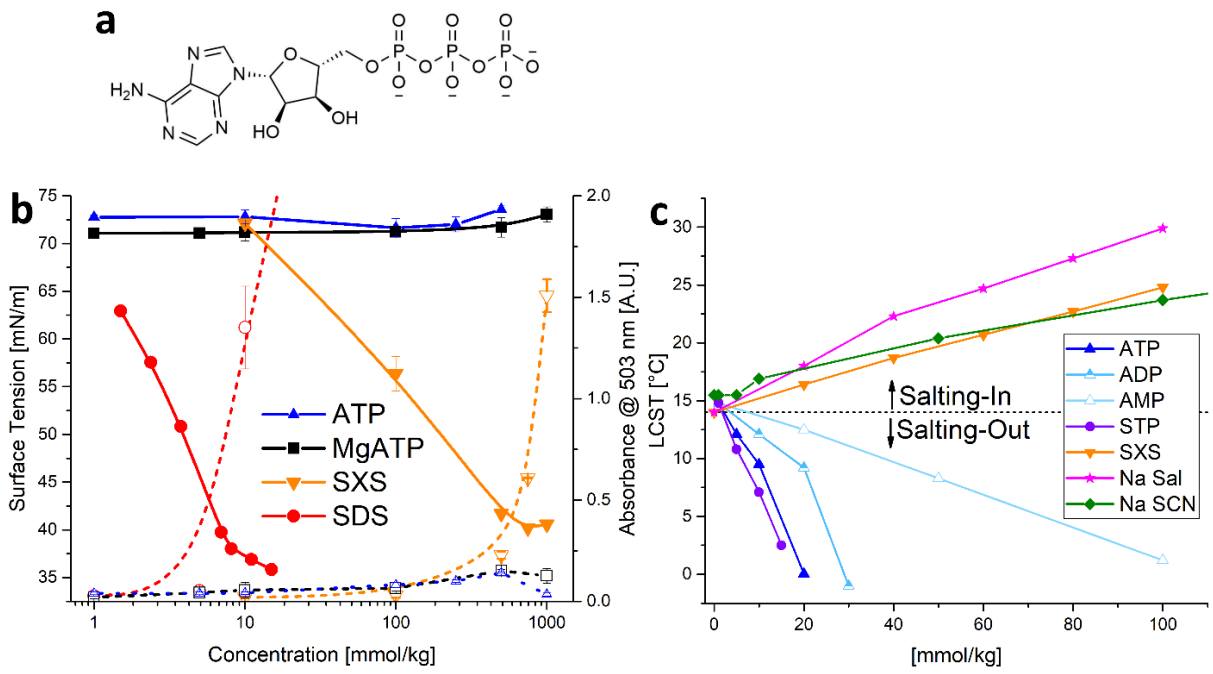

Figure 21 **a:** Molecular structure of ATP depicted in ionic form. **b:** Surface tension (filled symbols) and Disperse Red 13 solubilization (hollow symbols) in regards to additive concentration. Error bars mean ± SD (N=2). **c:** Evolution of the LCST of the DPnP/water (55/45 w/w) system after addition of different substances showing salting-in or salting-out behaviour.

As can be seen in Figure 21 a, the structure of ATP reveals a principally amphiphilic nature with a poorly water-soluble adenine moiety joined by a ribose unit to a very hydrophilic triphosphate headgroup. The compound studied in this work is used as the disodium salt at pH 7.4 (if not explicitly stated otherwise) and will hereafter simply be referred to as "ATP". In order to check the physicochemical properties of ATP for hydrotropic behaviour, a variety of experiments were conducted. First, we tested the influence of increasing amounts of ATP (or the magnesium salt MgATP) on the solubility of the scarcely soluble dye Disperse Red 13 (DR). This assay was previously used by Bauduin et al. to quantify the hydrotropic efficiencies of various compounds.[143] As can be seen in Figure 21 b, the solubility of the hydrophobic substance was not significantly enhanced at any concentration of the added ATP or MgATP up to 1M. In contrast to that, the same experiment carried out for the surfactant SDS and the well-known

hydrotrope SXS showed predictably an increase of dye solubilization in their respective concentration ranges. In addition to that, the surface tension of all four compounds were measured in relation to their concentration. The results show strong surface activity for small SDS and medium SXS concentrations but no drop in surface tension for ATP or MgATP. This is in line with the results for the Disperse Red Assay and suggests poor or no surface activity of ATP salts (cf. section Chapter 2:).

In a second series of experiments, we considered the influence of different compounds on the lower critical solubilisation temperature (LCST) of the binary mixture DPnP-water (dipropylene glycol propyl ether). As described elsewhere, any salting-out (i.e. solubility diminishing) agent lowers the LCST of this system, whereas any salting-in (solubility-enhancing) agent increases it (cf. also section 2.3).[13,113,119] The results are shown in Figure 21 b. The use of hydrotropes such as SXS and Sodium Salicylate (NaSal) as well as the chaotropic salt NaSCN exhibit a salting-in behaviour as per definition. On the contrary, ATP (as well as ADP and AMP) are strongly salting-out. This effect is a consequence of the charged phosphate groups as can be seen by comparing the different adenosine derivatives: The salting-out capacity correlates with the number of phosphate units attached to the adenosine-residue. Additionally, a strong similarity with the inorganic triphosphate (STP) and ATP becomes apparent.

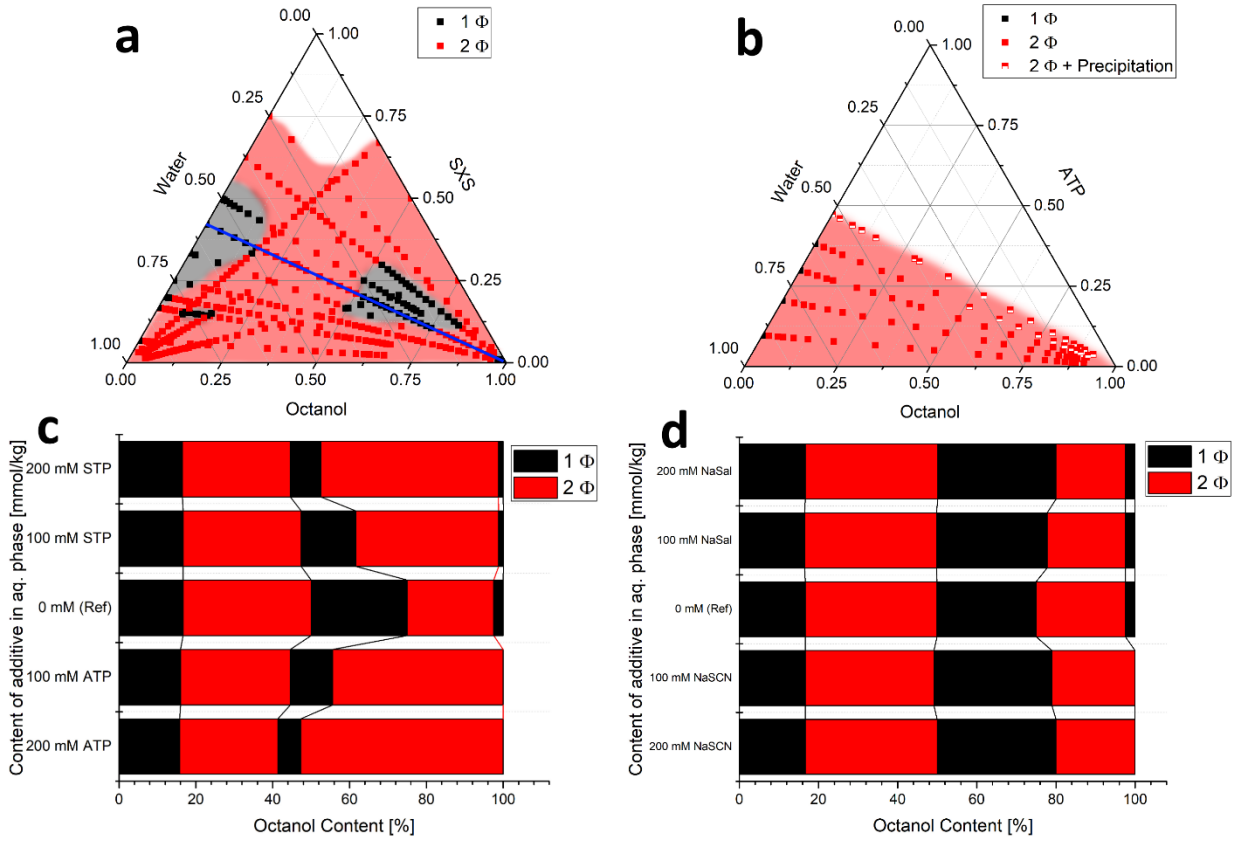

Figure 22 : **a:** Ternary Phase diagram of SXS/Octanol/Water. **b**: Ternary Phase diagram of ATP/Octanol/Water. **a & b**: One phasic area (Black squares), two phasic/immiscible regions (red squares) and visible precipitation (half shaded square) are marked. White areas were not measured due to limited solubility of the additive. **c & d:** Pseudo-ternary phase behaviour of SXS/octanol/water + additive mixtures diluted along to the blue line in diagram **a**. Black denotes one phasic, red two phasic/immiscible behaviour. Additives were ATP, STP, Na Sal and NaSCN in 100 and 200 mmol/kg concentrations

In order to examine whether ATP exhibits any solubilization behaviour at all, a ternary phase diagram of an Additive/Octanol/Water system was measured. This and similar systems have been used previously to exhibit the hydrotropic effect of various compounds.[144,145] Typically, a rather large one-phasic region is to be expected for good (liquid) hydrotropes, where a considerable amount of a hydrophobic component can be solubilised.[44] For solid hydrotropes that have a somewhat limited solubility in water, two smaller one-phasic regions (oil-rich and water-rich) can be observed as seen in Figure 22 a for SXS. ATP, on the contrary, does not exhibit any one-phasic areas apart from the binary water/ATP mixtures (see Figure 22 b). Any addition of octanol will immediately cause a phase separation and at high octanol high ATP conditions will even start to drive the ATP out of the aqueous phase (precipitation). Furthermore, it was

investigated, whether ATP can at least help to enhance the solubilization of octanol in a SXS/water mixture. For this, a pseudo ternary dilution series (by octanol) according to the blue line in Figure 22 a was examined with fixed ATP and STP content in the aqueous phase. Figure 22 c & d shows how the phase behaviour changes with rising additive content in regards to the reference taken form the ternary phase diagram for SXS (blue line in Figure 22 a). It can be seen that ATP and STP behave alike, reducing the size of the one-phasic (oil rich) area significantly while simultaneously shifting its onset to lower octanol contents. This can be explained with the strong salting out behaviour of phosphates (including ATP), which push the SXS out of the aqueous phase and toward the interface effectively increasing its local concentration.[146] At the same time, the increased hydrophobicity leads to a much earlier collapse of the system. Adding a "salting in" compound (NaSCN) or an additional hydrotrope (NaSal) led to the opposite effect, with the one phasic region expanding further into the oil-rich domain (see Figure 22 d).

It becomes apparent that ATP behaves almost exactly like sodium triphosphate in all of our physicochemical experiments and acts in the opposite fashion to what would be considered a solubilizer. This indicates that ATP functions here purely as a Hofmeister salt via its triphosphate moiety rather than a hydrotrope despite its amphiphilic structure.

We thusly conclude that (amphiphilic) organic molecules with negatively charged phosphate groups can be salting-out and in this case cannot be hydrotropes in the common sense of the word. On the contrary, ATP can even decrease the solubility of organic, hydrophobic molecules in water as was previously shown for caffeine.[147] Therefore, ATP can even be considered an "anti-hydrotrope" as defined in the previous chapter (see section 2.4).

Nevertheless, Patel et al., besides others[148], found a strong protein solubilising effect of ATP, so there must be an interaction of some nature between ATP and proteins. In order to look deeper into this specificity, we consider the effect of ATP and its constituents on proteins in the next section.

3.3.2 Effect of ATP on various proteins in solution

In order to examine the effects of ATP on biological macromolecules, experiments were carried out to measure the structural stability (via denaturation temperature) as well as the colloidal stability (via particle growth and turbidity) of various proteins in solution. The results were then compared to STP and SXS.

3.3.2.1 Denaturation

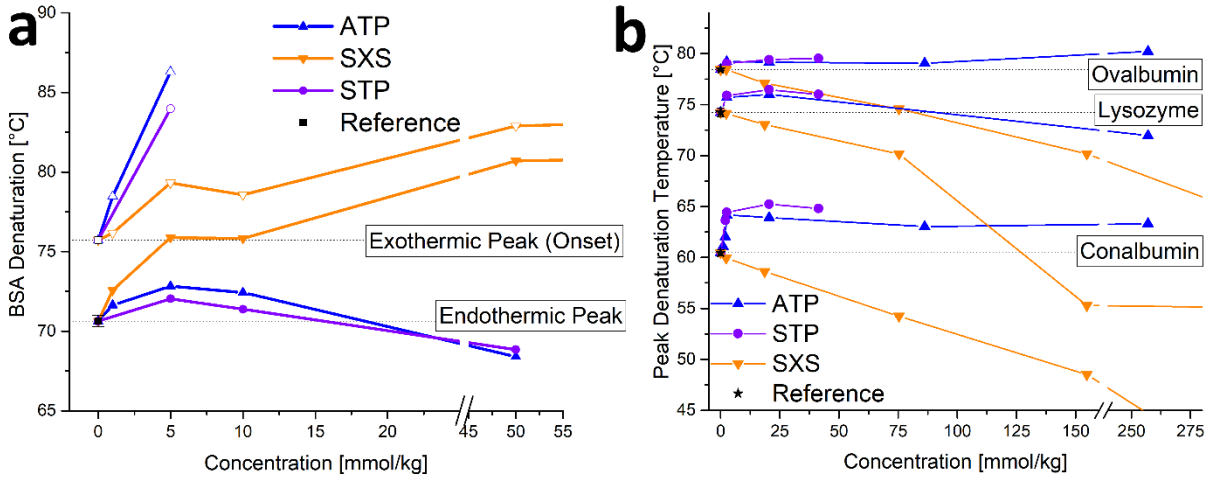

Figure 23 **a:** Endothermic denaturation peak (filled symbols) and (exothermic) aggregation peak onset (hollow symbols) of 1 wt% BSA in 50 mM TRIS pH 7.4. Error bars for Reference mean ± SD (N=3). **b:** Peak denaturation temperatures for CCEW in 50 mM TRIS pH 7.4 separated for individual main protein fractions conalbumin, lysozyme and ovalbumin with additives. Error bars for reference mean ± SD (N=3).

Figure 23 a & b reveal the effect of the mentioned additives on the peak denaturation temperature of bovine serum albumin (BSA) and the main protein fractions in crude chicken egg white (CCEW). For BSA, it becomes apparent that ATP and STP slightly raise the peak denaturation temperature (i.e. the conformational stability), as it is expected for kosmotropic anions.[13,78,134,149–151] Further, the onset of the second (exothermic) peak is quickly shifted outside the temperature window of the DSC. This second peak is most probably connected to protein aggregation, as samples with this peak had jelled in the measuring vessel, while samples without this peak remained liquid and much less turbid.[95] For SXS, it was found that the denaturation temperature was increased even more strongly than that for the phosphates. This somewhat counterintuitive observation could be explained by the role BSA plays in vivo. Normally BSA is used to transport very hydrophobic molecules such as fatty acids through the body, hence it can

also bind to hydrotrope-like molecules such as ethanol[97]. It has been proven in the past that binding ligands can lead to a thermal stabilization of BSA (cf. also section 1.3.2).[98,99]

For the major protein fractions in CCEW (see Figure 23 b and Figure 9 a), it can be seen that SXS and NaSCN decrease the peak denaturation temperature for conalbumin, lysozyme and ovalbumin with rising concentration. This is no surprise, as both SXS and NaSCN are salting-in: one as a classical hydrotrope (with a soft headgroup), the other one as a chaotropic salt. They facilitate the unfolding of polypeptide chains by solubilizing the hydrophobic protein residues through preferential adsorption.[81,99,139,140,149] In contrast, ATP, STP and Na_2SO_4 all raise the denaturation temperatures of said proteins. Again, this behaviour is in line with the observed effects of the Hofmeister series: strongly hydrated anions are preferentially excluded from the protein surface, thus forcing its ternary structure to remain compact with hydrophobic moieties mostly buried in the protein interior (cf. also section 0.2.1 and Figure 9 a).[38,139,152]

3.3.2.2 Aggregation

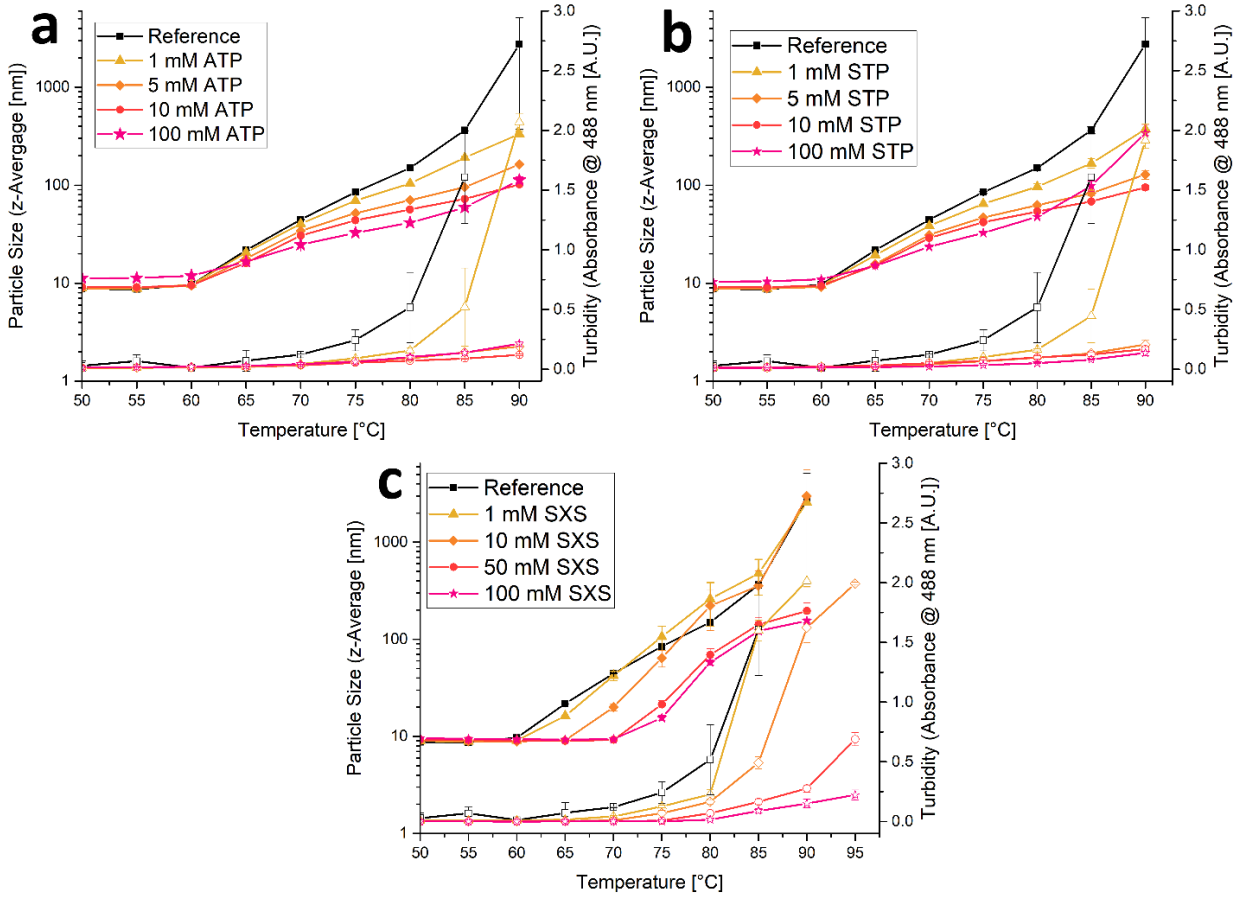

Figure 24 **a-c:** Particle size (filled symbols) and turbidity (hollow symbols) of 1 wt% BSA in 50 mM TRIS at pH 7.4 in dependence of temperature. Additive are ATP (**a**), STP (**b**) and SXS (**c**). Error bars mean ± SD (DLS: N=2, Turbidity N=3).

Solutions of 1 wt% BSA were submitted to thermal stress by heating until 90°C at a physiological pH of 7.4 and the corresponding change in turbidity was recorded. In a second experiment, the heating was repeated but the particle growth was monitored via DLS. As can be seen in Figure 24 a-c, the particle size and turbidity remain constant until the denaturation temperature of BSA is reached (roughly 60 °C; cf. Figure 23 a), at which denaturation followed by aggregation sets in. However, both the severity of the appearing haziness and the particle growth are hindered with rising concentration of ATP, STP and SXS although not to the same extent. While for SXS, concentrations of at least 50 mM are necessary, ATP and STP behave very much alike and are effective at containing particle growth and aggregation at concentrations as low as 5 mM.

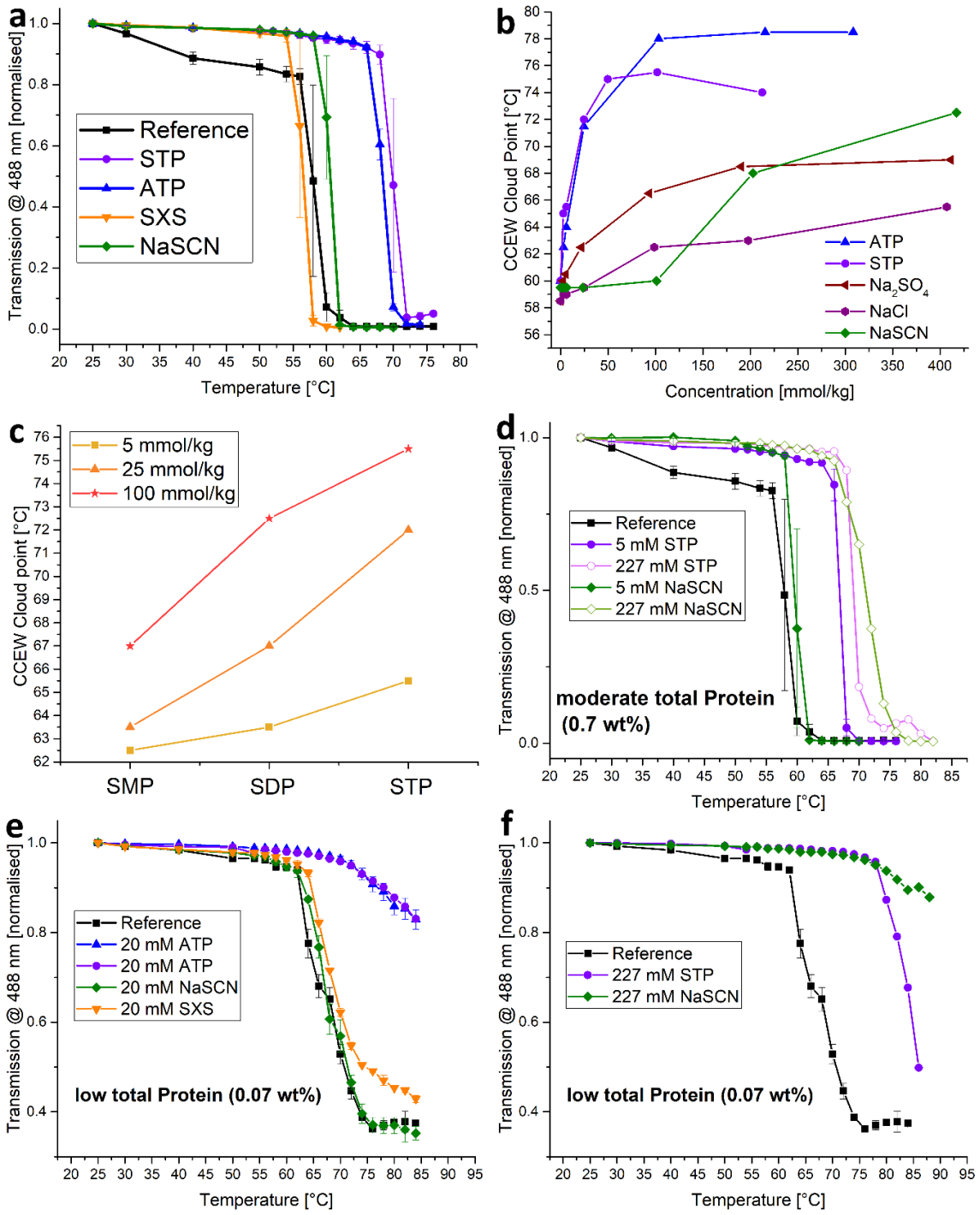

Figure 25 **a:** Transmission of CCEW in 50 mM TRIS pH 7.4 in dependence of temperature with 20 mM of additives. Error bars mean ± SD (N=2). **b**: Cloud point of CCEW in 50 mM TRIS pH 7.4 in regard to additive concentration. **c**: Cloud points of CCEW in 50 mM TRIS pH 7.4 for sodium mono- (SMP), di- (SDP) and tri-phosphate (STP) at various concentrations. **d**: Transmission of CCEW in 50 mM TRIS pH 7.4 in dependence of temperature with low (5 mM) and high (227 mM) concentration of additives. Error bars mean ± SD (N=3) where given. **e & f**: Transmission of 1:10 diluted CCEW in 50 mM TRIS pH 7.4 in dependence of temperature at low (20 mM; **e**) and high (227 mM; **f**) concentration of additives. Error bars mean ± SD (N=3) where given.

A similar experiment was carried out for CCEW in 50 mM TRIS at pH 7.4, where the temperature was increased slowly and the corresponding transmission was recorded (see Figure 25 a). In separate experiments, the cloud points of CCEW solutions were determined visually and plotted against the additive concentrations (Figure 25 b). As can be seen in Figure 10 h, SXS exhibited almost no effect at low, and limited effects at medium concentrations. In contrast, ATP and STP showed a strong increase in cloud point temperature of CCEW already at low concentrations (> 5 mM; Figure 25 a & b). This stabilization effect of CCEW by ATP has been reported also by Patel et al.[82] However, similar to the effect in Figure 21 c, this appears to be connected to the number of phosphate groups involved, as can be seen for inorganic phosphates in Figure 25 c. This stabilizing behaviour can also be seen for other kosmotropic compounds such as Na_2SO_4, whereas the effect of the, in Hofmeister terms, neutral NaCl is much less pronounced (Figure 25 b, cf. also Figure 10). Interestingly, NaSCN, a salting-in compound that decreases the conformational stability of CCEW (cf. Figure 9 a), did also increase the cloud point, although it required much higher concentrations (Figure 25 a & b; cf. chapter 1).

As seen in the previous section, ATP does not act like a classical salting-in hydrotrope, but much more similarly to the kosmotropic triphosphate (see section 3.3.2.1). As such ATP and STP contribute to stabilizing the conformationally correct folded state of the examined proteins (BSA, lysozyme, conalbumin, ovalbumin) and as a consequence delay the onset of denaturation and subsequent aggregation as seen in Figure 24 and Figure 25.[76,78,134,153] Equally important, however, is the direct effect of salts on the particle growth of denatured proteins into larger aggregates. This process can be divided into *diffusion-limited cluster aggregation* (DLCA) and *reaction-limited cluster aggregation* (RLCA) (cf. also section 0.2.3.4).[93,94] These two factors are inversely coupled to the protein concentration, as crowded environments limit diffusion yet increase the chances of protein-protein interactions. Hence, RLCA dominates in areas with higher protein contents, as found in our experiments or most physiological systems. Now, contrary to the well-known effect of salts on protein solubility, particularly at high salt concentrations (> 500 mM), chaotropic anions can actually positively contribute to the RLCA and facilitate protein-protein interactions (e.g. via bridging effects).[24,154] Kosmotropic anions can, in

turn, slow down RLCA considerably, leading to smaller particles sizes and lower turbidity of thermally aggregated protein samples (cf. Figure 7 and section 0.2.3.4).[79,94]

As mentioned above, the protein concentration can influence the aggregation behaviour mediated by specific ion effects. It was reported by Iwashita et al., that for CCEW the Hofmeister series reverses from low protein content (1 mg/mL) to high protein content (10 mg/mL). Therefore, (salting-out) kosmotropes can become stabilizing for thermally aggregating proteins, while (salting-in) chaotropes will enhance aggregate formation.[94] Similar observations were made in the past for high (soy and oat) protein and high salt contents.[78,153]

These results were in part reproduced with the CCEW system used in this work: As Figure 25 d shows, at moderate protein and low additive concentration STP hinders aggregation while NaSCN has very little effect. This difference becomes almost negligible at high additive concentrations (227 mM). In this case, aggregation sets in almost at the same point as for 5 mM STP. The salt concentrations, however, are still about 50% lower than what was used in the experiments by Iwashita et al. It appears the reversed Hofmeister series is not limited to high protein high salt content, but is also in effect at low salt concentrations. At low protein low additive content (20 mM), it was found that SXS and NaSCN have almost no effect, while STP and ATP have a strong aggregation-hindering efficiency (Figure 25 e). At high additive low protein conditions, STP will lead to strong aggregation (although significantly later than the reference), while the sample of NaSCN remains mostly transparent (Figure 25 f). This is in line with the data form Iwashita et al., who found a direct Hofmeister series for low protein high additive scenarios meaning “salting-out” ions will increase thermal aggregation. This, however, does not seem to be the case for small (<20 mM) salt concentrations. At these low salt contents, “salting-out” i.e. decreasing the solubility and facilitating thermal aggregation does not appear to be relevant.

Again, it shows that for globular proteins, ATP acts in the same fashion as STP, indicating a purely Hofmeister-type effect on the aggregation of thermally denatured proteins. It also became apparent that the shift of the cloud point temperature alone is not sufficient to conclude on the effect of additives, as the underlying mechanisms might be very different, e.g. aggregation suppression vs. conformation stabilization (cf. Figure 7).

3.3.2.3 Fibrillation

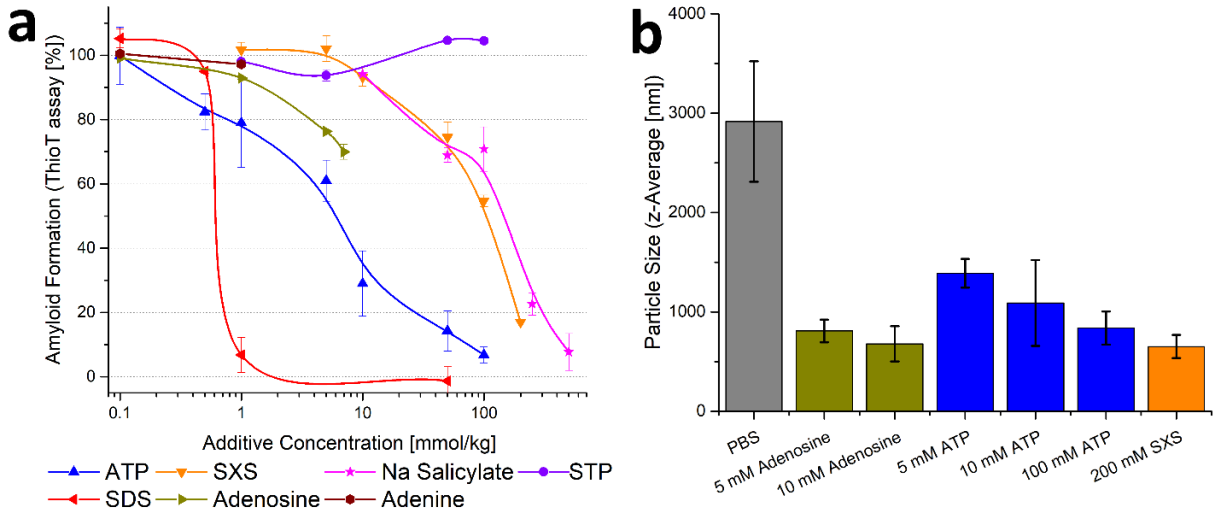

Figure 26 **a:** Amyloid fibre formation from amyloid beta 1-42 protein measured by Thio T assay in 10 mM PBS pH 7.4. Values expressed as fluorescence intensity compared to control groups (positive control = 100%, negative control = 0 %). Error bars mean ± SD (N=3). **b:** Particle size (z-Average) of amyloid aggregation as measured with DLS in 10 mM PBS pH 7.4 with various additives. Error bars mean ± SD (N=2).

The phenomenon called "fibrillation" is possible due to a specific folding of otherwise *intrinsically disordered peptides* into species that are very prone to form linear aggregates with a well-defined structure.[155,156] Hence, this process differs significantly from the aggregation of *globular proteins*, either by precipitation (modulating solubility) or denaturation (affecting ternary structure).

The protein fragment amyloid beta 1-42 (Aß42) is known to be labile in aqueous solutions and has a strong tendency to aggregate, forming amyloid-type fibres already at room temperature. These aggregates can be measured and quantified using the fluorescent hydrophobic dye Thioflavine T (Thio T), which specifically binds to amyloid-fibres. Patel et al. and Coskuner and Murray reported that ATP can effectively limit Aß42 fibrillation.[82,157] To examine the exact origin of the capacity of ATP to prevent fibrillation, it was compared to its free constituents, namely Adenine/Adenosine and STP, see Figure 26 a. It becomes apparent that inorganic STP has practically no effect over a broad range of concentrations, ruling out a Hofmeister-type interaction with the protein fragment.[149] On the contrary, both, salting-in and salting-out salts have shown to, if anything, increase aggregation of amyloid beta.[158] Adenosine, however, making up the other half of the ATP molecule, appears to have a very similar efficiency to prevent

fibrillation at similar concentrations to ATP, but runs out of solubility, before it reaches the levels of maximum effect (> 10 mM). Similarly, adenine is not soluble enough to even reach concentration levels, where an effect could be expected. SXS and sodium salicylate also exhibit a strong inhibitory effect similar to the observations of Patel et al.[82], although at significantly higher concentrations (> 100 mM), as is to be expected for classical hydrotropes. The mode of action is probably a solubilization of the Aß42, hence, the effective concentration range for hydrotropes overlaps with their surface activity behaviour and hydrophobic dye solubilization observed in Figure 21 b. SDS, a potent surfactant, prevents aggregation almost entirely already at 1 mM. This is even below its cmc, and a co-aggregation of SDS and amyloid peptides forming very small particles (but no fibres) has been proposed in the past as a potential mechanism.[159] Additionally, DLS experiments were conducted to measure the size of the formed aggregates, see Figure 26 b. Again, the addition of small quantities of adenosine or ATP (5 or 10 mM) effectively reduced the size of the measured particles in comparison to the control (PBS only). The reported particle sizes might not accurately represent the actual physical size of the fibres/aggregates, as DLS theory assumes spherical particles rather than oblong shapes. However, it has been shown in the past that DLS correlates well with the Thio T assay[160] and the relative size differences observed in our measurements are in good agreement with our fluorescent measurements. In conclusion, it becomes obvious that, while surfactants such as SDS can prevent fibrillation at very low and classical hydrotropes at high concentrations, adenosine and ATP fall in the middle and probably effect aggregation via a completely different mode of action: as ATP has been shown to not exhibit a classical hydrotropic behaviour (see above), and yet shows similar efficacy as adenosine, it can be postulated that the effect relies solely on the nucleobase moiety, as was suggested recently by Kurisaki et al.[161] The drawback of this compound, however, is adenosines' poor water solubility, which is compensated for by the addition of the triphosphate part to the molecule, making ATP a highly soluble adenosine derivative. The enhanced solubility then also leads to an enhanced anti-fibrillation performance at least one order of magnitude more effective than a classical hydrotrope, as seen in Figure 26. It has been suggested in the past that amyloid aggregation can be prohibited via π-π stacking interactions by suitable molecules with an emphasis on the presence of at least two aromatic

rings and a number of hydroxy-groups in near vicinity.[162–164] This would be the case for ATP and adenosine, which have a π-system that stretches over two rings as well as several ribose hydroxy groups close by. This might enable the compounds to intercept the aggregation of amyloid peptides by interfering with the π-stacking of certain amino acid side chains.[83,157,163,165,166]

3.4 Conclusion

The results give rise to the view that ATP is lacking any signs of a hydrotropic behavior in its traditional sense and is neither surface active nor "salting-in" for hydrophobic molecules. On the contrary, it even lowers the solubility of organic compounds in water. However, strong interactions between ATP and peptides/proteins were observed that manifested in a variety of effects (Td, aggregation, fibrillation). In conclusion, the increase in stability of proteins against denaturation, caused by ATP, is indeed a typical specific ion (Hofmeister) effect and not a classical hydrotropic (Neuberg) effect. Furthermore, the inhibition of fibrillation of intrinsically disordered proteins caused by ATP, is due to the specific interaction of adenosine with proteins and cannot be attributed, neither to a classical hydrotropic nor a Hofmeister effect. The triphosphate primarily serves to increase the solubility of adenosine.

A clear differentiation of the relevant interactions between ATP and organic molecules as well as proteins has implications far beyond pure semantics. It also shows the complexity and the subtlety of interactions in such biologically most relevant scenarios.

CHAPTER 4: PHOSPHORYLATED RESVERATROL AS A POTENT AGGREGATION SUPPRESSOR

4.1 Introduction

Protein aggregation plays an important role not only for medical reasons as in conformational diseases (proteopathy), but also for a variety of technical applications. Hence, compounds that can suppress misfolding and subsequent aggregation of proteins have a wide field of application[167,168].

In a simplified model, one can discriminate between three conceptually different types of aggregation: one that forms from native protein that has surpassed its solubility or is complexed by bridging ions (e.g. multivalent salts) to form loose aggregates, that can be re-dispersed by changing the solvent environment. The second type of aggregation is preceded by a denaturation step where the peptide-chain starts to unfold, exposing hydrophobic patches normally buried inside the protein[7176]. This will lead to a virtually irreversible aggregation, which is solidified by inter-molecular crosslinking (e.g. disulfide shuffling).[76] Further details on protein aggregation can be found in the introductory sections 0.2.1 & 0.2.3. Additionally, other non-native aggregation forms such as fibrillation are known. Here, proteins (often without well-defined native ternary structure) assume a beta-sheet rich conformation, that will eventually lead to the formation of fiber-like aggregates (cf. chapter 3). These amyloid-type fibers are associated with a variety of conformational diseases such as glaucoma, amyloidosis, Alzheimer's and Parkinson's disease.[20,21,169]

The compound examined in this paper is a phosphorylated derivative of trans-resveratrol, a well-known polyphenolic substance of natural origin. Trans-resveratrol has been reported in the past to potentially have positive effects on human health regarding obesity, diabetes, various forms of cancer, Alzheimer's and cardiovascular diseases besides others.[170] The underlying mechanisms are not entirely clear, but a variety of effects have been suggested in the past. As an anti-oxidant, trans-resveratrol is assumed to reduce oxidative stress in cells by radical-scavenging[171,172], but it was also shown that it can directly interact with gene expression.[173,174]

Concerning conformational diseases, the effect of trans-resveratrol is in part exerted by preventing the fibrillation of pathogenic proteins such as amyloid beta [175–177]. This effect is thought to be owed to π-π interactions[178], besides other binding modes relying on hydroxyl groups.[177]

The solubility of trans-resveratrol is, however, very low (≤300 µM with sonication)[179], making formulations that achieve high bioavailability very challenging.[180] To this end, a variety of delivery systems and derivatives (i.e. prodrugs) have been devised to approach this issue.[181] By introducing phosphate groups to the molecular structure through esterification of the hydroxy-groups, the compound becomes highly water soluble and can also exert specific ion effects. Hence, phosphorylated resveratrol (PR) can affect proteins (in-vitro and in-vivo) through the special interactions of its extended π-system, while potentially featuring a better (bio)availability. This interesting combination of properties has noticeable consequences on various proteins studied in this work, and affects mostly aggregation and fibrillation.

This chapter will be published as: "Phosphorylated resveratrol as a protein aggregation suppressor in-vitro and in-vivo (J. Mehringer, J. Navarro, D. Touraud, S. Schneuwly and W. Kunz, *RSC Chemical Biology*, 2022)". The in-vivo experiments were conducted by the author at the department of biology (University of Regensburg). Juan Navarro has contributed as an advisor and helped with experiment planning and the analysis of the reported in-vivo data.

4.2 Experimental

4.2.1 Chemicals

Chemicals – Thioflavine T and disperse red 13 (95%), were purchased from Sigma-Aldrich. The acetonitril (99.5%) was acquired from VWR Chemicals. The phosphorylated resveratrol (PR, 60-85%) was obtained from Ajinomoto OmniChem as a free sample and was marketed as "resveratrol triphosphate trisodium salt". The pH was adjusted using HCl (1 N, VWR Chemicals) and NaOH (1 N, Roth). Deionized water (Millipore quality) with a resistivity of 18 MΩ·cm was used. The fly food was prepared from formula 4-24 drosophila instant medium by Schlüter Biologie.

Polypeptides – Amyloid β protein fragment 1-42 (≥95%) and human insulin solution (BioXtra) were obtained from Sigma-Aldrich. Egg white was prepared from fresh chicken eggs bought in local supermarkets.

Histology – Rabbit anti-oligomer (A11) by Invitrogen, rabbit anti-amyloid fibrils OC (AB2286) by EMD Millipore Corp. and mouse anti-aβ 1-16 (6E10) by BioLegend were used as primary antibodies in combination with goat anti-mouse or anti-rabbit alexa flour 555 by Thermo Fisher as secondary antibodies for immunostaining. Specimen mounting was done using VECTASHIELD by Vector laboratories. Fly fixation was done using PFA (>95%) by Merck and Triton x 100 by Roth.

qPCR reagents – qPCR was performed using SYBR ORA qPCR green ROX by highQu, Quanti Tect Reverse Transcription Kit by Qiagen, DEPC water (≥97%) by Roth, 2-propanaol (100%) by VWR and TRIZOL (ambion) by life technologies. The primer RNAs used were ABpBACFW, ABpBACRV, 2xABFW, 2xABRV, RP49RTFw and RP49RTRv by Invitrogen (cf Table 4 for sequences).

4.2.2 Methods

Disperse Red 13 – Sample solutions were prepared in their respective concentrations in MilliQ. Then 2 mL of each solution were added to 10 mg of Disperse Red 13 and stirred in the dark for 24h. After that, the solutions were filtered by means of a 200 nm syringe filter and measured for absorbance at 503 nm using a Perkin Elmer Lambda 19 Spectrophotometer. Samples exceeding 1.5 absorbance were diluted accordingly. All measurements were done in duplicates and the results averaged.

Turbidity – Turbidity was measured at 488 nm by means of a photometer. For temperature scans, 20 mL of the sample solution was heated in a water bath at a constant rate of 1K/min. At appropriate temperature increments, a small volume was retrieved and subjected to absorbance/transmission measurement. All measurements were done in duplicates or triplicates and the results averaged.

Thioflavine T Assay (Amyloid) – The Thioflavine T assay was performed in black half area 96 well plates utilizing a nano M Multimode plate reader by Tecan. For this, 70 µL of sample (or background) was mixed with 10 µL of 0.11 mM Amyloid42 in 50/50 Acetontril/Water (or blank)

and incubated at room temperature for 1 h. Then 20 µL of 75 µM Thioflavine T solution was added, pipette-mixed and immediately submitted for fluorescence measurement (λ_{exc} = 450 nm, λ_{det} = 490 nm). All solutions were prepared in 10 mM PBS at pH 7.4. The fiber content is expressed as percentage in regards to control groups (negative = 0%, positive = 100%). All measurements were done in triplicates and the results averaged.

Insulin Aggregation and Fibrillation – Samples with appropriate RP concentrations were prepared in 10 mM PBS and the pH adjusted to 7.4. Then, a human insulin stock solution (10 mg/mL) was added to yield a final protein concentration of 2 mg/mL. Identical control samples (without protein) were prepared simultaneously and subjected to the same treatment. A total of 2 mL for each solution was transferred to GC vials and submerged in a water bath at 37°C. Magnetic stirrers inside the vials provided constant agitation (500 rpm). At appropriate time intervals, small aliquots (50 µL) were retrieved and transferred to a (half area) 96 well microplate. Then, absorbance was measured using a Tecan nano M multimode plate reader at 600 nm. After this, 25 µL of a Thio T solution (45 µM in PBS) was added to each vial, pipette-mixed and the fluorescence was measured (λ_{exc} = 450 nm, λ_{det} = 482 nm). All necessary background corrections were made and each sample was measured at least in triplicates and the results averaged.

HPLC – HPLC was performed on a Waters 717plus with a RP-18 column at 30°C. Detection was done photometrically at λ_{Det} = 310 nm by use of a Waters 2487 unit. HPLC-MS was carried out by the central analytics laboratory of the department of chemistry (University of Regensburg) using an Agilent Q-TOF 6540 UHD. The PR sample was dissolved in water/acetonitrile 98/2 at pH 7.0 in a concentration of 0.2 mg/mL.

Table 1: Gradient table for HPLC measurements of PR. Solvent A: 0.085% phosphoric acid (pH 2.5). Solvent B: acetonitrile.

Time [min]	%A	%B
0	98	2
25	79	21
50	79	21
51	60	40
60	60	40
61	98	2
70	98	2

Fly keeping and incubation – Fly stocks were kept in glass vials containing drosophila standard medium and stored in a humid incubator at 18°C, a relative humidity of 65% and a 12 hour light/dark cycle. In order to overexpress Aß, Aß40 and Aß42 fly stocks were obtained from the Bloomington Stock Center (numbers 64215 and 64216, respectively) and 2xAß42 as a kind gift from Sergio Casas-Tinto (UAS-Aß42(2x)). UAS-GFP lines (Bloomington Stock number 5431) served as a control group. The panneuronal Elav-GAL4 line (Bloomington Stock number 458) was combined with temperature sensitive GAL80 protein alleles under the control of a ubiquitous promoter (TubG80ts, Bloomington Stock number 7018) to suppress the expression of toxic amyloid proteins during drosophila development. Here, GAL80 binds to GAL4 and prevents GAL4-mediated transcription activation. At 18°C, the temperature-sensitive GAL80 protein is stable and active but becomes degraded and inactive at 29°C. The expression of the UAS-GAL4 system is repressed at 18°C, but will be reinstated once the flies are shifted to 29°C.[182]

Female virgins were crossed with various UAS lines and the hatched offspring was selected for the correct phenotype by visual inspection for genetic markers (cf. Table 2). The flies were transferred into new vials and split into two groups: normal food (nf) and food fortified with 480 µM of PR (PR). After breeding and hatching at 18°C, the adult flies were transferred to 29°C for an incubation period of 10 days. The flies were transferred into new food every 2-3 days on a fixed schedule. All experiments were carried out with males flies exclusively, except for qPCR

which was done with female flies only. The experiments were conducted several times with independent setups (2-3 replicates) running in parallel.

Table 2 List of performed crosses.

Virgin females	Males	Selected F1 Genotype
$Elav-\mathrm{GAL4};\ \frac{Tub\text{ - GAL80}^{ts}}{\mathrm{TM6B}}$	UAS-GFP (II)	$Elav-\mathrm{GAL4};\frac{\mathrm{UAS}-GFP}{+}\ ;\ \frac{Tub\text{ - GAL80}^{ts}}{+}$
$Elav-\mathrm{GAL4};\ \frac{Tub\text{ - GAL80}^{ts}}{\mathrm{TM6B}}$	UAS-AB^{1-40} /TM3	$Elav-\mathrm{GAL4}\ ;\ \frac{Tub\text{ - GAL80}^{ts}}{\text{UAS-}AB^{1-40}}$
$Elav-\mathrm{GAL4};\ \frac{Tub\text{ - GAL80}^{ts}}{\mathrm{TM6B}}$	UAS-AB^{1-42} /TM3	$Elav-\mathrm{GAL4}\ ;\ \frac{Tub\text{ - GAL80}^{ts}}{\text{UAS-}AB^{1-42}}$
$Elav-\mathrm{GAL4};\ \frac{Tub\text{ - GAL80}^{ts}}{\mathrm{TM6B}}$	2x UAS-AB^{1-42} /CyO	$Elav-\mathrm{GAL4};\frac{2\text{xUAS-}AB^{1-42}}{+}\ ;\ \frac{Tub\text{ - GAL80}^{ts}}{+}$

Fly negative geotaxis assay (climbing) – The locomotor ability was measured by transferring individual flies into clear, graduated plastic pipettes. For this, the flies were temporarily incapacitated with cold temperatures and allowed to recover for 1 h after transfer. By slightly tapping the pipette on a table surface, the flies were relocated to the bottom and prompted to immediately climb upwards (negative geotaxis behavior). A timer was set to 12 seconds and the maximum vertical distance covered was noted. 10 flies per genotype were measured 3 times. The experiments were conducted in a controlled environment (temperature, humidity, light).

Wholemount immunostaining – Aged (10 days at 29°C) flies were fixed in fixation buffer for 2 h at room temperature (4% PFA in 0.5% PBST, prepared freshly). After washing with PBS twice, the flies were dissected under the binocular and the brains washed thrice with 0.1% PBST. The primary antibody (1:100 in 0.5% PBST-10% NGS) was applied over night at 4°C. Then the brains were washed thrice with 0.1% PBST and the second antibody (1:80 in 0.5% PBST-10% NGS) was again applied at 4°C over night. All staining was conducted in the dark. After this, the brains were again washed thrice with 0.1% PBST and mounted onto confocal slides with vectashield, sealed with nail polish and stored in the dark at 4°C until used.

Confocal microscopy and image handling – All samples were scanned on a Leica TCS SP8 confocal microscopy and image acquisition settings were kept constant for every condition. The specimen were excited with a DPSS laser at 561 nm. The fluorescence signal was detected with a HC PL APO 40x/1.30 oil CS2 objective at 565 nm. Images were taken at a resolution of 1024 x 1024 pixels. The brains were scanned in z-stacks (1 µm per slice) resulting in 30-35 images per specimen. Subsequent analysis was carried out using the image processing software Fiji 2.0.0.[183] For this, the background was subtracted via the *rolling ball* method (radius = 50 pixels) and maximum projections of fifteen slices were made. The resulting image was again background subtracted and the contrast was adjusted to improve signal quality.

Fly-head Thio T assay – Male flies were fixed as described above. Then, exactly ten heads for each group were manually removed and transferred to exactly 100 µL of PBS in an Eppendorf snap-cap. The heads were homogenized thoroughly using a vortex-mixer. The snap-caps were centrifuged for 5 min at 2000 rpm to remove debris. The 95 µL were retrieved and transferred to a new tube. 505 µL of PBS was added and pipette-mixed. Then, for each group 6 wells of a half area black µclear 96-well plate were filled with 80 µL of solution and the absorbance at 280 nm was measured to adjust for protein content. Subsequently, 20 µL of Thio T stock solution (in PBS, target conc.: 15 µM) or PBS (for background correction) were added into three wells each and pipette mixed. Endpoint fluorescence was then measured ($\lambda_{exc.}$ = 450 nm, $\lambda_{det.}$ = 490 nm, fixed gain). The measurements were carried out on a Tecan Infinite M nano multi-mode plate reader. The triplicates were corrected for protein content and background and the results averaged.

qPCR – Female flies were frozen after incubation (10 days at 29°C) and kept at -80°C until needed. 20-30 frozen fly heads were removed mechanically using sieves. The heads were homogenized in 200 µL TRIZOL using a vortex-mixer. Then, TRIZOL was added to a total volume of 1 mL. Debris was removed by centrifugation at 12400 rpm for 10 min at 4°C. 200 µL of chloroform were added and thoroughly mixed. After centrifugation for 15 min at 12400 rpm (4°C), the aqueous supernatant was transferred to a new vial. Then, 0.5 mL of isopropanol was added and incubated for 10 min (at r.t.) to precipitate the RNA. Centrifugation for 10 min at

12400 rpm (4°C) yielded a pellet that was washed with 75% ethanol (in DEPC water). Subsequent centrifugation (5 min at 9800 rpm, 4°C) and air drying (37°C heat block) yielded a pellet that was redissolved in 30 µL DEPC water. The samples were then incubated for 10 min at 60°C. The RNA concentration and purity (RNA/DNA ratio) was determined using nanodrop measurements (Nanodrop 1000 by peQLab). Then the RNA samples were mixed with gDNA-wipeout buffer in the according concentrations and incubated for 2 min at 42°C. By mixing with a RT-PCR quantiscript master mix (RT buffer, reverse transcriptase, primer), the RNA was translated into cDNA by incubating at 42°C for 40 min and subsequent quenching with 95°C for 3 min. cDNA samples were diluted with Biopak water, mixed with SYBR green and primers (cf. Table 4) and transferred into the RT-PCR machine (CFX Connect by BIO RAD). Each reaction was composed of 0.5 µL cDNA, 5 µL SYBR green, 0.5 µL 10 µM primer fw, 0.5 µL 10 µM primer rv and 10 µL water. Samples were run with two different primers and a house keeping gene (RP49 for internal control) in triplicates according to the PCR program in Table 3.

Table 3 qPCR program used

Step/Repeats		Temperature	Duration
Pre-denaturation and activation of polymerase		95°C	2 min
Denaturation	40x	95°C	10 s
Annealing		60°C	10 s
Elongation		65°C	30 s

The results were analysed using the comparative C_T (threshold cycle) method. The ΔC_T value represents the difference between the C_T of the target gene and that of the housekeeping gene. Comparing the ΔC_T values of different sample groups (normal food and PR) yields the $\Delta\Delta C_T$ value which was used to calculate the final ratio as $2^{-\Delta\Delta CT}$. The mean ΔC_T value of all control (normal food) reactions for a given gene was used as a reference and the other values were referred to this for the final fold change. The qPCR experiments were carried out twice for every genotype with independent setups and the results were averaged.

Table 4 qPCR primers used in this work for Aß42 and 2xAß42 genotypes

Primer	Sequence
ABpBACFW	ATGGCCCAGTTCCTGCGCC
ABpBACRV	TGCACCTCGTAACCGC
2xABFW	ACAAACCGCAAGAAAACAAC
2xABRV	AGGCATGATTTATGACTCTGAC
RP49RTFw	GCATACAGGCCCAAGATCCGT
RP49RTRv	CAATCTCCTTGCGCTTCTTG

4.3 Results and Discussion

4.3.1 Phosphorylated resveratrol composition

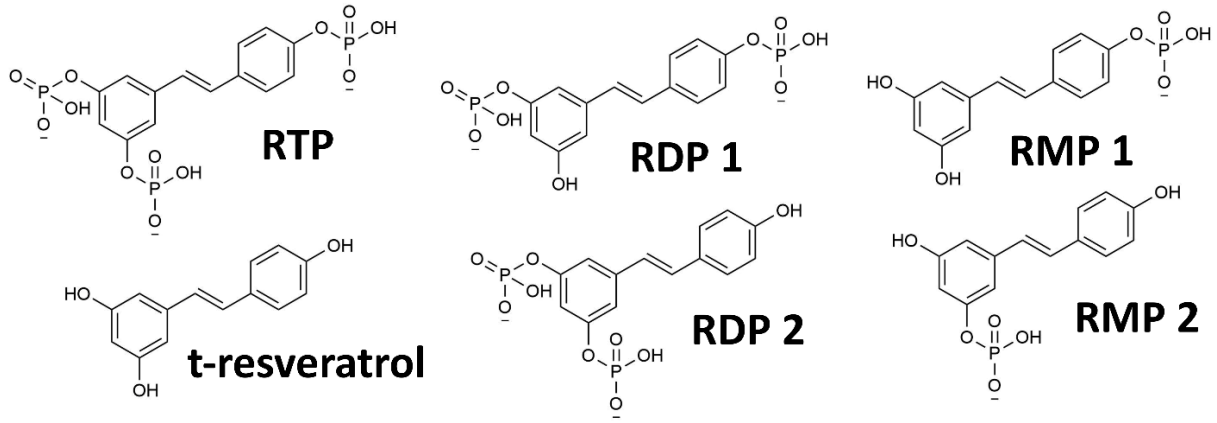

Figure 27 Molecular structures of various PR derivatives: RTP, RDP and RMP (both with two structural isomers denoted 1 and 2) and the parent compound trans-resveratrol.

PR (cf. Figure 27 for the molecular structures) as used in this study comes as a mixture of sodium salts. The actual composition can be found later in this section (Figure 30 b). As the phosphorylated resveratrol derivatives are very similar in size and solubility characteristics, separation and isolation in reasonable quantities would prove to be a difficult challenge (cf. Figure 28). For many experiments, this attempt would also be rendered futile, as PR is not stable in in-vivo conditions and will be hydrolyzed enzymatically to derivatives with a lower number of phosphate units (or free t-resveratrol) anyway.[184,185] Instead, the compound was treated as a mixture of chemically related substances, that, in essence, present a water-soluble form of t-resveratrol with potentially augmented characteristics.

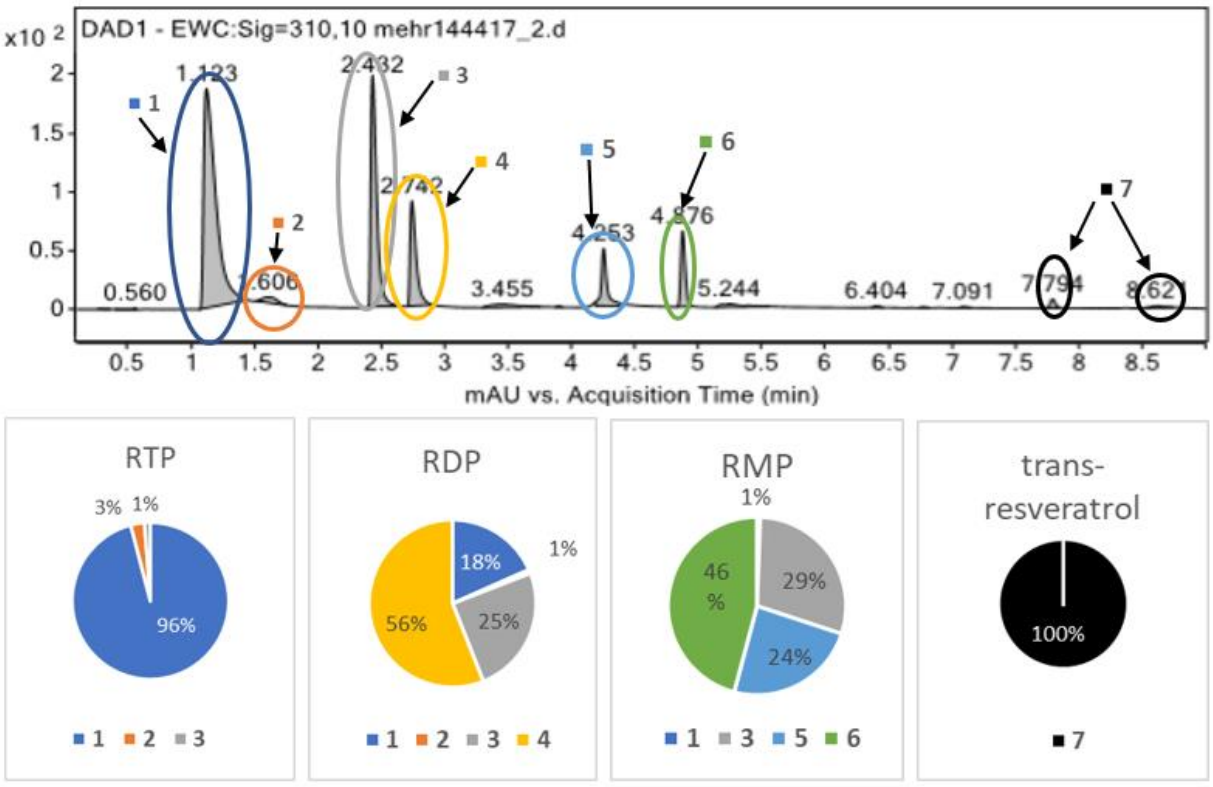

Figure 28 Chromatogram and LC-MS results for PR mixture. The pie charts depict the distribution of individual PR derivatives (determined by mass) across the 7 main peaks.

Using liquid chromatography in combination with mass spectroscopy, the actual composition of the PR mixture was analyzed. Expectedly, the mixture separated into rather distinctive peaks (see Figure 28, top picture) as was reported in a patent on this compound.[185] However, the peak assignment in the patent appears to be rather crude, as our mass spectroscopy data revealed a poor separation of different PR derivatives leading to mixed peaks. This can be seen in Figure 28, where the discrete mass signals for the derivatives of PR (namely RTP, RDP, RMP and trans-resveratrol) can be found not only in their designated main peaks but often also in preceding or trailing peaks. The compound RTP for example (identified by its distinctive mass) can be found mostly in the first peak, but also to a much lesser extent in the second and third peak. Similarly, RDP can be found mostly in two distinctive peaks (as was expected for the two structural isomers of RDP, cf. Figure 27), but also to a significant amount in the first RTP main peak. Pie-charts accompanying the chromatograms in Figure 28 give an impression of the distribution of each derivative across the peaks as determined by HPLC area. Taking the varying extinction

coefficients for different PR derivatives into account [186], no quantitative results can be gathered from LC measurements. However, it shows that different PR species appear to have a strong interaction with each other, making a separation with HPLC difficult and incomplete. This suggests that PR compounds can also have strong interactions with various other compounds, that share similar features (e.g. extended π-systems), which is important for potential mechanisms in in-vitro and in-vivo applications (see section 4.3.2).

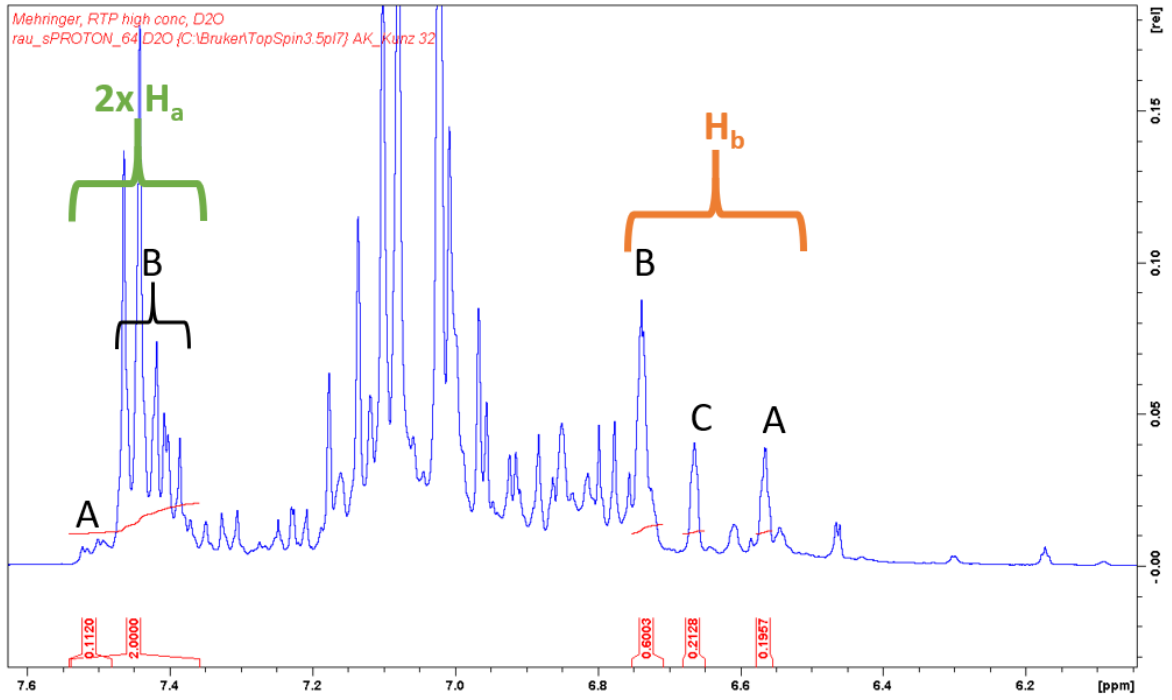

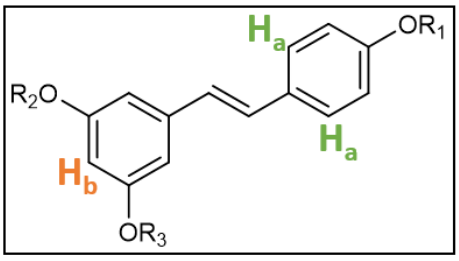

	H	Phosphate	H/Phosphate
NMR Peaks	A	B	C
R_1	5.6%	94.6%	
R_2 & R_3	19.3%	59.3%	21.3%

Figure 29 Proton NMR analysis of PR mixture. Relative integrals of distinctive protons yield the ratios of phosphorylated/unphosphorylated ester bonds.

In order to determine the composition of the PR mixture as well as identifying impurities, NMR measurements were conducted (Figure 29). The proton NMR was found to be relatively messy at first glance, but this can be explained by considering the mixture of PR derivatives present in the sample. The number of different permutations (number and position of phosphate groups)

inevitably leads to an overlay of NMR signals from various compounds that are shifted slightly up- or downfield. This makes correct peaks assignment almost impossible for most protons. However, two proton types (H_a and H_b) are conveniently located at either end of the spectrum and relate to positions in either ring (see Figure 29, bottom). Using the chemical shifts reported for pure compounds by Aleo et al.[186], the peaks and their integrals could be assigned to different PR subspecies, which allowed the calculation of phosphorylated/unphosphorylated hydroxy group ratios as shown in Figure 29. Using an internal standard, the molar purity in regards to resveratrol-bearing structures was calculated to be about 60% of what would have been expected for a pure product containing RTP exclusively.

a

Compound	Content
t-resveratrol	1.1%
RMP	19.4%
RDP	23.5%
RTP	56.1%
Total phosphorylation degree (calculated)	78.2%
Measured phosphorylation (^{31}P-NMR)	80.3%

b

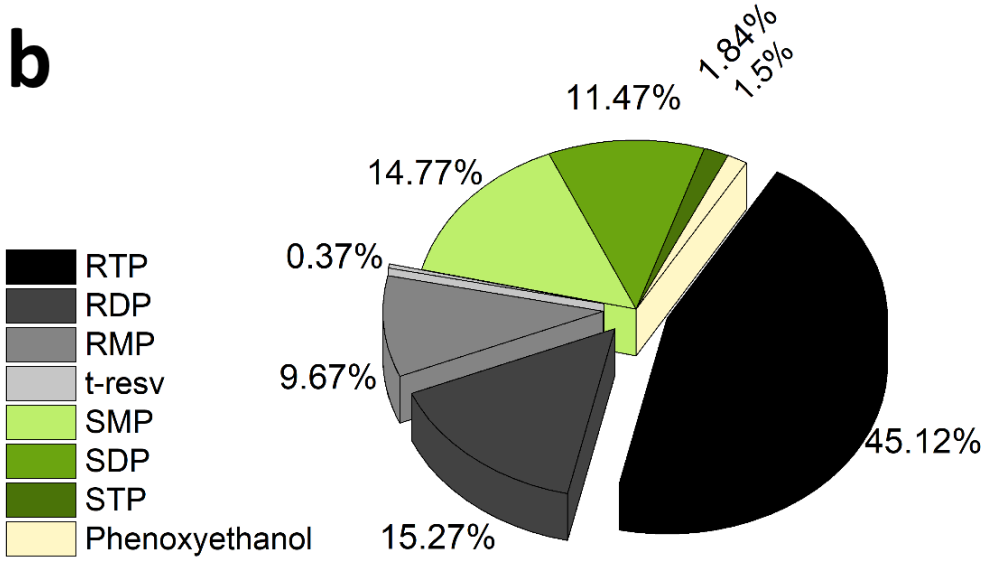

Figure 30 Composition of PR mixture. **a:** calculated composition of resveratrol-bearing derivatives based on the phosphorylated/unphosphorylated ester bond ratios in Figure 29. Below is the theoretical total degree of phosphorylation based on the calculated composition with the actual measured phosphorylation degree as per ^{31}P-NMR. **b:** Total composition of PR mixture including inorganic impurities and traces of phenoxyethanol in mass percent.

Using the ratios of phosphorylated ester bonds in Figure 29 as a basis, the percentages of t-resveratrol, RMP, RDP and RTP could be calculated and are given in Figure 30 a. Using these figures, the degree of total phosphorylation in regards to the resveratrol-bearing structures present can be calculated and amounts to approximately 78%. This is in good agreement with ^{31}P-NMR measurements that gave a phosphorylation degree of about 80 % (using an internal standard). This translates to an average of 2.4 phosphate units per resveratrol structure. As further impurities, proton NMR revealed traces of phenoxyethanol (as per manufacturer data sheet) and ^{31}P-NMR showed significant amounts of inorganic mono-, di- and traces of tri-phosphate. The total makeup of the compound mixture can be found in Figure 30 b in mass percent: Apart from the main compound RTP (45.1 wt%), di- or mono-phosphates (RDP, 15.3 wt%, RMP, 9.7 wt%) were detected as well, most probably the product from either hydrolysis or incomplete phosphorylation during the production. Additionally, small traces of free trans-resveratrol (0.4 wt%) were also found. This concludes to about 70 wt% purity in regards to PR which matches the manufacturers specification (60-85%).

4.3.2 Physicochemical effects

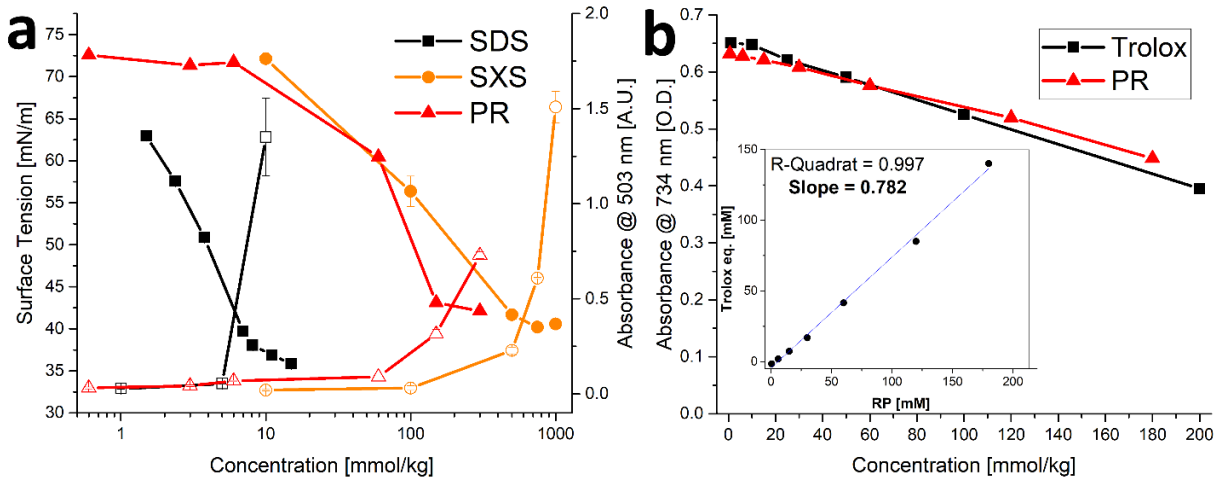

Figure 31 **a:** left axis: surface tension (filled symbols) and right axis: absorbance as measure of DR13 solubilization (hollow symbols) for SDS, SXS and PR. Error bars mean ± SD (N=2). Data for SDS and SXS are taken from Figure 21 **b:** Trolox anti-oxidant assay for trolox and PR. Error bars mean ± SD (N=2). Insert: Trolox equivalents of PR vs. PR concentration yielding the average trolox value as slope.

In order to examine the properties of the amphiphilic PR compounds, solubilization experiments were performed. It was found that relatively high concentrations of PR (> 100 mM) can solubilize the hydrophobic dye disperse red 13 (DR13), see Figure 31 a. This is normally only the case for surfactants (such as SDS) at low or hydrotropes (such as SXS) at high concentrations.[143] The significantly better performance of PR over the common hydrotrope SXS might be related to the similarities in molecular structure between the dye and RP. They both share a stilbene-type backbone, with the DR13 having an azo-group instead of a C-C double bond linking the two rings (cf. Figure 27). Therefore, specific π-π interactions can lead to complex formation making the dye somewhat soluble. This is often referred to as copigmentation.[187] It has been reported in the past that resveratrol can partake in copigmentation and thus contribute to the color of wine.[188] Hence, it is possible that the much more water-soluble phosphorylated derivative can likewise interact with compounds that share certain similarities and in this way facilitate the solubilization of minute yet measurable quantities of DR13. Further proof of this is the incomplete separation of PR compounds during HPLC, leaving mixed peaks that indicate strong interactions between the structural isomers and derivatives with varying phosphate content (see section 4.3.1). This is, however, not to be confused with general hydrotropic solubilization, even though π-π

interactions can play a secondary role for hydrotropes as well.[143] Furthermore, it can be assumed that decreasing phosphate content (RTP > RDP > RMP) will contribute significantly to a surface active behavior, as the salting-out characteristics of the phosphate headgroups will decrease, and the ratio of nonpolar surface/ionic headgroup will increase (cf. chapter 2). This is reflected by the surface tension measurements for PR, that show a significant decrease in surface tension at higher concentrations (Figure 31 a). Here, the minor compounds RDP and RMP will be present in significant enough amounts to exhibit a noticeable surface activity. This is likely to contribute significantly to the DR13 solubilization.

Trans-resveratrol is a known anti-oxidant[171,172], therefore, it was examined if and to what extent the phosphorylation affects this property. As can be seen in Figure 31 b, the trolox assay (using ABTS) was performed for PR yielding a trolox value of ≈ 0.78. This means that one molecule of PR is about 78% as effective as the reference anti-oxidant trolox. For trans-resveratrol, the literature reports a trolox value of approximately 0.33, albeit at a significantly lower concentration regime due to the limited solubility of trans-resveratrol.[189] We conclude therefore that the anti-oxidant capacity of PR is not affected by the phosphorylation. Instead, it was reported in the past that modification of the hydroxy-group to make it unavailable (e.g. by methylation) can help hinder the degradation of the resveratrol structure, particularly due to photochemical transformations.[190]

4.3.3 In-vitro effects

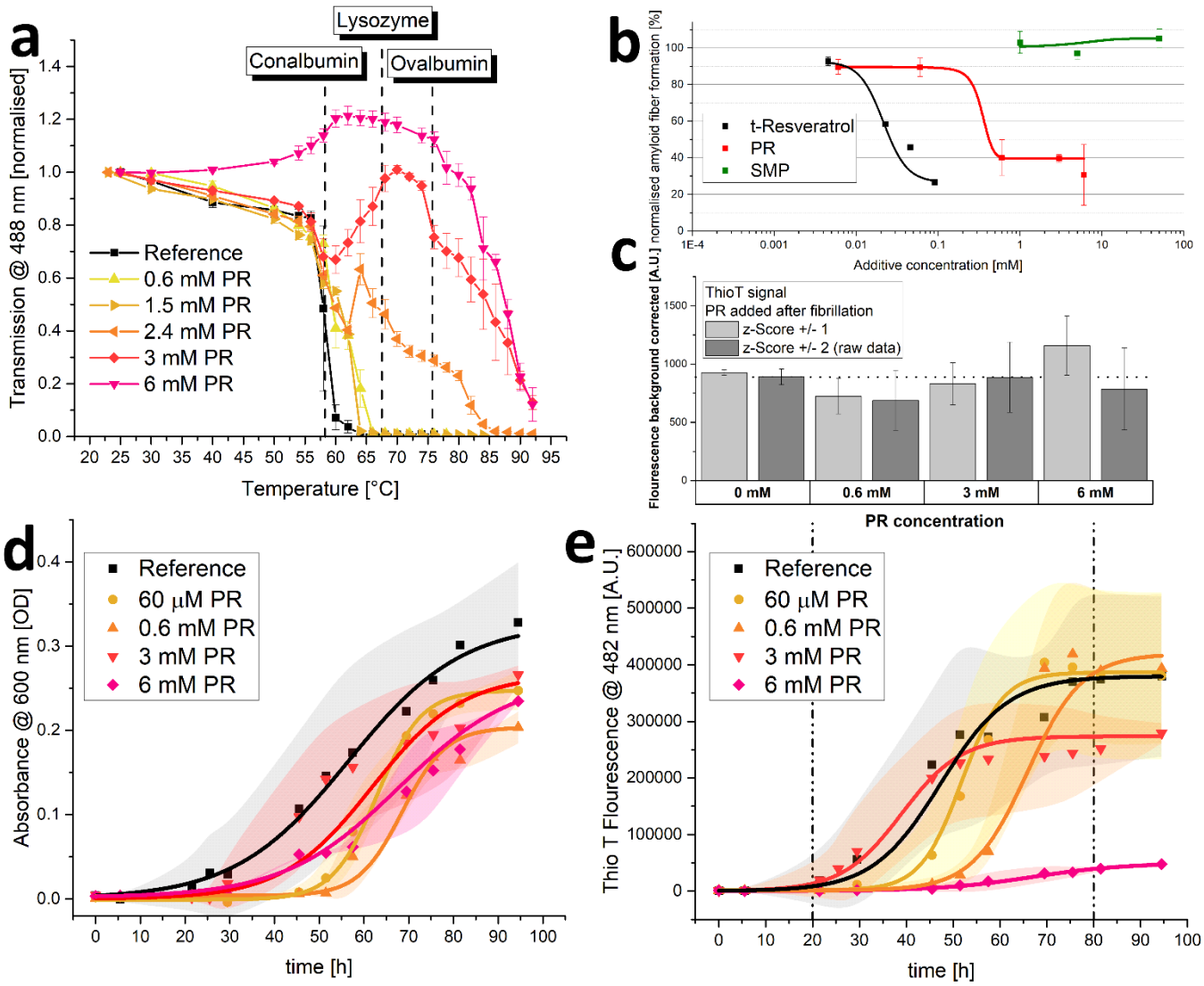

Figure 32 Biochemical effects of PR in-vitro. **a:** Turbidity of CCEW solutions (pH 7.4) with various PR concentrations as a function of temperature. Error bars mean ± SD (N=3). Indicated are the approximate denaturation temperatures of the main egg white fractions in CCEW as determined by DSC. **b:** Amyloid beta 42 fibrillation with various additives. Measured via Thio T staining and normalized according to reference (PBS only). Error bars mean ± SD (N=3). **c:** Thio T fluorescence of amyloid fiber-probe in presence of amyloid beta 42 with PR added after fibrillation to yield different concentrations. Data is represented as raw data (all points abide z-score ±2) and filtered data according to a z-score of ±1. Error bars mean ±SD (N = 3 for raw data). **d & e:** Insulin aggregation (**d**) and fibrillation (**e**) as measured by turbidity and Thio T fluorescence over time with various PR concentrations. Conditions were 2 mg/mL human insulin in 10 mM PBS (pH 7.4) at 37°C with constant agitation. Reference is in buffer only. The shaded areas represent ± SD (Reference: N=9, 60 µM, 0.6 mM & 6 mM: N=3, 3 mM: N=6).

In this section, the effects of PR on protein aggregation and fibrillation were examined. For this, solutions of diluted crude chicken egg white (CCEW) were heated and the subsequent denaturation followed by aggregation was monitored via turbidity measurements. As can be seen in Figure 32 a, increasing concentrations of PR lead to a reduction in turbidity and for 6 mM PR even increased the transmission up to 75°C until aggregation (presumably of more thermostable ovalbumin) set in. PR could apparently prevent the (partially) unfolded egg white proteins from sticking together to produce a large network, which is usually the principal cause for the observed turbidity.[92] While some limited effect on the aggregation is also observed for other ionic compounds (kosmotropic, chaotropic or hydrotropic), this behavior is very unusual and was not seen in this quantity or quality with a variety of other substances (see Figure 10).

Next, a specific subspecies of protein aggregation, namely fibrillation, was examined. During fibrillation, susceptible proteins undergo a transformation toward a beta-sheet-rich conformation which will in turn facilitate the aggregation into highly structured fibrils often called amyloid-like. The appearance of these aggregates is associated with a variety of neurodegenerative or conformational diseases such as amyloidosis, Alzheimer´s and Parkinson´s diseases.[20,21,169] The intrinsically disordered peptide amyloid beta 42 (Aß42) is known to be very prone to fibrillation and easily forms amyloid type fibers in aqueous environments. The amount of formed fibrillose material can be quantified using the highly specific fluorescent probe Thio T (cf. also section 3.3.2.3). As can be seen in Figure 32 b, the addition of PR can reduce the amount of formed fibers at concentrations below 1 mM. It was reported in the past that resveratrol is also effective in preventing the fibrillation of amyloidogenic peptides[176,177], which is also represented in Figure 32 b. Here, it appears that PR is actually less effective than trans-resveratrol, as it requires roughly ten times the concentration. It is likely that different PR derivatives have varying efficiencies in preventing fibrillation, including the possibility that some derivatives have little or no efficiency at all. In a previous work by Sciacca et al., the resveratrol monophosphate RMP 1 was shown to be very effective in preventing amyloid growth of human islet amyloid peptide, outperforming trans-resveratrol at small concentrations.[191] Assuming that resveratrol derivatives with a low degree of phosphorylation are predominantly responsible for

this effect, it does not come as a surprise that higher quantities of PR are necessary, as only about 20% of the PR is present in monophosphate form (RMP 1 & 2, cf. Figure 30 a).

It was reported in the past that some polyphenolic substances can intervene in fluorescence assays to detect amyloid fibers. Competitive binding with the dye can lead to false positive anti-aggregation activities and additional experiments to exclude this possibilities are advised.[192] Therefore, an Aß42 aggregation assay, akin to what was reported in Figure 32 b, was run in PBS buffer only. Then, after completion of aggregation, PR was added to yield a final concentration that matched the ones used in the actual assay. The results showed little effect of PR additive on the recorded fluorescence signal (see Figure 32 c), indicating no major interference with the assay. This also shows that the formed fibrils are stable and do not dissolve into non-fibrous material upon mixture with PR (with little to no incubation time), which would have resulted in significantly lower fluorescence signals.

Next, the aggregation of human insulin (HI) was examined. It was reported in the past that HI will aggregate and form amyloid-type fibers under a variety of conditions.[193,194] The experiment showed that at physiological conditions (pH 7.4, 37°C), HI will aggregate during constant agitation after an induction time of roughly 24 hours resulting in increasing turbidity of the solution (see Figure 32 d). Adding varying amounts of PR had only minor diminishing effects on the apparent aggregation. Further evaluation using Thio T fluorescence, however, revealed the effect of PR on fibrillation, as the amount of formed amyloid-type fibers are detected as opposed to the overall amount of aggregation (including amorphous aggregates) using turbidimetry only. As can be seen in Figure 32 e, the fibrillation principally follows a sigmoidal curve for all samples with an induction period of about 1 day and a plateau after 4-5 days, indicating an endpoint to the fibrillation. As can be expected[195], time resolved experiments are very prone to kinetic effects, resulting in broad standard deviations and the behavior during growth phase (indicated by broken lines) does not strictly correlate with the amount of PR added. However, the endpoint does depend on the PR content, yielding significantly lower fiber fluorescence signals for 3 mM and almost no fluorescence for 6 mM of PR. It should be noted that this experiment is conducted with a relatively high protein load of 2 mg/mL, which increases fibrillation (both, quantity and

kinetics).[193] It also requires higher additive concentrations to achieve additive/protein ratios necessary to inhibit the formation of fibers. While PR cannot prevent the aggregation of HI entirely, it can inhibit the fibrillation. This indicates that PR can steer the aggregation pathway away from amyloid-fibers and toward other, possibly amorphous aggregates. This effect was also previously reported for trans-resveratrol on human islet amyloid peptide.[177]

4.3.4 In-vivo effects

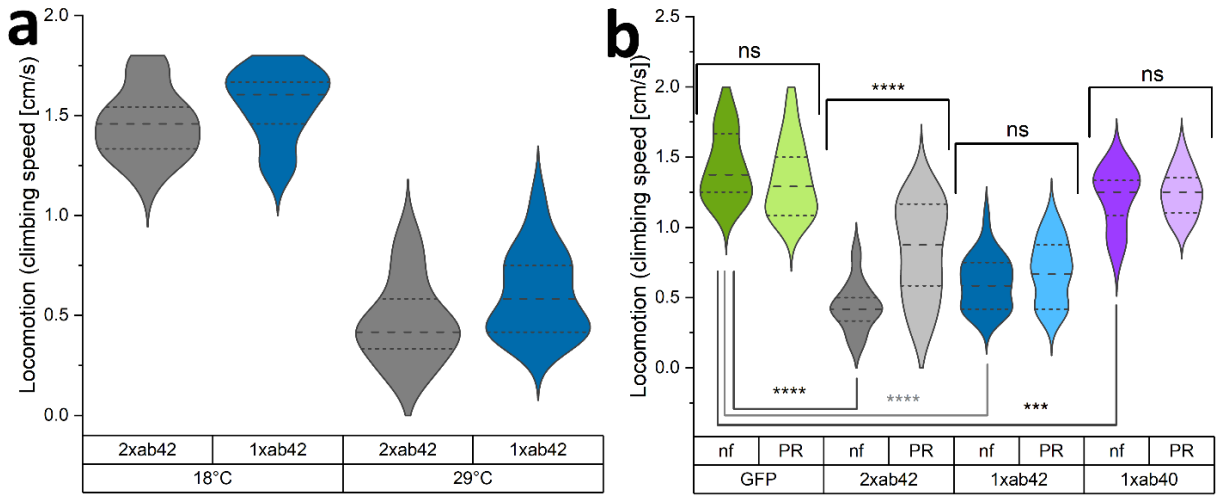

Figure 33 **a:** Locomotor data (climbing speed) for amyloid flies kept at 18°C or 29°C for 10 days (N=18). **b:** climbing speed for various genotypes after 10 days at 29°C (N=24-30). nf groups have been fed with normal food, PR groups have been fed with PR spiked (480 µM) fly food during development and aging.

The in-vivo capabilities of PR were examined by using drosophila melanogaster as a model organism. To this effect, genetically modified flies were used to simulate Alzheimer´s type amyloid overexpression and pathological protein build-up.[196,197] Two different fly strains were used to provoke Alzheimer´s disease phenotypes, carrying either one or two copies of the Aß42 mutant transgene (1xAß42, 2xAß42). As controls, genotypes with an overexpression of an innocuous protein such as green fluorescent protein (GFP) and the overexpression of the wildtype Aß (1xAß40) were included. As Aß42 expression strongly impairs fly development, a temperature sensitive inhibitor gene (TubG80ts) was deployed to allow a healthy development from larvae to fully hatched flies. Figure 33 a shows the effect of temperature incubation in 10-day-old flies when the expression of Aß is blocked at 18°C and when it is promoted at 29°C. At the lower temperature, the inhibitor gene is activated and suppresses the expression of Aß42.

This results in agile and healthy flies that exhibit normal climbing speeds (cf. GFP flies at 29°C in Figure 33 b). Transgenic Aß flies that were incubated at 29°C on the other hand exhibited severe locomotive impairment, with a reduction of around 60% in their climbing speeds. To see if the PR-supplementation can counteract the neurological manifestations of Aß42 overexpression, flies were bred and incubated (at 29°C for 10 days) in fly food that was spiked with 480 µM of PR versus a control group in normal food (nf). The results for various genotypes can be seen in Figure 33 b: here, GFP flies served as a "genetically healthy" reference setting the climbing speed benchmark. While the locomotive impairment is substantial for 1xAß42 and 2xAß42 genotypes, Aß40 flies exhibited only a slight reduction in agility, as this amyloid subtype is less aggregation-prone and neurotoxic.[198,199] Importantly, for the most affected 2xAß42 flies a significant difference among the food groups was detected: For this genotype a notable conservation of locomotor abilities was observed in the PR fed group, suggesting a physiological effect of the additive. To investigate this further, histological brain examinations were carried out.

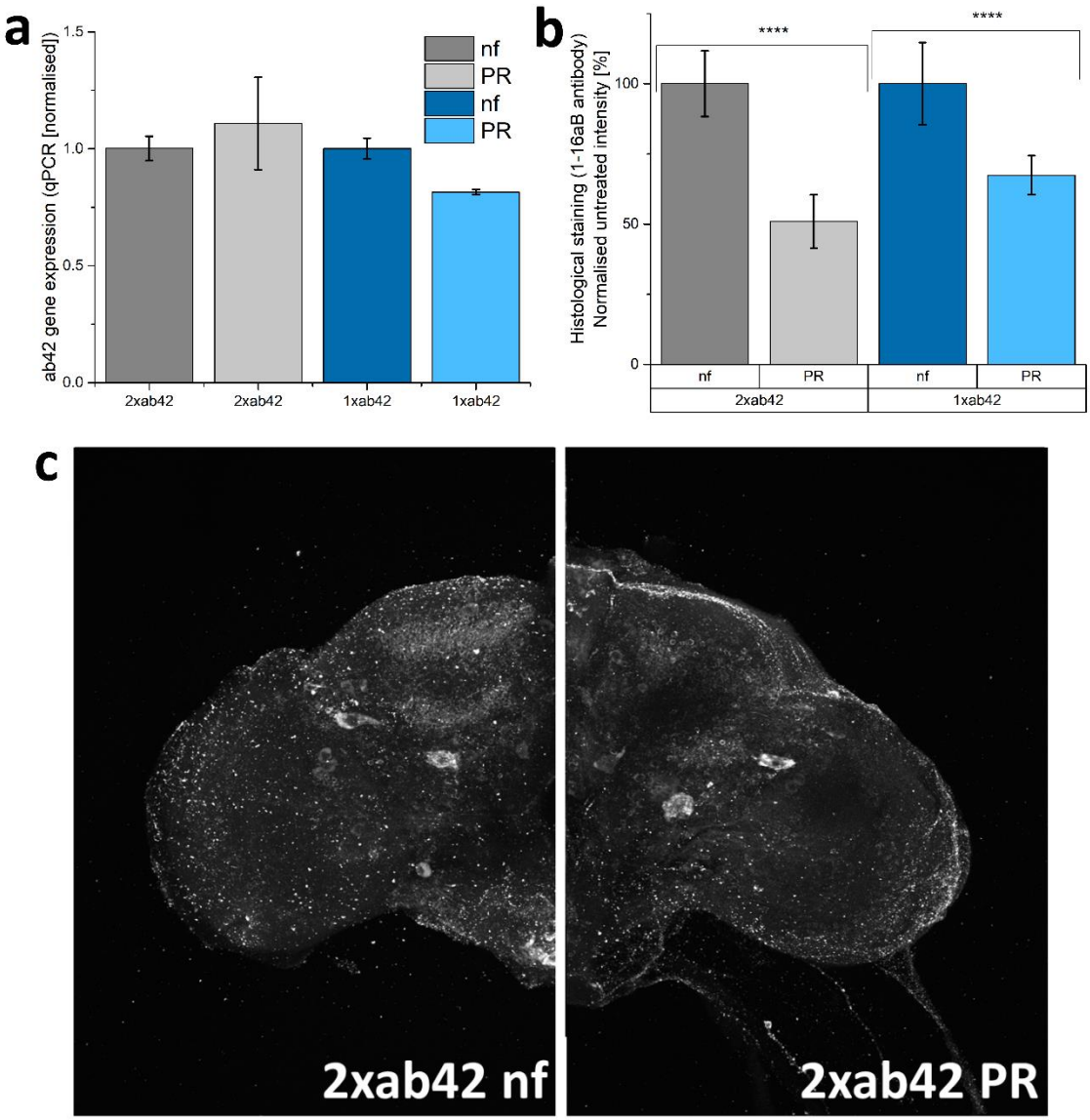

Figure 34 **a:** Aß42 gene expression as measured by qPCR. Data was collected in two independent experiment and qPCR runs and the results averaged. **b:** Integrated density of the fluorescence signal for a sequence specific Aß42-antibody (1-16ab). For each group 10-12 brains were analysed using confocal microscopy. The brains for each group were gathered in 4 independent experiments. **c:** Confocal microscopy pictures (max. intensity projection) of drosophila brains exemplifying the difference in sequence specific antibody binding between the two food groups.

In order to see the correlation of physical fitness and supplementation with PR, the amount of Aß42 inside the fly brain needs to be quantified. As this is also a function of gene expression, the effect of PR on the amount of Aß42-RNA was investigated using qPCR. Figure 34 a shows relatively uniform RNA levels for both food groups, giving no indication for a gene-regulating effect. Next, the influence of PR on the accumulation of Aß42 protein in the fly brains was

investigated by confocal microscopy. For this, dissections were performed with subsequent whole-mount immunostaining using a sequence specific amyloid-antibody. The results in Figure 34 b reveal a clear reduction in Aß42 levels, for both genotypes examined (1x Aß42 & 2xAß42). The confocal microscopy images in Figure 34 c are representative for nf and PR food groups. The detected signal, however, does not differentiate between Aß42 conformers (fibre, oligomer, amorphous), which are known to vary greatly in neurotoxicity.[200] Therefore, aggregation specific antibodies were deployed next to further investigate the effect of PR.

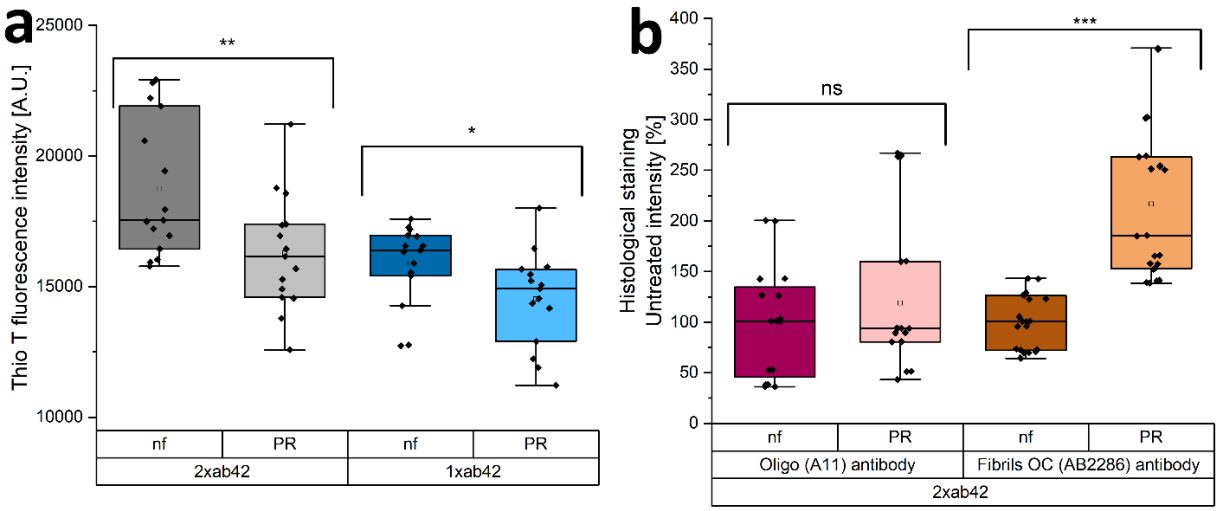

Figure 35 **a:** Thio T fluorescence of homogenized fly-head extracts. The box plot shows data gathered in 5 separate experiments (N=5x10). **b:** Integrated density of the fluorescence signal for aggregation-specific Aß42-antibodies (oligomer & fiber). The data was gathered in 3 separate experiments. For each group at least 5 brains were analysed using confocal microscopy (N=3x5-7).

For this, homogenized fly head extracts were measured with the fluorescent Thio T dye (cf. previous section). As can be seen in Figure 35 a, the strength of the fluorescent signal was dependent on both, the amount of Aß42 gene copies as well as the food group. It showed that samples prepared from PR fed flies exhibited a significantly lower Thio T fluorescence, indicating a reduced amount of amyloid fibres.[201] In additional experiments, whole-mount immunostaining with aggregation specific antibodies was used to elucidate the aggregation state for 2xAß42 genotype flies (see Figure 35 b). The staining with the oligo-specific antibody (A11) exhibited no statistically significant difference across the two food groups. The signal, however, was much weaker than for the sequence specific antibody, resulting in an overall poor signal-to-noise ratio. For the fiber-specific immunostaining, a much stronger signal was detected. Here, the PR food

group specimen showed a significantly increased fluorescence. A previous study on drosophila Aß42 models related higher fiber content with better physical fitness, as this appears to be the less neurotoxic morphology compared to oligomers or pre-fibrillar states.[202] While this appears to disagree with the Thio T results (see Figure 35 a), one must take into account that according to the manufacturer, the deployed antibody (AB2286) does not exclusively bind to fibrils but also to a lesser extent to Aß42 monomers. On top of this, fibril OC antibodies were found to be rather selective for specific fiber polymorphisms revealing varying binding affinities.[203] Hence it is likely that antibody and Thio T results cannot be compared directly.

While the exact mechanism remains unclear, the reduced amounts of Aß42 protein (Figure 34 b) could be related to a modulating effect on aggregation morphology (Figure 35) and an improved peptide clearance.[199,202] Both would result in a reduced neurotoxicity, explaining the improved locomotive abilities (Figure 33 b) for PR supplemented flies.

4.4 Conclusion

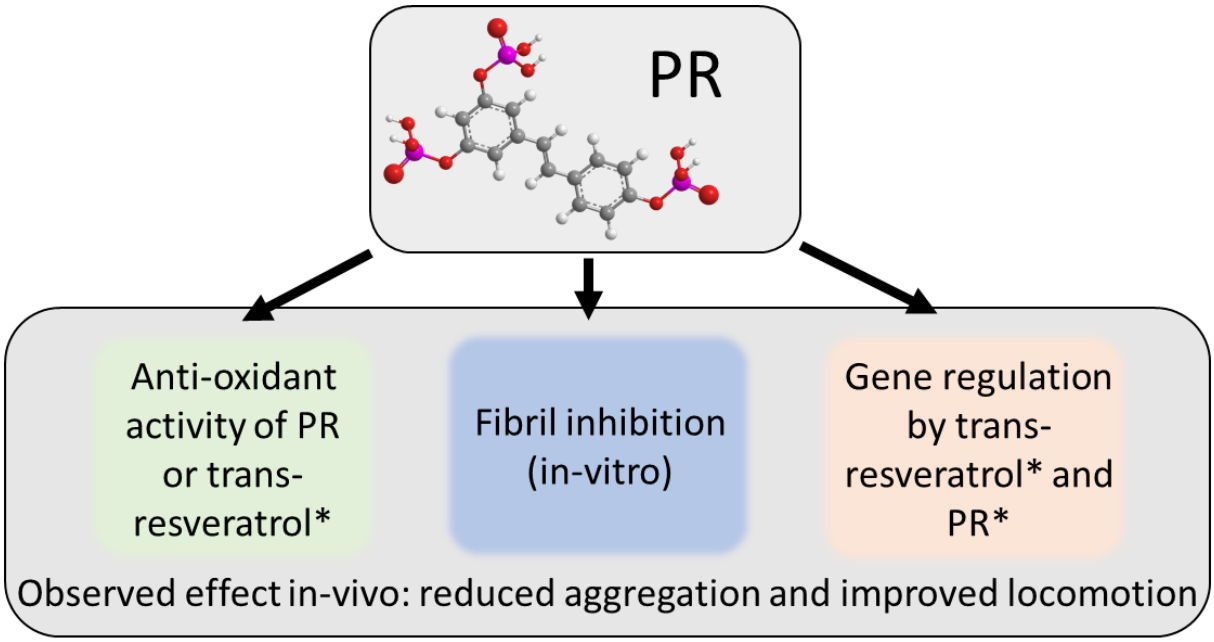

Figure 36 Scheme summarizing various mechanistic pathways of PR as a direct active or potential prodrug for in-vivo formation of trans-resveratrol. Aspects marked with an asterisk were not the subject of this publication but can be found elsewhere in the works cited in this section.

The PR compounds are an interesting set of molecules that show a variety of effects that have their roots in multiple pathways (see Figure 36). As it became apparent in Figure 31 b, PR retains the anti-oxidant behavior known for the free t-resveratrol compound. A previous dietary study with RTP showed a significant reduction of oxidative stress in-vivo.[204] This was , in part, also attributed to gene regulatory effects of RTP. A property that has also been reported for t-resveratrol.[173,174] Besides this, PR also exhibited potent anti-fibrillation characteristics in-vitro (cf. Figure 32), which potentially relies on π-π interactions as reported for t-resveratrol.[178] This property also extended into in-vivo experiments using drosophila as a model organism (see section 4.3.4). Here, the aggregation of Aß42 could be significantly reduced, resulting in better locomotor abilities suggesting a neuroprotective effect. Similar results showing a clear correlation between in-vitro experiments and in-vivo drosophila models of Aß42 were reported in the past for compounds such as curcumin and doxycycline.[199,202]

It was suggested previously that PR has an improved bioavailability over t-resveratrol due to its much higher water-solubility.[170] Aleo et al., however, also reported different biological activities

for various PR derivatives, which might be connected to different membrane interaction characteristics.[186,205] This unresolved discussion was circumvented by deploying a whole host of different PR compounds at once, but could and should be the target of a future inquiry. This way, PR could also be considered as a potential prodrug for individual degradation products (cf. Figure 27), as phosphate groups are gradually cleaved off in-vivo.

The author is aware that PR derivatives might qualify as pan-assay interference compounds (PAINS), as is the case for t-resveratrol.[206,207] While an adverse effect on some assays cannot be excluded, the wealth of previously reported data and the results of this work justify a genuine optimism regarding the present findings. In particular the indirect effects of nutritionally supplemented PR on physiological changes as detected in in-vivo experiments will be difficult to invalidate with known interference patterns of PAINS.

In conclusion, PR could prevent the aggregation of CCEW and the fibrillation of Aß42 and insulin in-vitro. Additional drosophila fly models also exhibited significant effects, leading to reduced Aß42 aggregation in-vivo and improved locomotion behaviour (neuroprotection).

CHAPTER 5: PHOSPHATE FREE DISH WASHER FORMULATION - SUBSTITUTION OF HEDP

5.1 Introduction

The deposition of calcium and magnesium carbonates ("scaling") as well as organic matter ("fouling") in industrial and domestic applications (e.g. dishwashers) still poses a remarkable challenge. While modern high-capacity builders (such as polycarboxlyates) and crystal growth inhibitors can tackle scaling issues when using hard feedwater[208,209], fouling is currently mostly suppressed by the use of phosphonate additives such as HEDP. These small, usually non-polymer based compounds can reduce the amount of organic deposits on glass- and tableware during dishwashing cycles which would otherwise often lead to irreversible staining. As these products are deployed all over the world in large quantities, the increased release of phosphor-containing wastewater has proved to be a challenge for the environment in general and sewage treatment plants in particular. This process is often referred to as eutrophication, and as a result, phosphate-free alternatives that can replace the conventional additives are a sought-after commodity.[210,211]

Even though they were listed as two separated phenomena, scaling and fouling are actually closely interrelated. Hard ions will not only form inorganic deposits on glass- and tableware ("filming") besides reducing the effectiveness of detergents, but also lead to additional "spotting" by insoluble proteinaceous soil complexes. Sequestering hard ions via the usage of builders will effectively curb filming issues, and the use of deposition inhibitors will slow down or contain the growth of crystalline precipitates also known as "threshold effect". Organic spotting, however, can still occur even in softened water. Therefore, soil dispersing agents are necessary. It becomes apparent that compounds typically used to soften feedwater can sometimes also effectively reduce the deposition of organic residues that are suspended in the aqueous phase.[210,212] Such compounds (e.g. phosphates/phosphonates, citrate, low molecular polycarboxylates) are usually of the kosmotropic variety, meaning they carry strongly hydrated moieties. According to the implications of specific ion effects, kosmotropes generally affect

protein solubility and stability, as well as the solubility of hydrocarbons.[5,26,119] In the context of nucleation and crystallization, it was shown that kosmotropic compounds can suppress aggregation (of calcium carbonate) and lead to more soluble pre-nucleation clusters (exclusion and threshold effect).[132]

In this work the focus is set on the prevention of (re-)deposition of mostly organic (proteinaceous) matter on surfaces in dishwashing applications by use of phosphate-free agents. For this, model systems were deployed utilizing genuine dishwashing liquor with a protein rich solid content load ("KS Dirt").

5.2 Experimental

5.2.1 Chemicals

1,2,3,4,5,6- Cyclohexane-hexacarboxylic acid – monohydrate (CHC) (>97.0%) was purchased from TCI. Dextran sulfate (MW: 4000 Da), etidronic acid monohydrate (HEDP) (≥95.0%), sodium poly acrylic acid (SPAA, MW: ≈2100 Da), sodium alginate, calcium chloride dihydrate and magnesium chloride hexahydrate were acquired from Sigma Aldrich. Citric acid monohydrate (p.a.) was supplied by Merck. The KS-Dirt and the Trilon M was both supplied by the BASF SE. The pH was adjusted using 1M NaOH by Roth and 1M HCl by VWR Chemicals. All chemicals were used without further purification. Aqueous solutions were prepared using deionized water (MilliQ) with a resistivity of 18 MΩcm.

5.2.2 Methods

QCM – Quartz chips microscale measurements were conducted on an Omega Auto by Q-sense. The fouling experiments were carried out on gold and silica quartz chips at 55°C and pH 9. At first the chips were primed for 30 min with MilliQ (pH 9). Then, a fouling step was carried out using a 1000 ppm KS-Dirt solution in either MilliQ or 21°dH + 160 ppm Tri M solvent (optionally including various additives) for 30 min with an additional rinsing step with MilliQ (pH 9) for another 30 min. The flow rates for each step were 20 µL/min.

XPS – X-ray photoelectron spectroscopy (XPS) analysis was carried out by a technician at the BASF SE research facility in Ludwigshafen, Germany on my behalf.

Glass-slide fouling – To measure the fouling and subsequent hazing of glass slides, 1000 ppm KS-Dirt solutions were prepared in either MilliQ or 21°dH + 160 ppm Tri M solvent (optionally including various additives) and the pH adjusted at 60°C (pH 9, if not stated otherwise). Then, two clean glass slides (duplicates) were submerged into the stirred KS-Dirt solution (500 rpm, 60°C). After exactly 30 minutes the slides were retrieved and immediately transferred into a beaker with stirred MilliQ water for rinsing. Again, after 30 min the slides were removed from the water, excess liquid wicked off (without touching the slide faces) and air-dried. Then, the slides were analyzed on a conventional office flatbed scanner against a matte black background. Using a photo-analyzer software (Fiji ImageJ), a region of interest (ROI) well within the submerged slide surfaces was selected and the mean gray value was calculated. This result was corrected for the value measured for clean glass slides (background correction). Negative mean gray values are an artefact of the background correction and can best be interpreted as *zero mean gray value [corrected]*. The results for each set of duplicates were averaged and the standard deviation was calculated. For some experiments, slides were subjected to repeated fouling an rinsing cycles (up to three).

Transmission – The transparency of the KS-Dirt solutions that were used for the glass-slide fouling tests were measured by means of a photometer. For this, the transmission at 488 nm was recorded and the background (100% transmission) was set for MilliQ water.

Zeta-Potential – The surface charge of suspended KS-Dirt particles was determined using a Zetasizer by Malvern. Sample solutions were prepared according to the method described in the glass-slide fouling section. Then a small quantity was transferred into a DTS70 cuvette and the surface potential was measured. Samples were prepared in duplicates and measured at least three times each. The results were averaged and the standard deviation was calculated.

5.3 Results and Discussion

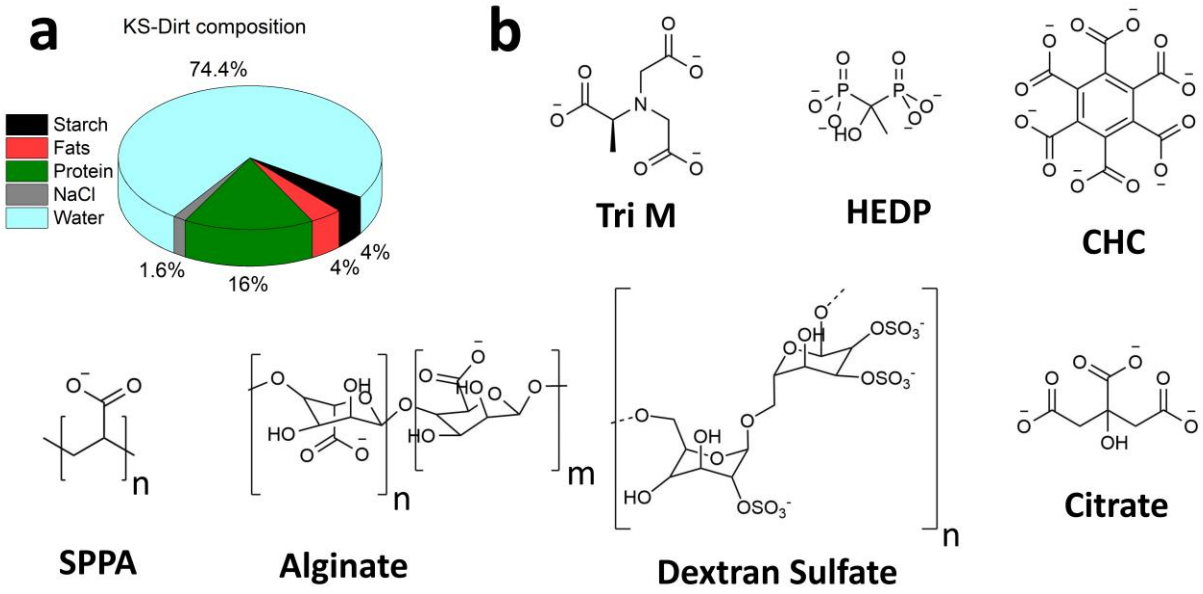

Figure 37 **a:** Composition of KS-Dirt used for fouling and deposition experiments. Constituents are expressed as mass-volume. **b:** Molecular structures of compounds and additives used in this study depicted in ionic form.

In the following, a variety of experiments was conducted to examine the fouling of proteinaceous material onto surfaces ("spotting") akin to what can be observed during a washing cycle in a conventional household dishwasher. For this, a blend of materials was used as a model dishwasher fluid termed "KS-Dirt" ("KS" means "Klarspüler", referring to the rinsing program in automatic dishwashers). The makeup for this suspension can be found in Figure 37 a. The majority of the solid content is proteinaceous (ca. 63 %) in nature with a small admixture of fats (ca. 15%) and other constituents (salt and starch; ca. 22%). To examine the effect of anti-fouling additives, a variety of compounds have been tested in this study (Figure 37 b). If not explicitly stated otherwise, hard-water (21°dH) as solvent usually contained a fixed amount of 160 ppm Trilon M (Tri M) as a standard water softener as is found in conventional dishwasher detergent formulations. The compounds used in this study (CHC, dextran sulfate, citrate and, to a smaller extent, alginate, SPAA) were compared against HEDP, which is a current industry standard anti-fouling additive. At the pH values where the experiments were conducted (pH 9 & 11), all additives are present in ionic, deprotonated form (cf. Figure 37 b). CHC has been proposed in

the past as a promising phosphate-free anti-scaling agent[213], but due to its profound kosmotropic character, could also function as a potential anti-fouling additive. Similarly, the high charge density of dextran sulfate or alginate might render these compounds a viable alternative, as they share certain similarities with polymeric builders.[209,214] Additionally, citrate was considered in some experiments as it has been used as a phosphate free builder in the past.[210,215]

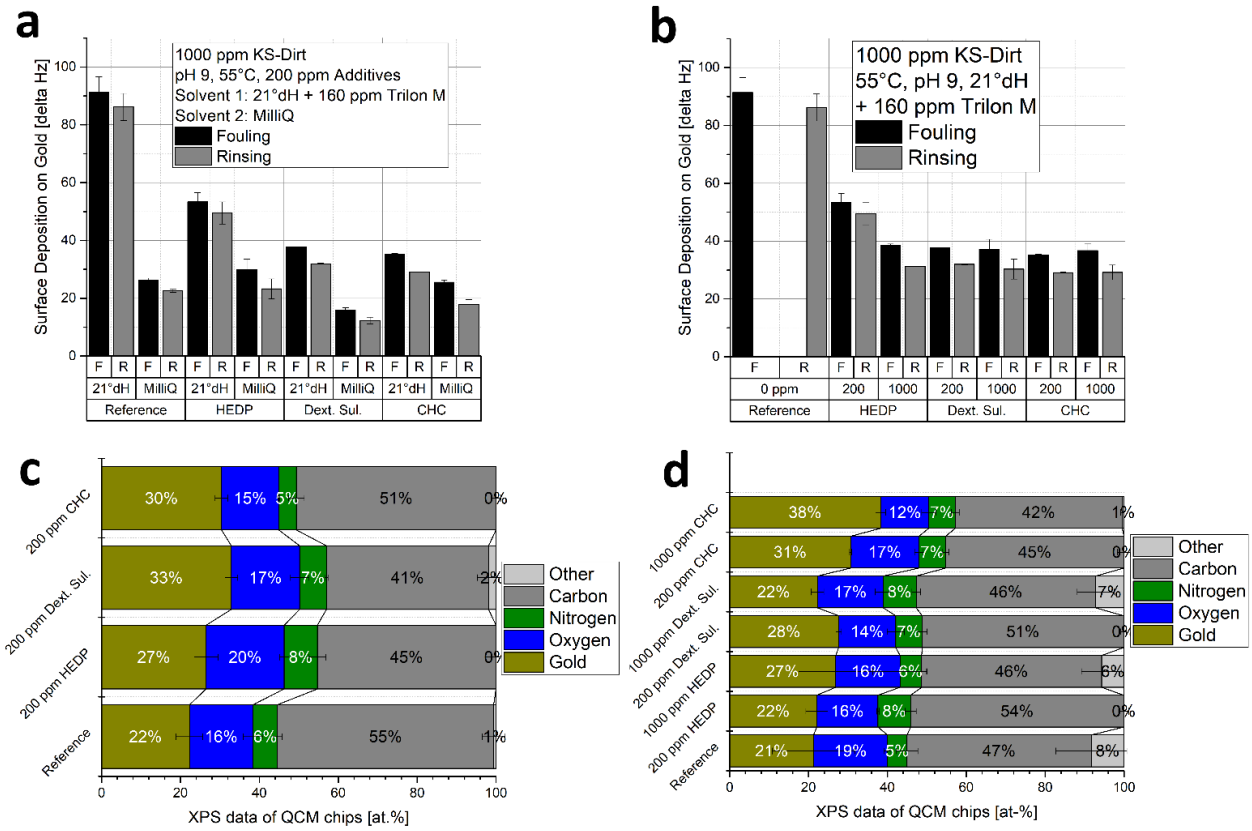

e

Additive	Gold (substrate)	Proteinacous Organics	Residual Organics	Other
	[atomic %]			
21°dH + 160 ppm Trilon M – Reference	21.3	28.5	41.9	8.3
21°dH + 160 ppm Trilon M – 200 ppm HEDP	22.1	47.31	30.49	0.1
21°dH + 160 ppm Trilon M – 1000 ppm HEDP	26.9	31.35	36.05	5.7
21°dH + 160 ppm Trilon M – 200 ppm Dext. Sul.	27.7	38.19	34.21	0
21°dH + 160 ppm Trilon M – 1000 ppm Dext. Sul.	22.3	47.88	22.62	7.2
21°dH + 160 ppm Trilon M – 200 ppm CHC	30.7	38.76	30.54	0
21°dH + 160 ppm Trilon M – 1000 ppm CHC	38.3	38.19	23.01	0.5
MilliQ – Reference	22.3	35.34	41.76	0.6
MilliQ – 200 ppm HEDP	26.5	47.88	25.62	0
MilliQ – 200 ppm Dext. Sul.	32.9	38.76	26.44	1.9
MilliQ – 200 ppm CHC	30.4	25.65	43.95	0

Figure 38 QCM and XPS data for KS-dirt fouling experiments. **a:** Surface deposition of KS-Dirt in the presence of various additives in MilliQ and hard water. **b:** Effect of additive concentration on the surface deposition. **c & d:** Composition of the gold substrate surface by atomic percentage for different additives (**c**) and various additive concentrations (**d**). **e:** Crude calculation of the protein-content of surface deposits as measured in the QCM.

QCM experiments were conducted with KS-Dirt solutions under varying solvent conditions. Besides measurements in MilliQ water, solutions with a water hardness of 21°dH (+160 ppm TriM) as well as additive solutions that contained additional compounds were examined. On gold

chips (“substrate”) the experiments revealed a close correlation of water hardness with the amount of deposited material (Figure 38 a). Here, hard water led to four times as much fouling compared to MilliQ water. In all cases the deposition of material on the surface was final and a subsequent rinsing step (with MilliQ) appeared to remove only small amounts of presumably loose material. The addition of potential anti-fouling compounds to MilliQ based KS-Dirt solutions had little effect on the surface deposition and the results are similar to what was observed for KS-Dirt in MilliQ only. The only exception being dextran sulfate, for which at 200 ppm, a slightly lower surface deposition was observed. More importantly, however, was the effect of said additives on hard-water KS-Dirt solutions. Here, the fouling could be reduced considerably already at 200 ppm yielding a reduction in surface deposition of 40% for HEDP and about 60% for Dextran Sulfate and CHC (Figure 38 a). At 1000 ppm of additive content all tested additives reach this level, see Figure 38 b. A closer inspection of the examined gold substrates with XPS revealed the composition of the deposited material (see Figure 38 c - e). It becomes clear that all substrates treated with additives or MilliQ as solvent for the KS-Dirt exhibit a higher atomic percentage of gold on the surface. This can be interpreted as larger areas of uncovered surface, showing a protective effect against particle adsorption. While the QCM data showed much lower total deposition by weight, XPS showed that the surface coverage is very similar between the substrates treated with KS-Dirt in MilliQ and 21°dH + 160 ppm Tri M (No additives/references each; Figure 38 e). In systems without hard ions (MilliQ), additives still exhibited a positive effect. Here, the uncovered gold surfaces are larger and the effect of the additives ranks in the same order as what was observed in the QCM (HEDP < CHC < dextran sulfate). For samples with hard ions present, a larger content of additive led to larger uncovered areas (more exposed gold surface) for HEDP and CHC. For dextran sulfate, despite obvious effects in regards to total deposition by weight, 1000 ppm additive content led to less exposed gold surface than 200 ppm.

In general, differences in QCM and XPS data must be attributed to the nature of the deposited matter. For most samples with anti-fouling additives a reduction of adsorbed material of at least 50% in weight was observed in the QCM, while the uncovered surface grew larger by a much smaller amount. This means that covered areas must have either thinner or less dense layers of

deposited material, or a different composition of the material (e.g. rich or lean in protein). A percentage breakdown by elements allows a crude calculation of the protein content on the substrate surface (Figure 38 e). Surprisingly, the relative amount of proteinaceous matter adsorbed onto the gold surfaces is in almost all cases higher than the references (with the exception of 200 ppm CHC in MilliQ). While QCM revealed that clearly much less overall material was deposited, the anti-fouling additives were apparently more effective in preventing the adsorption of non-proteinaceous organics (fats and starch). A potential reason for this might be the presence of fatty acids stemming from hydrolysed fats (cf. Figure 37 a). In combination with free hard ions, these can form insoluble soap scum that will readily precipitate.[216] Competitive binding of hard ions with the anti-fouling additives might curb this trend effectively.

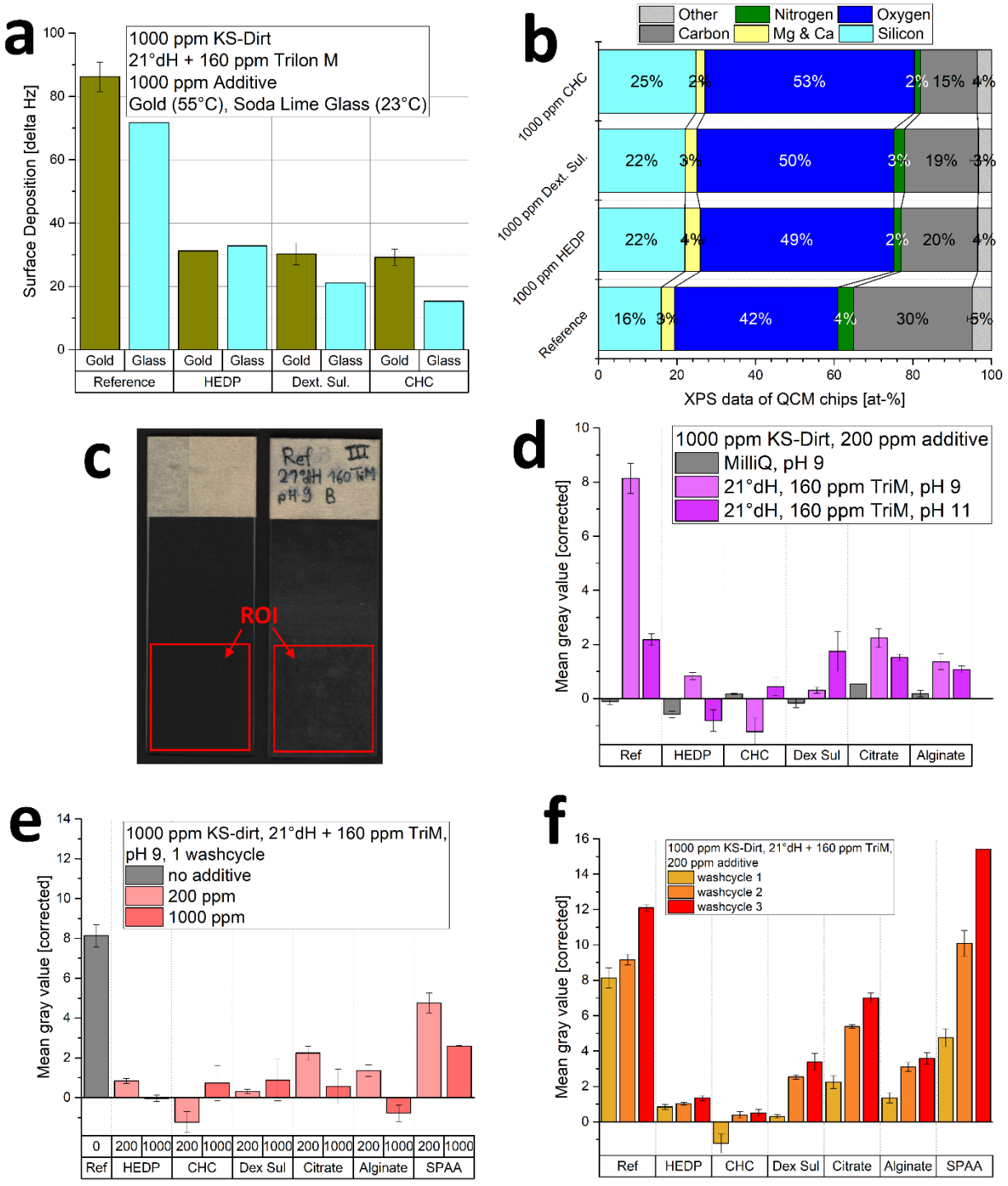

Figure 39 KS-Dirt fouling on glass surfaces. **a:** Comparison of glass and gold surfaces in QCM experiments, **b:** Surface composition of QCM glass chips, **c:** Examples of a clean and hazed glass slide with an approximate region of interest (ROI), **d:** Fouling on glass slides in various solution conditions (pH, hard ions, and additive presence), **e:** Additive concentration dependence of fouling on glass slides, **f:** Effect of repeated washing cycles on glass slide fouling in the presence of various additives.

Additional experiments were carried out to examine the fouling properties of KS-dirt solutions on glass substrates. Figure 39 a shows that in QCM experiments the general trend observed in the previous section for gold surfaces also holds true for glass substrates. Again, much lower dirt adsorption (by weight) was observed for additive solutions containing 1000 ppm of additive. Similarly, XPS data revealed that the non-covered surface, measured as atomic percentage of silicon, is larger, while the amount of carbon is significantly lower (Figure 39 b). To examine these effects further, clouding experiments of glass slides with KS-Dirt solutions were performed. The surface deposits could be seen clearly and were quantified after a rinsing step with MilliQ by determining the mean gray value of a selected ROI (Figure 39 c). For samples without additives, the clouding was dependent on water hardness and pH (Figure 39 d): While KS-Dirt in MilliQ water did not cause any hazing of the glass slides, at pH 9 a significant amount of material was deposited, leading to extensive clouding. At pH 11, the observed hazing was much lower. This was most probably due to the lower availability of free magnesium and calcium ions as they will be increasingly bound in suspended hydroxides particles at such high pH levels.[217] The addition of various additives (at 200 ppm), again led to much lower clouding of the glass slides at pH 9. Here, citrate and alginate showed a better effect at higher (1000 ppm) concentrations (Figure 39 e). At pH 11, dextran sulfate, citrate and to some extent alginate had little anti-deposition effect beyond what was observed for the reference, while HEDP and CHC were still effective (Figure 39 d). SPAA as a powerful (polymeric) sequestering agent was also examined, but it proved to be much less effective at 200 and 1000 ppm (Figure 39 e).

In Figure 39 f, the effect of repeated “washing cycles” on the clouding of the glass slides was examined. For this, a KS-Dirt solution in 21°dH + 160 ppm Tri M solvent was used. Expectedly, the reference without any additives had extensive hazing of the glass surface that grew more prominent with every cycle. HEDP and CHC showed a good protective effect across all washing cycles (at 200 ppm), while dextran sulfate lost some of its effect after the first cycle. Citrate and alginate showed only moderate anti deposition behaviour, that became worse after the first washing cycle (particularly for citrate). This is most likely related to the overall weaker effect of the latter additives at 200 ppm (cf. Figure 39 d). SPAA showed the worst anti-deposition behaviour, even surpassing the reference after three washing cycles. From visual inspection, it

appeared the SPAA was compromising the emulsion stability of the washing solution and led to a precipitation onto the glass slides that seemed “waxier” (fat containing) in nature.

In conclusion, the effects observed for the clouding of glass slides by KS-Dirt solutions were consistent with the results found in QCM measurements on glass and gold surfaces.

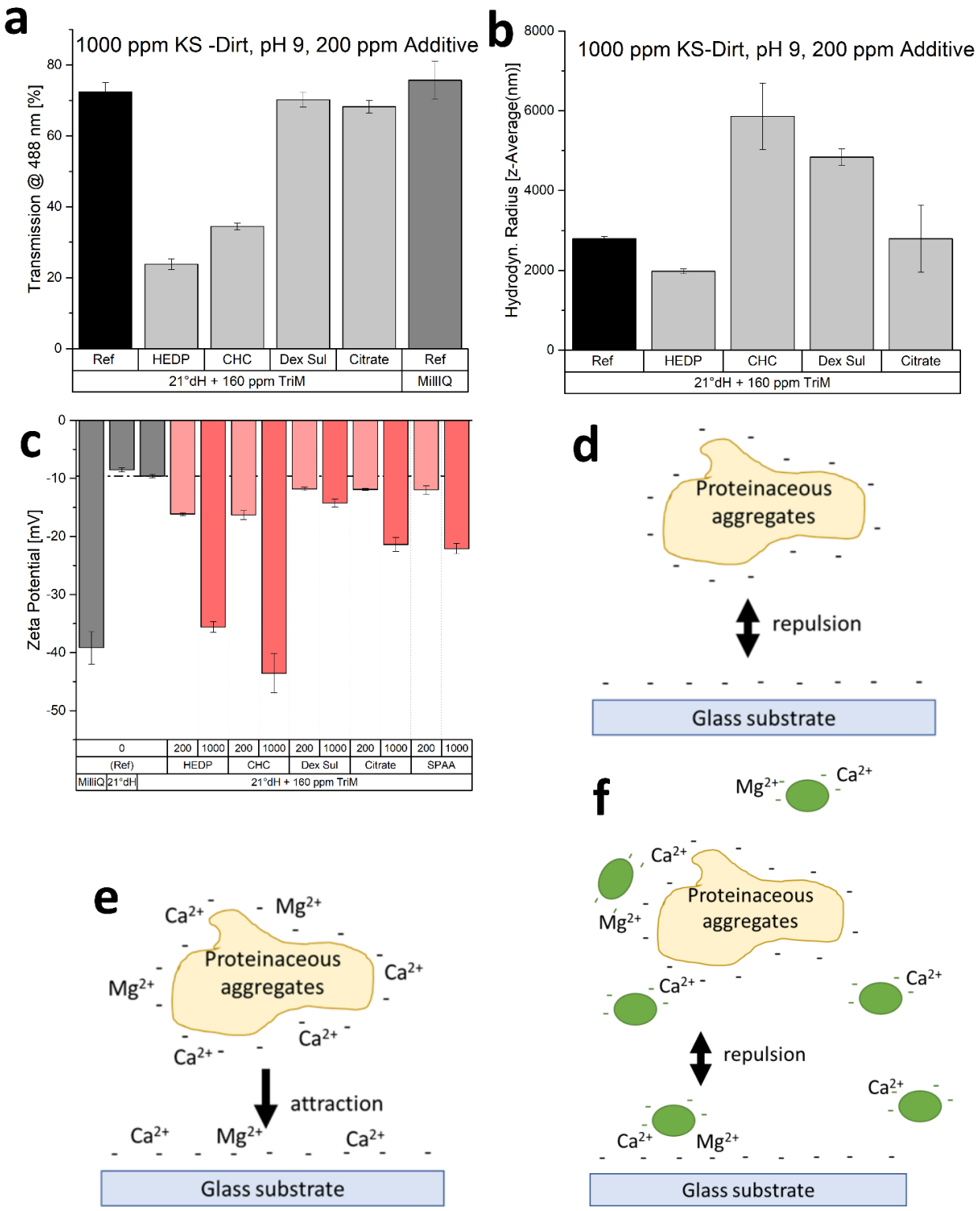

Figure 40 KS-Dirt solution turbidity (**a**), hydrodynamic radius (**b**) and zeta potential (**c**) for various solvent conditions. **d-f:** Scheme of possible interactions between suspended KS-Dirt particles (yellow), substrate, hard ions and anti-fouling additives (green).

In order to examine the effect of additives on the suspended protein-rich KS-Dirt particles, the turbidity, the hydrodynamic radius and the zeta potential of the examined washing solutions was measured. As can be seen in Figure 40 a, the turbidity of the washing solution is not related to the tendency of material deposition. Solutions containing the very effective HEDP and CHC are noticeably less transparent, which indicates a much more aggregated and less finely disperse particle distribution. Dextran sulfate and citrate, on the other hand, appear just as translucent as the reference in 21°dH + 160 ppm Tri M or MilliQ. Additional measurements have shown, that in MilliQ (pH 9), all solutions regardless of the additive appear equally transparent (Transmission ≈ 90%), indicating a stable suspension of small particles. On the contrary, solutions of HEDP and CHC with hard ions (21°dH + 160 ppm Tri M) but without KS-Dirt start to become turbid at elevated pH (≈ pH 9, data not shown). This might indicate the formation of microscopic particles comprised of anti-fouling additives (HEDP or CHC) and hard ion hydroxides. This appears to be the primary reason for the less transparent KS-Dirt solutions with these additives. The hydrodynamic radius of the suspended particles varies with different additives, but does not appear to correlate with the deposition behaviour observed in the QCM or glass slide fouling experiments either (Figure 40 b). Instead, the relative sizes might indicate that some additives (CHC and Dextran Sulfate) have a bridging effect, binding two or more dirt particles together. Further investigation revealed the effect of hard ions and additives on the zeta potential (surface charge) of the suspended KS-Dirt particles (Figure 40 c). The proteinaceous particles exhibit a strongly negative surface charge of around -40 mV in a MilliQ solvent without any hard ions present. This will allow an effective electrostatic repulsion between particles (cf. DLVO theory). As gold or glass surfaces are negatively charged at pH 9 or higher[218,219], this will also ensure a sufficient repulsion between the particles and the substrate surfaces. As a consequence, both the turbidity of the solution (Figure 40 a) as well as the fouling on surfaces (Figure 38 a) is low. In contrast, particles suspended in hard water (21°dH) have a severely reduced surface charge of less than -10 mV, which is only marginally improved on by the addition of 160 ppm Tri M (Figure 40 c). For the additives HEDP and CHC, a marked increase of the surface charge is observed already at 200 ppm (- 15 mV). At higher concentrations (1000 ppm), the observed zeta potential rises to levels that are similar or greater to what was measured for MilliQ (-35 to -44

mV). The additives dextran sulfate, citrate and SPAA show a much lower enhancement of the surface charge (both at 200 and 1000 ppm, respectively), which corresponds with their lower anti-fouling effect observed in Figure 39 d & f. It is clear that the effect of all tested additives on the surface charge is the main contributor to the adsorption of proteinaceous material onto substrate surfaces. The schemes in Figure 40 d-f help to illustrate this point. At pH 9, protein aggregates will carry a negative surface charge, as all negative amino acid side chains (carboxy groups) and all otherwise positive side chains (amino moieties) will be deproteinized. As stated, the electrostatic repulsion between particles and surfaces will be sufficient and the colloidal stability leads to a stable suspension (Figure 40 d). Hard ions, however, will attach to the negative particles and screen the charges, leading to a severely reduced zeta potential. Additionally, QCM measurements indicate an adsorption of hard ions onto the glass or gold surface at pH 9 (data not shown), which will in turn also reduce the zeta potential of the exposed substrates. This allows the particles to exert a van-der-Waals (and possibly electrostatic) attraction to glass and gold surfaces, leading to strong adsorption (Figure 40 e), that cannot be rinsed off easily (cf. Figure 38 a).

Adding anti-fouling compounds, such as the frequently used HEDP or the possible alternative CHC and to some extent dextran sulfate, effectively curbs this process. This is done by competitively binding to the hard ions (“sequestration”), thus removing them from the suspended particles. Additionally, it is possible that such compounds might coordinate themselves in the vicinity of the bound hard ions close to the surface of the dirt particles, effectively creating a highly negatively charged second layer around the suspended dirt (Figure 40 f).[212] In this case, the spatial arrangement would set strict size and shape requirements for the additives to be effective. Large molecules or polymers (such as heavy polycarboxylates or SPAA) would have trouble covering the particle surfaces effectively and might end up bridging various particles and thus reduce the overall colloidal stability. Therefore, very small, yet highly charged molecules might be more efficient. This could explain the observed differences for the small HEDP and CHC compared to the charged polymer dextran sulfate, alginate and SPAA.

5.4 Conclusion

The goal of this study was the replacement of HEDP as an anti-deposition additive (anti spotting) for automatic dishwasher applications with a phosphate-free alternative. The main focus was on protein-rich dirt solutions. It became apparent that CHC, a small and highly charged molecule, can achieve equal or better results for model systems, such as QCM or glas-hazing experiments. Limited success was also made with the medium-length polymer dextran sulfate, while other compounds such as SPAA, alginate and citrate were of lesser efficiency. Analysis of the (proteinaceous) particle surface charge revealed the main driving force behind the spotting effect: Screening of the negative surface charge due to hard ions (magnesium and calcium) led to a severe reduction in colloidal stability. This enabled attractive forces between the particles and the substrate (i.e. glassware) to dominate, yielding strong and irreversible material-deposition/spotting. The simple sequestration of hard ions by high-capacity complexing agents such as SPAA or Trilon M was not sufficient in restoring the particle surface charge and thusly the colloidal stability. On the contrary, polymeric compounds appeared to be detrimental, possibly due to bridging effects. Instead, specific requirements such as high charge and low molecular weight (i.e. small molecular size) appear to be vital.

CHAPTER 6: FUNCTIONAL PROTEIN STABILITY AND ACTIVITY WITH IONIC ADDITIVES

6.1 Introduction

Polypeptides can be broadly grouped into structural and functional proteins. The former serve either as building blocks (e.g. elastin) or storage (e.g. casein, ovalbumin) while the latter perform (often) catalytical reactions that are essential to all cellular life processes (cf. section 0.2.3.1). In this chapter, the focus will be directed toward the activity and stability of functional enzymes and how they can be modified using ionic additives. As mentioned in section 0.2.3.3, stability and activity are inherently connected, as one is the prerequisite of the other. Beyond this, however, the activity of functional proteins can be tuned by the addition of various additives. Specific ion effects, again, can have a strong influence on the activity of enzymes.[32]

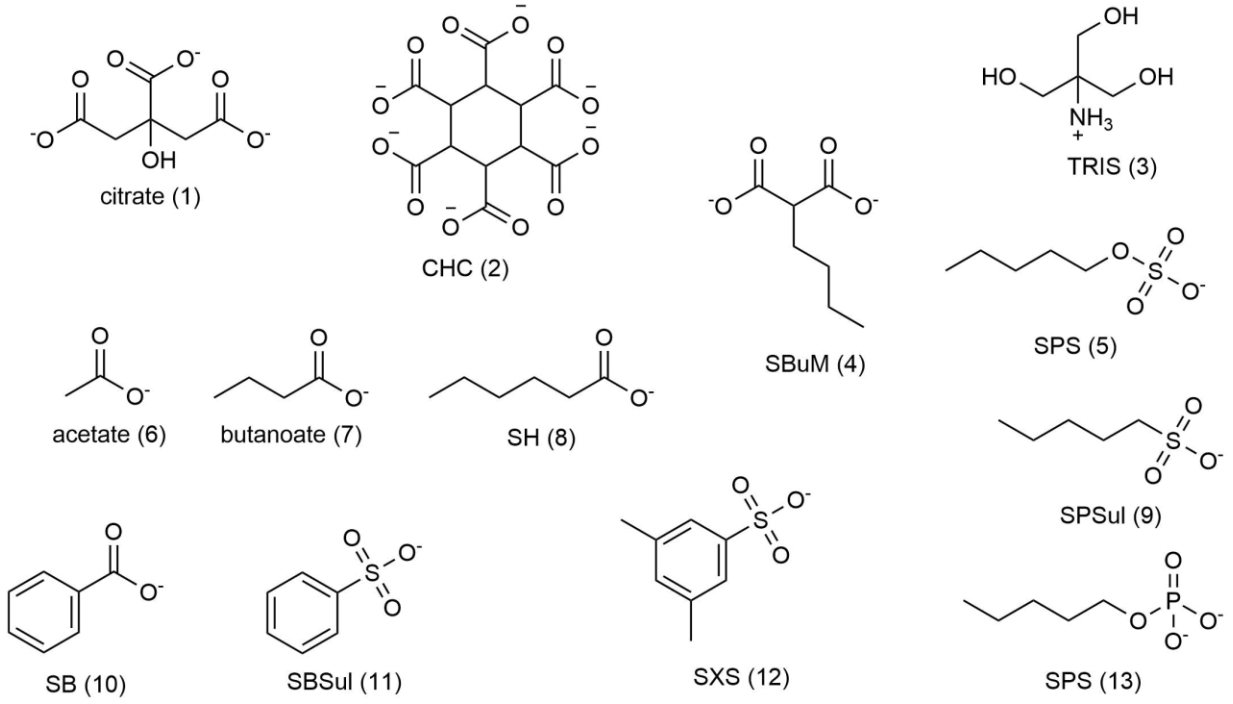

Figure 41 Molecular structure and abbreviations of used compounds and additives depicted in ionic form. Sodium salts were used exclusively.

Figure 41 gives an overview of the used compounds in this study. Besides kosmotropic inorganic ions (sulfate, phosphate) and the chaotropic ammonium and thiocyanate ions, amphiphilic compounds with varying headgroup ionicity (cf. chapter 2) were deployed.

6.2 Experimental

6.2.1 Chemicals

Lysozyme (ultra-pure) was sourced from VWR. Bovine pancreas protease type I, savinase (protease from bacillus sp.), casein from bovine milk and the bacteria micrococcus lysodeikticus was purchased from Sigma Aldrich. Phytase was supplied as a 24 wt% stock solution directly from BASF SE. Trishydroxymethylaminomethane (TRIS, 99.8 %), sodium sulfate (99 %), citric acid monohydrate (98 %), sodium chloride (99.5 %), sodium butanoate (98 %), tetrasodium diphosphate decahydrate (≥99.0%), sodium dihydrogen phosphate (≥99.0%), sodium triphosphate (≥98.0%) and sodium acetate were all sourced from Merck. Ammonium chloride (99.5 %), sodium benzoate (99.5 %), butylmalonic acid (99 %), sodium benzenesulfonate (97 %), sodium xylene sulfonate (≥ 90%), sodium thiocyanate (≥98.0%) and trichloroacetic acid (TCA, 99 %) were purchased from Sigma Aldrich. Sodium hexanoate (99 %), sodium pentylsulfonate (98 %), and 1,2,3,4,5,6-cyclohexanehexacarboxylic acid (97 %) was sourced from TCI. Sodium pentyl sulfate (99%) was acquired from Alfa Aesar. All chemicals were used without further purification, and all solutions were prepared with millipore water ($\rho \geq 18$ MΩcm).

6.2.2 Methods

Turbidity and Zeta Potential measurements – Solutions were prepared in MilliQ with 1-3 wt% of protein and the pH was continuously adjusted using HCl or NaOH to achieve a range of acidic to basic conditions at room temperature. For each suitable pH increment, a small quantity of protein solution (< 1 mL) was retrieved to measure the transmission at 488 nm using a Hitachi U-1000 photometer against a blank sample (water only). Similarly, samples were taken to measure the Zeta Potential using DTS1070 cuvettes in a Malvern Zetasizer. Measurements were done in triplicate and the results averaged. Error bars mean ± SD (N=3).

Lysozyme activity and aggregation assay – Native lysozyme activity: A stock lysozyme solution of 0.4 mg/mL and a bacteria (micro. lysodeikticus) stock solution of 1 mg/mL was prepared in TRIS buffer at pH 7.4. Then, additive solutions were prepared in the same buffer as a dilution series and the pH adjusted accordingly. Mixing with bacteria stock solution (750 µL + 740 µL) gave 1.5 mL of additive-bacteria substrate solution. To this 20 µL of 0.2 mg/mL lysozyme solution was added and the drop in absorbance at 600 nm was recorded between 30 s and 90 s after enzyme addition. The relative activity was then calculated using a 4-point calibration curve (in duplicate), that was recorded new for every lysozyme/bacteria stock solution used.

Heat treated lysozyme: A stock lysozyme solution of 0.4 mg/mL and a bacteria (micro. lysodeikticus) stock of 0.5 mg/mL was prepared in buffer (PBS or TBS) at pH 7.4. Then additive solutions were prepared in the same buffer as a dilution series and the pH adjusted accordingly. Mixing with lysozyme stock solution gave 4 mL of additive-lysozyme solutions each with 0.2 mg/mL of enzyme content in 4 mL drum vials. Heat treated samples were submerged in a water bath at a certain temperature (e.g. 98°C) for the specified time after which quenching in cold water stopped the aggregation/denaturation. Then, 20 µL of enzyme solution was added to 1.5 mL of bacteria stock solution the drop in absorbance at 600 nm was recorded between 30 s and 90 s after enzyme addition. The relative activity was then calculated using a 4-point calibration curve (in duplicate) that was recorded new for every lysozyme/bacteria stock solution used.

The heat-treated samples were also investigated for turbidity at 488 nm and checked for aggregation by filtration through a 200 nm syringe filter and subsequent absorbance measurement at 280 nm. By use of a calibration curve (in duplicate) with various lysozyme concentrations, the residual content of soluble enzyme could be calculated. All necessary background corrections were made.

All measurements were done in duplicate and the results averaged.

Protease activity assay – Protease stock solutions (Protease bovine: 1 mg/mL, Savinase: 4 mU/g) were prepared in 10 mM phosphate buffer at pH 7.4. Caseine substrate stock solutions (6.5 mg/mL) were prepared in the same buffer and heated to 85°C to yield a turbid but homogenous solution. After cooling to r.t. the pH was adjusted to 7.4. Additive solutions were prepared in the

same buffer at various concentrations (pH adjusted to 7.4) and mixed with the protease stock solution in equal parts. To 400 µL of these additive-protease solutions was added 2 mL of substrate solution and mixed by swirling. Then, the samples were immediately transferred to a water bath at 30°C and incubated for exactly 30 minutes. After, the samples were retrieved and the reaction was quenched by the addition of 2 mL of TCA (110 mM). 1 mL of turbid solution was transferred to Eppendorf tubes and centrifuged at 13.000 rpm for 20 minutes. The supernatant was measured for absorbance at 280 nm. The necessary background corrections were made and the relative activity was calculated using a 4-point calibration curve (in duplicate), that was measured new for every protease/substrate solution used. All measurements were done in duplicate and the results averaged.

Protein aggregation – Additive solutions were prepared in 50 mM TRIS Buffer at various concentrations and the pH was adjusted to 7.4. Then, the addition from a suitably diluted protein stock solution in 50 mM TRIS adjusted to pH 7.4 led to 1 wt% phytase in all samples. The samples were heated up slowly in a water bath, and small quantities of solution (< 800 µL) were retrieved at suitable temperature increments and measured for transmission at 488 nm on a Hitachi U-1000 photometer. Measurements were done at least in duplicate and the results averaged. Error bars mean ± SD (N=2-3).

Differential scanning calorimetry – Protein solution samples with various additives were prepared as described above and the pH was set to 7.4. Then, the denaturation curve was measured using a Setaram micro DSC III. The denaturation peak temperature was determined using the proprietary software Setsoft 2000. Protein concentrations used were 1 wt% for phytase.

6.3 Results and Discussion

6.3.1 Lysozyme

The first functional enzyme to be investigated is lysozyme. Generally, lysozyme is found in a number of secretions of humans and animals. In high concentrations it is found in egg white and it is part of the native immune defence especially against bacteria. As such, it directly attacks the cell membrane of bacteria. The protein is made of a single polypeptide chain containing 129 amino-acid residues. The chain is cross linked via four disulfide bonds. Out of the 129 amino acids the majority is basic, which results in a positive charge of the protein at physiological pH.[220] As such the protein serves as a suitable model enzyme to investigate the activity and stability in particular after applying stress. Therefore, we will first look at the native activity of lysozyme in the presence of various additives and then examine the resistance to denaturation and aggregation upon application of thermal stress. For this, buffer effects will be examined also, as they typically have ionic character and their application is ubiquitous in biochemistry.

6.3.1.1 Additive effects on native lysozyme activity

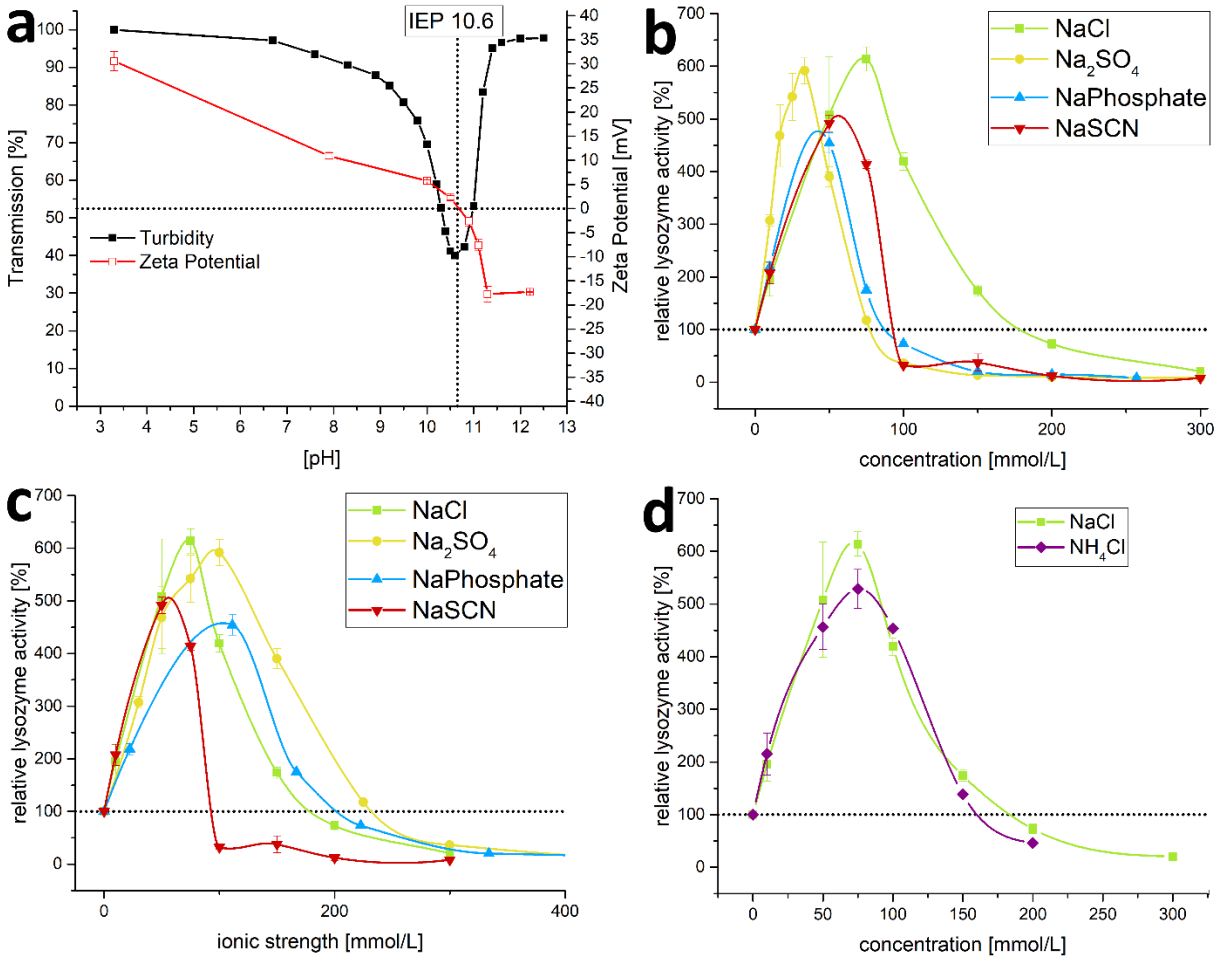

Figure 42 Lysozyme activity in presence of ionic additives in phosphate buffer. **a:** transmission and Zeta potential as a function of pH for lysozyme. Error bars mean ±SD (N=3). **b & c**: Relative lysozyme activity in 10 mM PBS (pH 7.4) with inorganic ions ordered by concentration (**b**) and ionic strength (**c**). **d**: Relative lysozyme activity with different cations. **b-d**: 100% activity relates to no additives present. Error bars mean ±SD (N=2).

As mentioned previously, lysozyme is positively charged at physiological pH (7.4) and has its iso-electric point (IEP) at around 10.6, which means the net-charge is zero at this pH and the colloidal stability is, therefore, the lowest, signified by an increased turbidity due to loose (reversible) aggregation (cf. Figure 42 a). Above this pH, the charge inverses to net-negative and the enzymes are dispersed again leading to the complete disappearance of turbidity. The activity of lysozyme depends largely on the salinity of the host-solution. As can be seen in Figure 42 b, different concentrations of common inorganic salts lead to an increase of up to 600% activity compared

to the reference (enzyme in PBS only) after which a steep drop-off leads to almost complete enzyme inhibition. If the results are plotted against the ionic strength instead of concentration, one can see distinct differences that arise from specific ion effects rather salinity (see Figure 42 c). Here, an ordering of anions according to the ionic strength when they first undercut the reference activity (i.e. deactivating behaviour), a direct Hofmeister series is observed. This means "salting-in" ions, that can cause protein denaturation, lead to a deactivation at lower concentrations than kosmotropic compounds. Ordering these inorganic ions by the value of their ionic strength at their maximum effect on enzyme activity results in: $SCN^- < Cl^- < SO_4^{2-} < H_2PO_4^-$ /HPO_4^{2-} . This order corresponds to the inversed Hofmeister series, which is often observed for positively charged proteins.[31] Arranging the ions by their effect of enhancing enzyme activity (i.e. maximum gain of activity), another trend is visible: $Cl^- > SO_4^{2-} > SCN^- > H_2PO_4^-$ /HPO_4^{2-}. As this order does not follow the Hofmeister series at all, one can assume that a balance of different underlying mechanisms (which follow the direct or indirect series) might be at play, which shuffles the ion order in an unusual way. Of all these inorganic ions, chloride has the highest effect on enzyme activity, possibly due to its intermediate position between chaotropes and kosmotropes ("borderline ion", cf. Figure 1).[121,122] This might allow chloride to balance direct and inverse ion effects and lead to an optimal enzyme activity. For cations this trend appears to be mirrored: The more chaotropic ammonium ion leads to a lower peak activity while also undercutting the reference line at a lower concentration than sodium (see Figure 42 c).

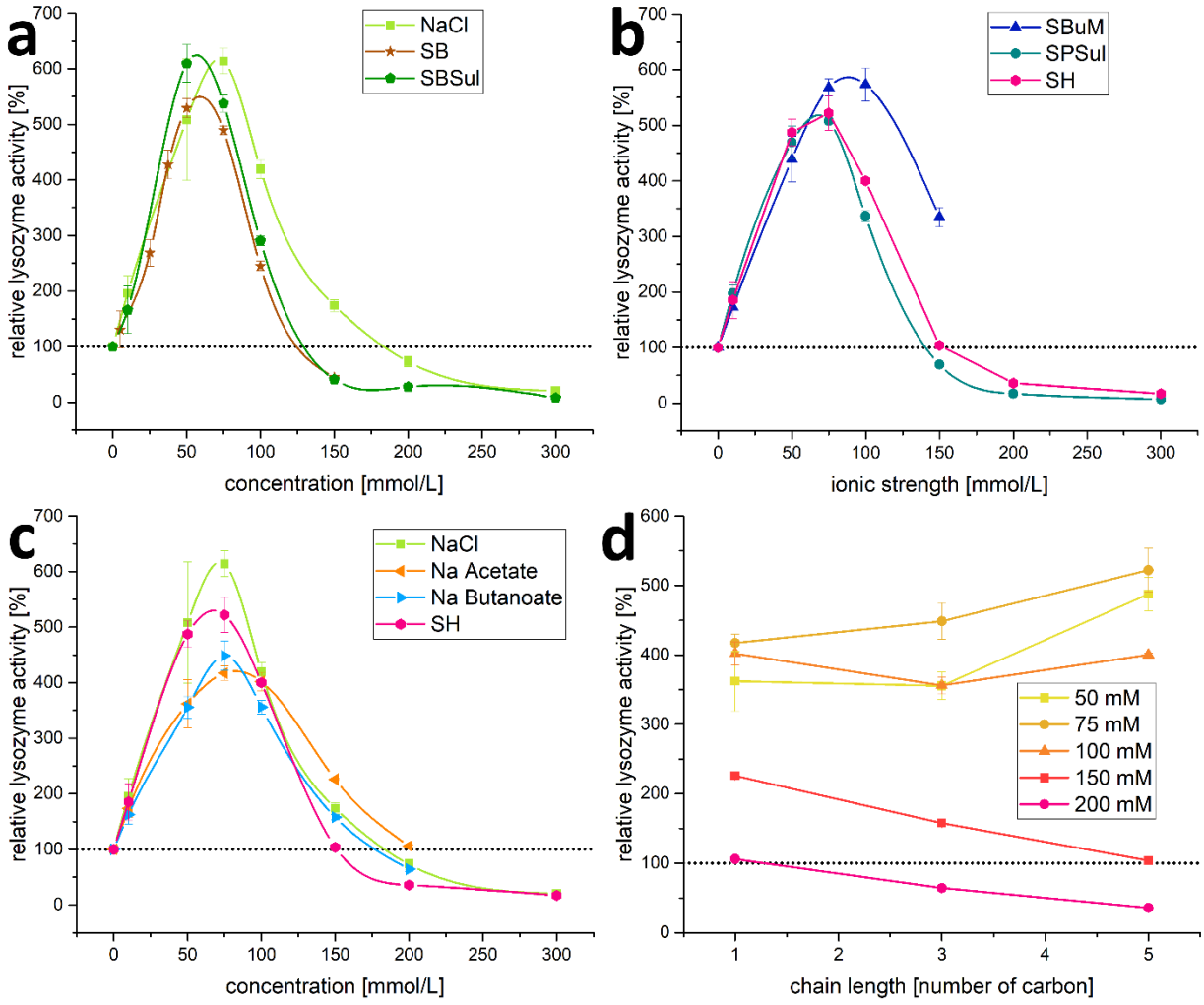

Figure 43 Lysozyme activity in presence of amphiphilic additives. Relative lysozyme activity in 10 mM PBS (pH 7.4) with benzene-derived hydrotropes (**a**), pentyl-derived amphiphiles (**b**) and carboxylic acid derived salts with varying chain length (**c**). **d:** Plot of relative lysozyme activity versus chain length and additive concentration. **a-d**: 100% activity relates to no additives present. Error bars mean ±SD (N=2).

Moving on to organic, amphiphilic anions, one can see that the ionicity provided by their polar headgroups leads to a strong increase of lysozyme activity akin to inorganic salts. For phenyl-derivatives such as benzene sulfonate (SBSul) and benzoate (SB), the peak activity is higher for the softer headgroup of the sulfonate similar to the equally borderline chloride ion (see Figure 43 a). However, both compounds are surface active hydrotropes and can denature proteins in higher concentrations. Therefore, they deactivate lysozyme at a lower concentration than chloride, much more similar to the salting-in thiocyanate (cf. Figure 42 c). For pentyl-derivatives similar observations were made (see Figure 43 b). Butyl malonate (SBuM), however, has a much

more kosmotropic head unit and is, despite its amphiphilic character, not surface active (see Figure 14). This results in a higher peak activity compared to surface active pentyl-derivatives. The reference activity will also be undercut at higher concentrations, indicating a low denaturation tendency for this compound. Focusing on linear alkyl carboxylates, the effect of the chain length on the enzyme activity was examined. This will impact the hydrophobicity and, therewith, the balance between specific ion effects and surface activity. As can be seen in Figure 43 c, all additives follow the same general concentration-activity relation as previously seen of other ionic additives, though shorter chains (acetate and butanoate) interestingly led to slightly lower peak activities. In turn, the more surface active (and therefore "salting-in") hexanoate undercuts the reference at a lower concentration. These seemingly conflicting effects can be better seen in Figure 43 d, where it becomes apparent that at lower concentrations (<75 mM), longer chains lead to a higher activity, while at higher concentrations (>100 mM) the opposite is true. This is in-line with previous results on cationic ammonium derivatives, showing a detrimental effect on lysozyme stability, with increasing hydrophobicity of the additive (longer alkyl chains).[221]

6.3.1.2 Additive effects on heat stability of lysozyme

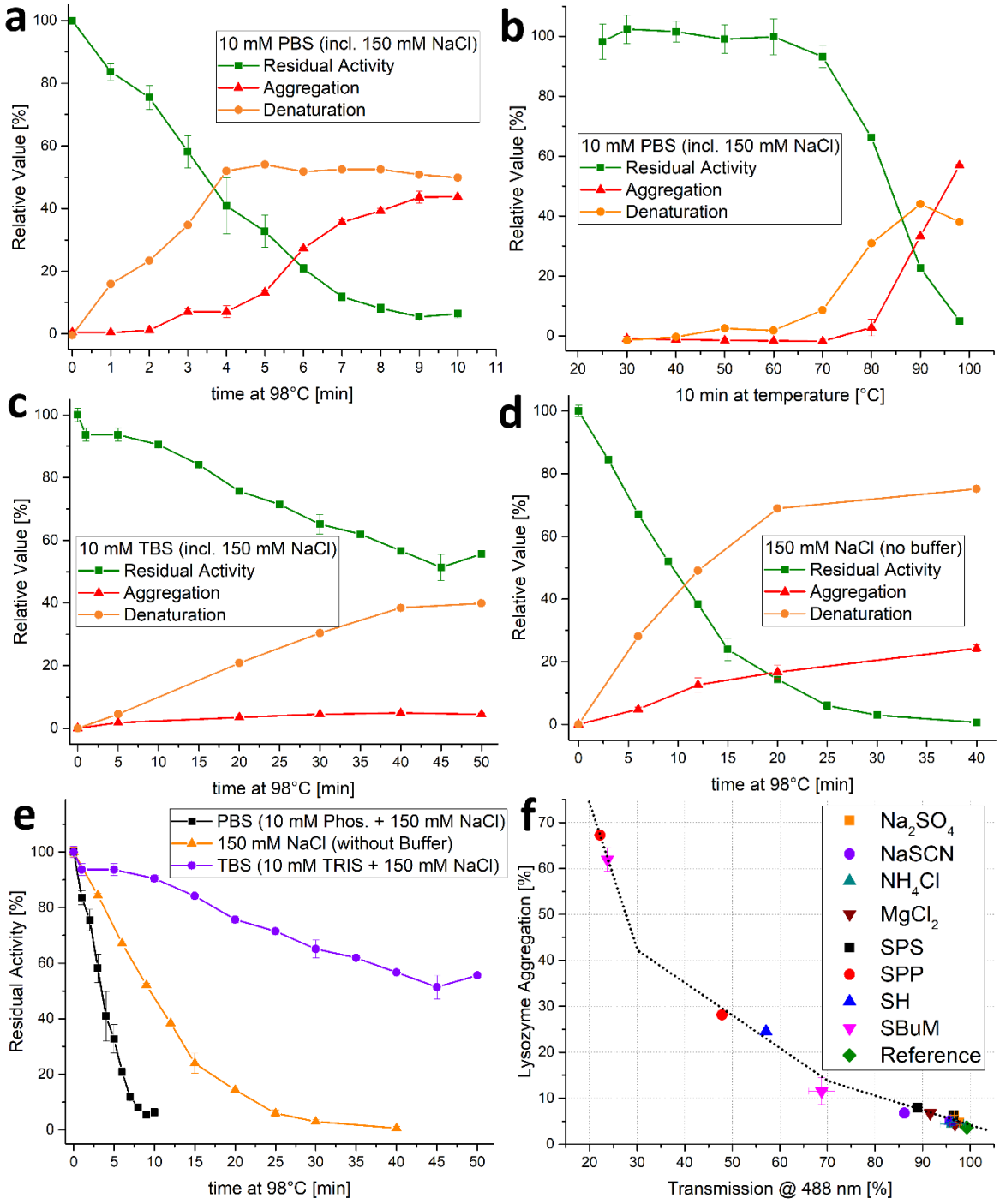

Figure 44 Heat deactivation of lysozyme in PBS and TBS. Residual activity, aggregation and denaturation of lysozyme in PBS according to time (**a**) or temperature (**b**) of applied thermal stress. Residual activity, aggregation and denaturation of lysozyme with time in TBS (**c**) and salt only solution (**d**). **e**: Comparison of residual lysozyme activities for various solution conditions. **f:** Lysozyme aggregation versus turbidity for various additives.

In technical applications, proteins are often exposed to mechanical or thermal stress. This will impair the longevity and activity of functional enzymes. To simulate this, lysozyme was subjected to a heat treatment that will lead to denaturation and aggregation with in turn lower protein activity. As can be seen in Figure 44 a & b, this effect is both time and temperature dependent, meaning a longer time at denaturizing temperatures or equal times at different temperatures will gradually reduce the residual enzyme activity while driving denaturation and aggregation. The latter two states represent inactive forms of the enzyme that are either soluble (denatured) or not (aggregated). These experiments were carried out in 10 mM PBS buffer, which indicates the presence of 10 mM of sodium phosphate and 150 mM of NaCl. This will greatly affect the activity and heat stability of lysozyme as becomes apparent in Figure 44 c. Here, the heat deactivation of lysozyme is measured in 10 mM TBS (10 mM TRIS + 150 mM NaCl). The protein activity is retained at a much higher level for a significantly longer heating period. While the amount of denatured protein reaches a similar level after 40 min compared to the 10 min in PBS, the aggregation levels remain very low throughout. Lastly, the same experiment was carried out in 150 mM NaCl only, without buffer (Figure 44 d). Here, it becomes apparent that the behaviour on activity, denaturation and aggregation is in some ways an intermediate between PBS and TBS (see also Figure 44 e), though pH control is compromised due to the lack of buffer compound. This means that phosphate as buffer is detrimental, and TRIS appears to be beneficial for lysozyme in heat-stress experiments. As can be seen in Figure 44 f, protein aggregation genuinely correlates well with the turbidity of the resulting solution. This includes cases with various additives (as measured in the following experiments) and shows that turbidity can be a useful measure for enzyme aggregation (e.g. in technical applications).

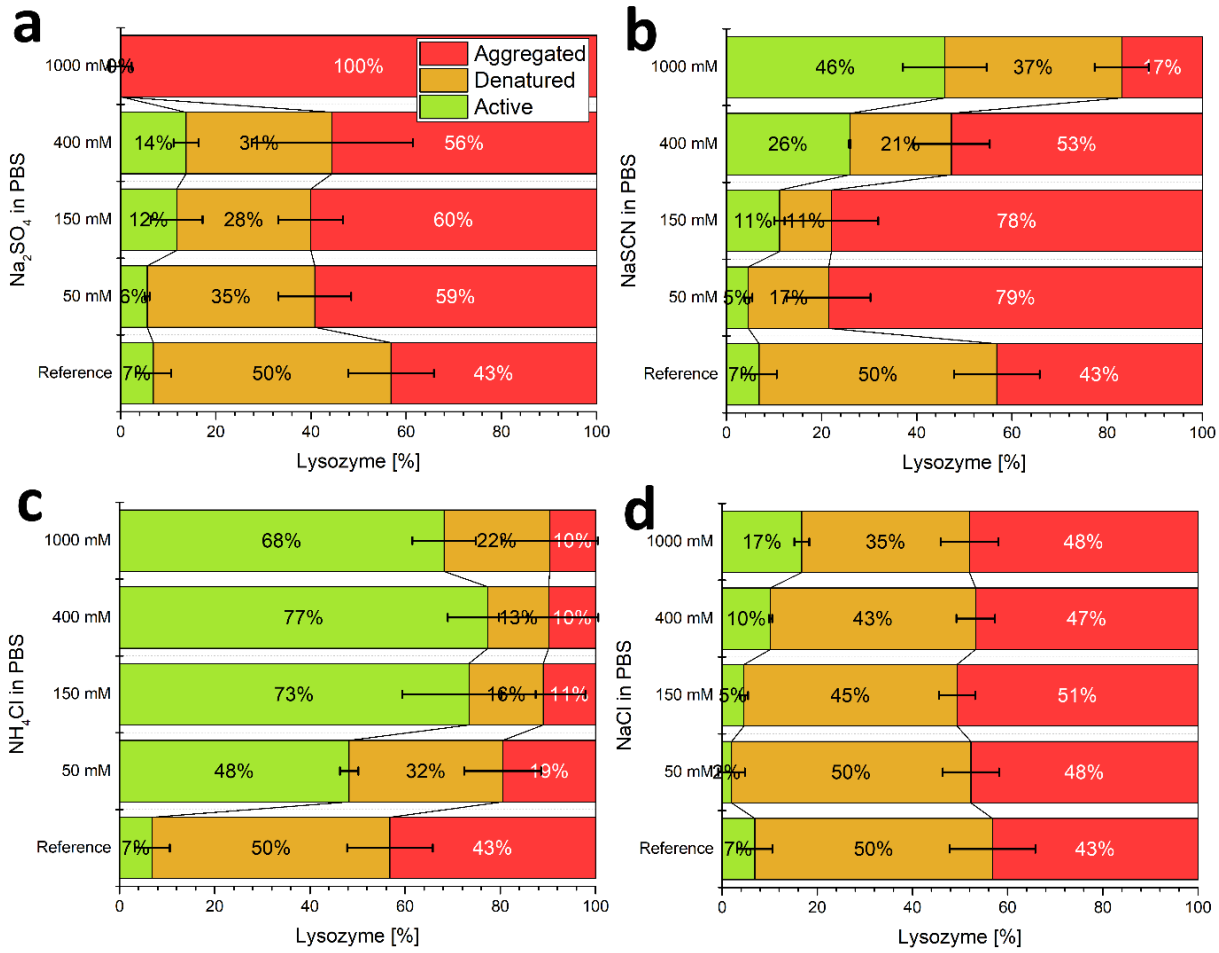

Figure 45 Effect of Hofmeister salts in PBS on lysozyme thermal stability. Additives were Na_2SO_4 (**a**), NaSCN (**b**), NH_4Cl (**c**) and NaCl (**d**) at 50, 150, 400 and 1000 mM after heat treatment. Different enzyme states labelled active, denatured (inactive but soluble) and aggregated (insoluble). Error bars mean ±SD (N=2).

In order to examine the effects of inorganic Hofmeister salts on the heat stability of lysozyme in PBS, experiments with various concentrations were carried out (see Figure 45). Due to a 1:75 dilution in the course of the experiment (after the heat treatment), the salt concentration will have only little effect on the resulting activity (as was the case for the previous chapter). Instead, the propensity to stabilize lysozyme during the heat-treatment and the capabilities to preserve its function will have the biggest impact on the remaining activity. The inactive lysozyme is further divided in denatured (soluble but inactive) and aggregated (insoluble) populations. It becomes apparent that in PBS, the best effect could be achieved by thiocyanate (chaotropic anion) in high concentrations (>400 mM) and ammonium (chaotropic cation) already in moderate concentrations (50 – 1000 mM). For thiocyanate, this effect is explained by facilitating

the correct refolding of proteins after the heat-stress (cf. also the lower aggregation at 1000 mM NaSCN in Figure 45 b).[32] This was previously shown for lysozyme with chaotropic guanidium and urea compounds[77], and for α-chymotrypsin with various chaotropic agents.[87] Mechanistically, the soft thiocyanate can attach to hydrophobic patches of the protein and increase its solubility, while preventing irreversible inactivation due to incorrect folding. For ammonium, its remarkable propensity at preventing specifically the aggregation of lysozyme (cf. Figure 45 c) has been reported previously.[222] This was attributed to the unique property of ammonium to adsorb on hydrophobic amino acids (due to its chaotropic character) and to increase the transition threshold for unfolded lysozyme to aggregate (as opposed to thiocyanate, which decreases the energy barrier for all transitions). This behaviour extends beyond the simple NH_4 cation to other more complex structures bearing an ammonium motif[223] and it is most likely also the reason for the significant stabilizing effect of TRIS buffer on lysozyme heat-stabilization seen in Figure 44 c (cf. Figure 41 for molecular structure of TRIS).

As the buffer already contains a kosmotropic anion (phosphate), additional sulfate (Figure 45 a) will have little (negative or positive) effect on the preservation of activity. A noteworthy exception is the total aggregation of lysozyme at 1000 mM Na_2SO_4. Similarly, NaCl, which is already present in 150 mM in the buffer, has little effect on the heat-deactivation or aggregation. In general, kosmotropic compounds destabilize the (thermally) unfolded state of lysozyme and, therefore, drive aggregation.[222] Hence, heat-stress experiments in PBS will always yield low residual activities except in the presence of strongly stabilizing compounds such as ammonium chloride.

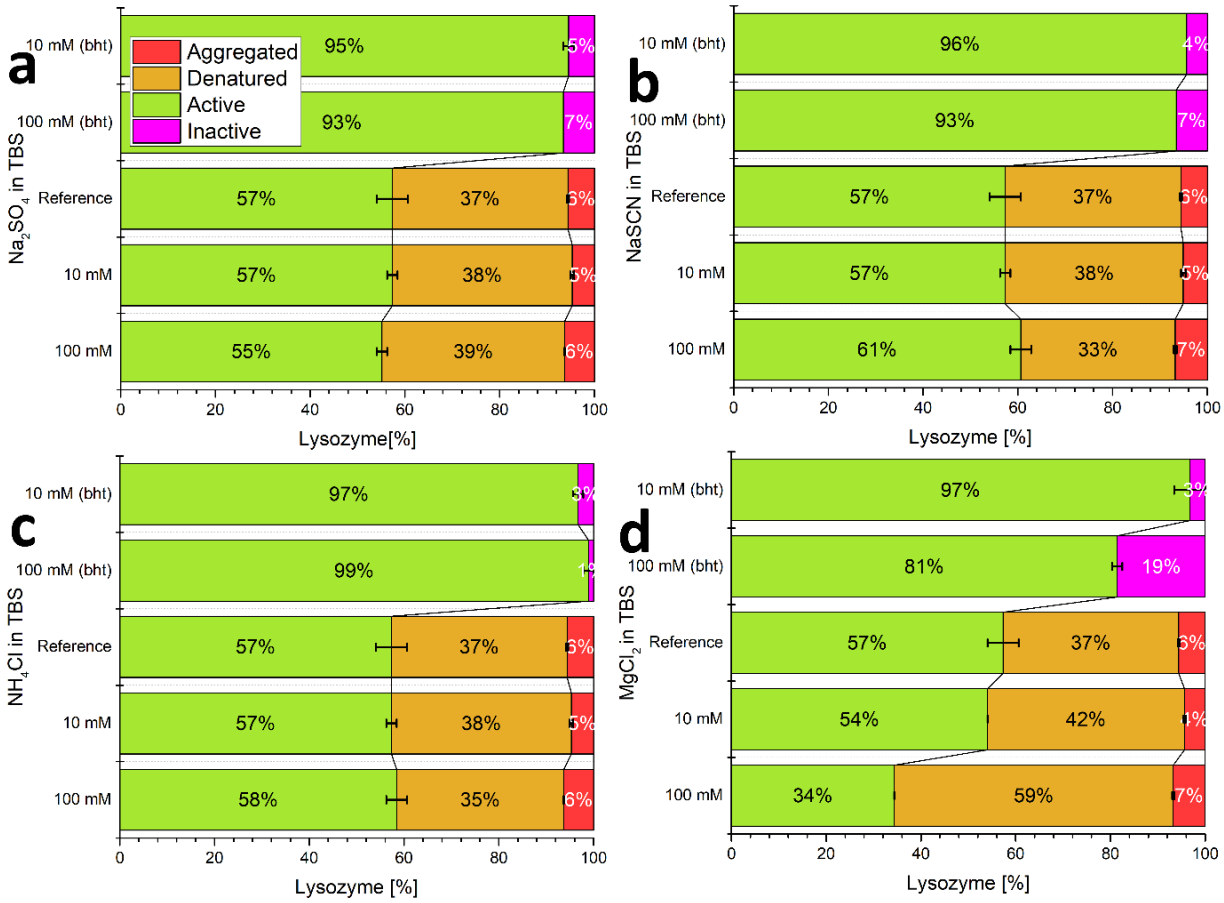

Figure 46 Effect of Hofmeister salts in TBS on lysozyme thermal stability. Additives were Na_2SO_4 (**a**), NaSCN (**b**), NH_4Cl (**c**) and $MgCl_2$ (**d**) at 10 and 100 mM after and before heat treatment (bht). Different enzyme states labelled active and inactive. For heat treated samples the latter is differentiated further in denatured (inactive but soluble) and aggregated (insoluble). Error bars mean ±SD (N=2).

To this, additional experiments were carried out with various Hofmeister salts in TBS (see Figure 46). Here, it can be seen that the stabilizing effect of the (chaotropic and cationic) TRIS buffer is so dominant that the detrimental effect of sulfate (Figure 46 a) and the beneficial effects of thiocyanate (Figure 46 b) and NH_4Cl (Figure 46 c) are only marginal. $MgCl_2$, however, which as a kosmotropic cation is a direct antagonist to the chaotropic ammonium can reduce the thermal stabilization of lysozyme significantly (see Figure 46 d). This is achieved not by increasing the aggregation, but by facilitating the denaturation during heat-treatment. It should be noted that $MgCl_2$ already significantly impairs lysozyme activity even before the heat treatment. This could be due to specific interactions of hard magnesium ions with hard anionic residues (carboxylates)

in lysozyme leading to the weakening of intra-molecular salt bridges in the protein with a subsequent loss of function.[224,225]

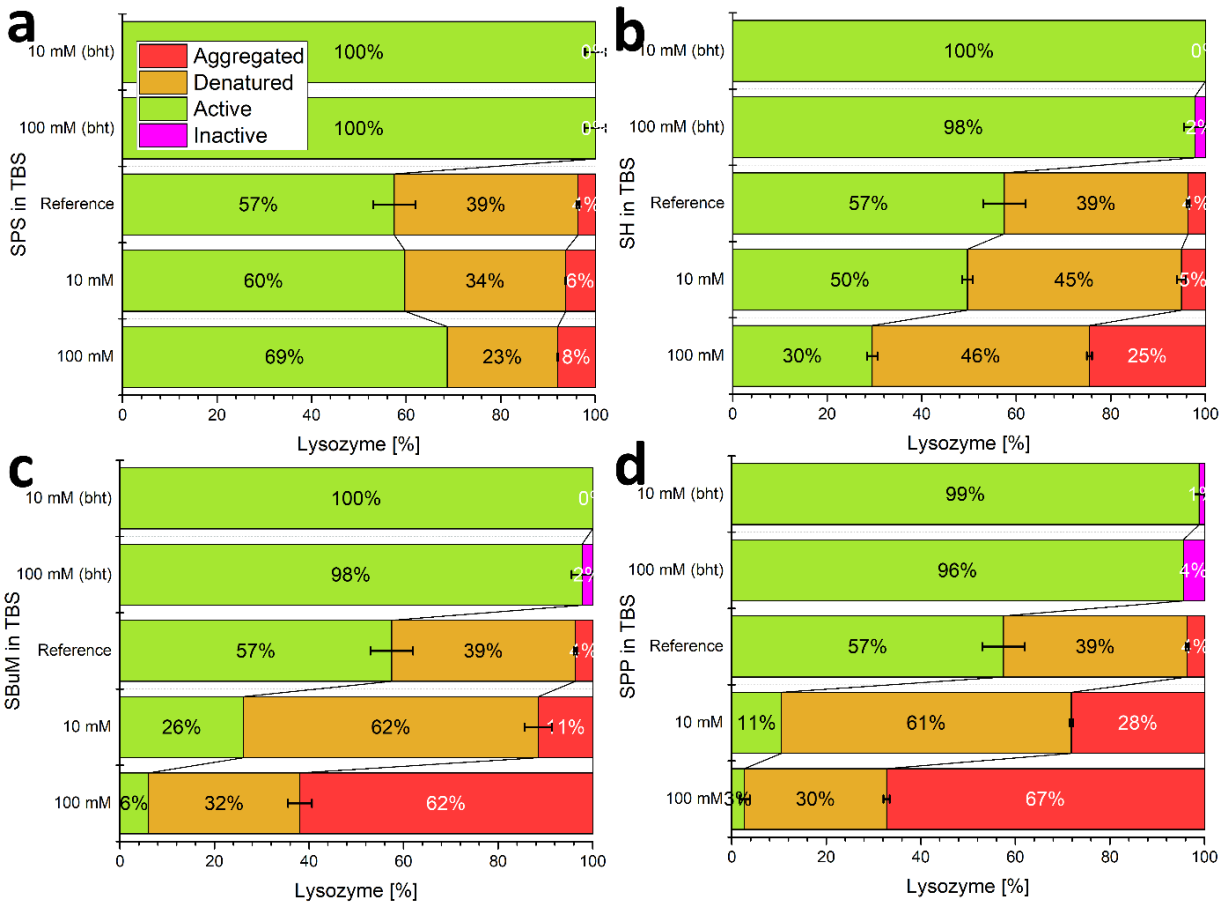

Figure 47 Effect of anionic pentyl derivatives in TBS on thermal lysozyme stability. Additives were SPS (**a**), SH (**b**), SBuM (**c**) and SPP (**d**) at 10 and 100 mM after and before heat treatment (bht). Different enzyme states labelled active and inactive. For heat treated samples the latter is differentiated further in denatured (inactive but soluble) and aggregated (insoluble). Error bars mean ±SD (N=2).

Lastly, experiments were carried out for lysozyme heat-stability in TBS with amphiphilic additives (Figure 47). More specifically pentyl derivatives with various anionic headgroups such as sulfate, carboxylate or phosphate units (cf. Figure 41 for molecular structures). Depending on the specific ion effects of the headgroup, these additives can be hydrotropic or salting-out in nature (cf. chapter 2). In general, the Hofmeister order of the headgroups is consistent with the effect on the heat-stability of lysozyme going from stabilizing for the most salting-in compound toward increasingly destabilizing for the more salting-out compounds. In detail, SPS can preserve the activity of lysozyme by reducing the population of the heat-denatured state (i.e. facilitation of

correct refolding) while only marginally increasing aggregation (see Figure 47 a). This effect seems to be analogous to the effect of thiocyanate (cf. Figure 46 b) but more pronounced. SH (while being genuinely a salting-in compound) appears to be already kosmotropic enough to facilitate both, aggregation and denaturation during heat treatment of lysozyme similar to what was observed chiefly for PBS and to some extend for sulfate (see Figure 47 b, cf. Figure 46 a and Figure 44 e). This trend is then increasingly prevalent for the even more kosmotropic SBuM and SPP, which both significantly increase denaturation at low concentrations (10 mM) and aggregation at high concentrations (100 mM) (see Figure 47 a & b), leading to low residual lysozyme activities. As kosmotropic additives destabilize the unfolded state, strong aggregation can be observed for SBuM and SPP at 100 mM, while SH seems to be surface active enough to favour incorrectly (re-)folded lysozyme over insoluble aggregates.

6.3.2 Protease (bovine pancreas)

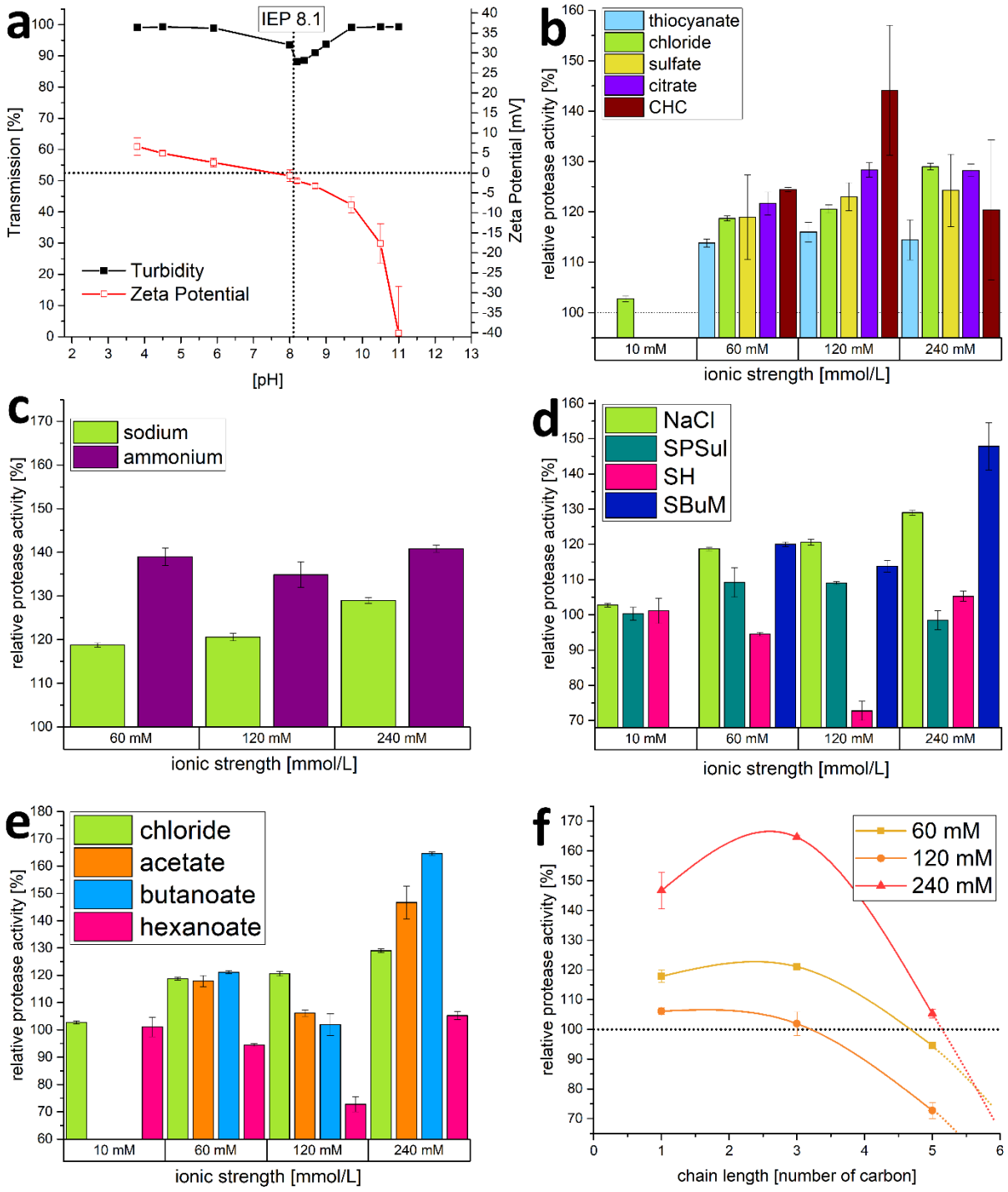

Figure 48 Bovine pancreas protease activity with various ionic additives. **a:** transmission and Zeta potential as a function of pH for bovine pancreas protease. Error bars mean ±SD (N=3) **b-e:** relative protease activity in presence of anionic additives (**b**), cationic additives (**c**), amphiphilic additives (**d**) and alkyl carboxylates with varying chain length (**e**). **f:** relative protease activity with varying chain length and concentration. 100% activity relates to no additives present. **b-f:** error bars mean ±SD (N=2).

The protease from bovine pancreas (thereafter referred to as “protease”) has an isoelectric point of 8.1, as can be seen from the zeta potential measurements in Figure 48 a. At this pH, the colloidal stability is also the smallest, leading to a local transmission minimum, that disappears once the protein regains sufficient charge. The activity experiments were carried out at physiological pH of 7.4. At this pH the protease carries a slightly positive charge but is almost neutral. As can be seen in Figure 48 b-f, the activity of the enzyme is generally enhanced with higher ionic strength much like what was observed for lysozyme. Beyond the effect of salinity, differences attributable to specific ion effects can be distinguished. More precisely, a direct Hofmeister series can be observed for anionic additives, at least in the range of 60-120 mM of ionic strength (see Figure 48 b). Here, the activity increases with the kosmotropic character, yielding the least activation in the presence of chaotropic thiocyanate and the most in the presences of kosmotropic CHC. At higher concentrations, the order starts to break up, indicating an optimum for some of the additives such as CHC and citrate. For cations, the order also follows the direct Hofmeister series, yielding higher activities for the more chaotropic ammonium from 60 to 240 mM (see Figure 48 c). Regarding amphiphilic pentyl derivatives, it can be noted that the kosmotropic and non-surface active SBuM has an equally enhancing effect (at 240 mM actually superior) as NaCl on the protease activity (see Figure 48 d). On the contrary, the more chaotropic and generally more surface active SPSul is less enhancing and in the case for SH can actually lead to a decrease in enzyme activity. This effect was examined further by measuring the effect of the chain length of alkyl carboxylates on the protease activity (see Figure 48 e). This shows that a short chain and high concentration (boosting salting-out properties) in beneficial to the enhancement of protease activity while a longer chain becomes detrimental to the enzyme. This effect is stronger for higher concentrations as becomes apparent in Figure 48 f.

The general agreement of enzyme activity enhancement with the direct Hofmeister series might be surprising, given the results that were reported for lysozyme in the previous section. Both enzymes are used below their IEP, meaning they principally carry a positive charge, which often results in inversions of the Hofmeister series. For this protease, however, the slope of the zeta potential is relatively shallow at moderate pH ranges (Figure 48 a). Therefore, there is only little surface charge at pH 7.4 which in turn might allow certain mechanisms to prevail allowing a

direct Hofmeister series to establish itself (for both cations and anions). It was reported previously that the enzymatic activity of chymotrypsin (a serine protease) could also be positively affected with increasingly kosmotropic additives when deployed below yet close to its IEP. This was also connected with an increased thermal stability of the protease and is assumed to be the result of direct protein-ion interaction.[226,227] In a different publication, the same effect was also shown for a variety of other proteases (some from animal pancreas) and was attributed to an increased stability of the active form and an improved binding affinity of the substrate to the active site of the enzyme in the presence of kosmotropic additives.[228]

6.3.3 Savinase (bacillus sp.)

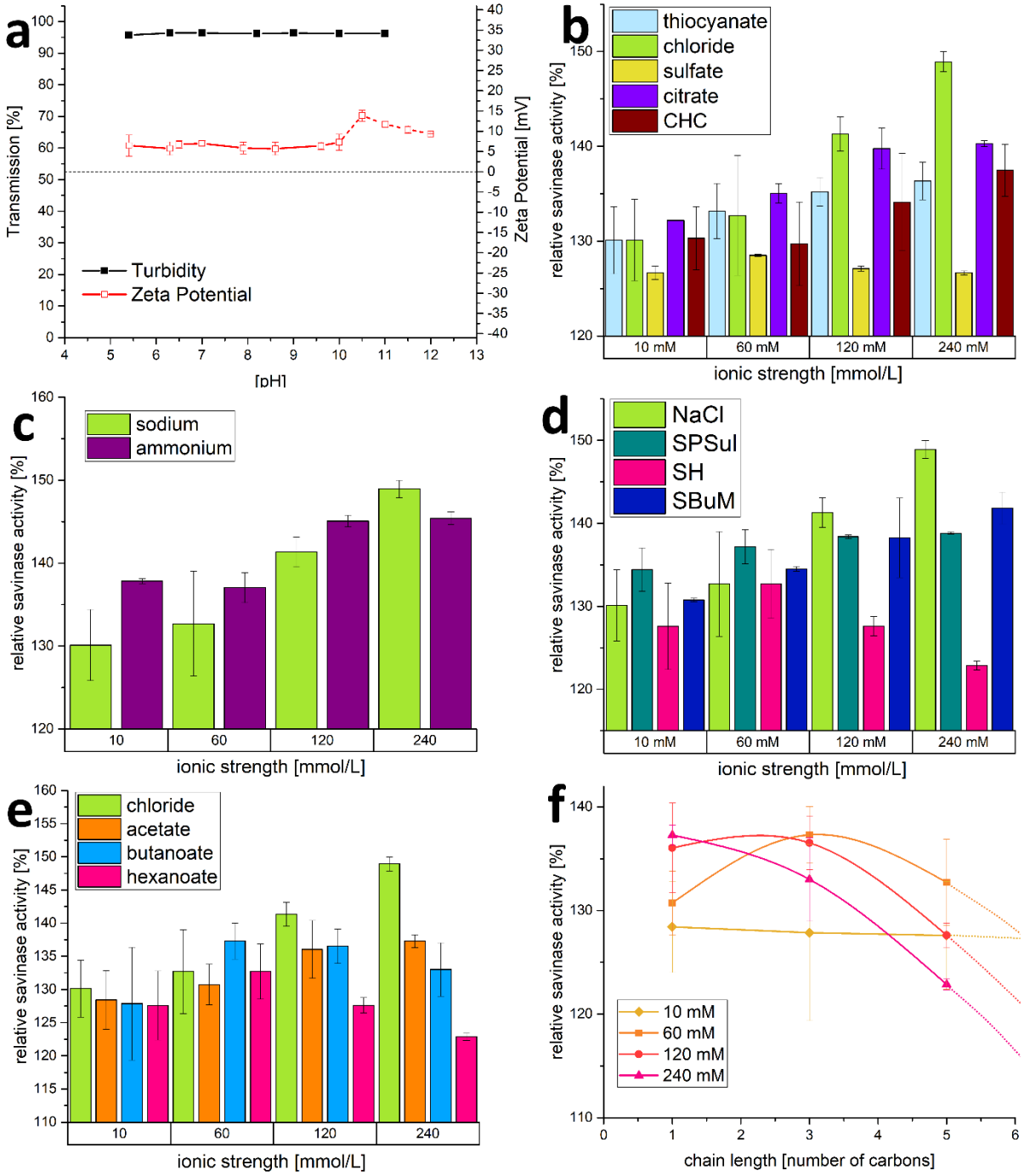

Figure 49 Savinase activity with various ionic additives. **a:** transmission and Zeta potential as a function of pH for savinase. Error bars mean ±SD (N=3). **b-e:** relative savinase activity in presence of anionic additives (**b**), cationic additives (**c**), amphiphilic additives (**d**) and alkyl carboxylates with varying chain length (**e**). **f:** relative savinase activity with varying chain length and concentration. 100% activity relates to no additives present. **b-f:** error bars mean ±SD (N=2).

The pH-dependent zeta potential of savinase enzyme (a type of protease from *bacillus sp.*) was examined in order to determine its IEP (Figure 49 a). It was found, however, that the protein remains positively charged at least until pH 10. Above this, the readings still indicate positive surface charge, but the cuvettes were not designed for such extreme pH values, hence the results could be compromised. Regardless, the IEP is assumed to be relatively high for this enzyme, ensuring a positive charge of roughly 7 mV at physiological pH (7.4). This is in line with the transmission measurements, that do not indicate an unstable region with loose aggregation due to low surface charges as was seen for protease from bovine pancreas or lysozyme (cf. Figure 48 a & Figure 42 a). As can be seen in Figure 49 b-e, increased salinity always led to an increased activity over the reference (which was 10 mM phosphate buffer only). The contribution of specific ion effects, however, appears to be very elusive. For anions, no clear Hofmeister trend is visible, with chloride yielding the highest activities in direct comparison (Figure 49 b). While the kosmotropic citrate is almost equally effective as the chaotropic thiocyanate, sulfate appears to be rather ineffective in boosting savinase activity. For cations, sodium and ammonium are generally very similar, with ammonium leading at lower concentrations as was observed for protease (Figure 49 c). For amphiphilic compounds with intermediate chain length (5 carbons), the effect on enzyme activity is lower than the chloride reference (at equal ionic strengths) across the board (Figure 49 d), which to some extent mirrors the results already observed for protease. In Figure 49 e, one can see that the chain length affects the boosting capabilities for aliphatic carboxylic acids. Here, longer chains lead to lower activities. This effect appears to be negligible at lower concentrations (10 mM), but will become more dominant at higher concentrations (see Figure 49 f). Similar to what was observed for lysozyme, the positive charge of savinase might lead to an inversed Hofmeister series for some specific ion effects. Consequently, the resulting activity order might be a compromise of various processes (e.g. colloidal and conformational stability, substrate binding) that scale with either direct or indirect Hofmeister series, allowing the borderline chloride to come out as most effective overall.

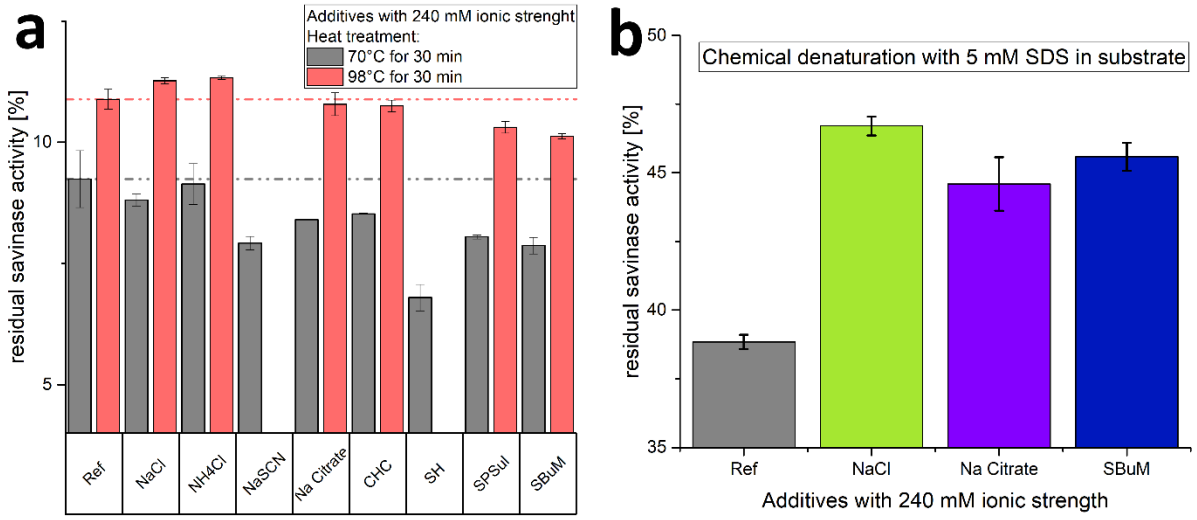

Figure 50 Stress-stability of savinase. **a:** heat treatment at 70°C and 98°C for 30 minutes. **b:** Chemical stress with 5 mM SDS. **a & b**: error bars mean ±SD (N=2).

In order to see the effect of ionic additives on the heat deactivation of savinase, experiments were carried out with the application of thermal stress (Figure 50 a). Here, it becomes apparent that heating for 30 minutes drastically lowers the residual activity of savinase. This deactivating effect is slightly more pronounced for incubating at 70°C than it is at 98°C. Contrary to experiments with lysozyme (see section 6.3.1), deactivation of savinase can be not only due to aggregation and denaturation but also due to autolysis.[229] The latter refers to the enzymatic degradation of savinase (or any protease) by itself. This could be responsible for the counterintuitive observation in Figure 50 a. At 70°C, the protein will not only denature, but some residual activity at this temperature will also degrade the (thermally) unfolded savinase. The activity will be significantly lower at 98°C, where most of the proteins will be unfolded or inactive. Additives that boost enzyme activity (see previous section) will actually become counterproductive during thermal stress, as they will boost the autolytic degradation of savinase equally well (see Figure 50 a). Besides thermal stress, chemical denaturation/deactivation is also a major challenge for functional enzymes such as savinase.[230] For this, experiments were carried out with 5 mM of SDS background (in the casein substrate solution; Figure 50 b). As expected, this led to a significantly lower savinase activity, though the addition of ionic additives improved on this by almost 10 percentage points. However, the ion specificity for this was negligible, continuing the trend that was already observed for the boosting effect (see previous section).

6.3.4 Phytase

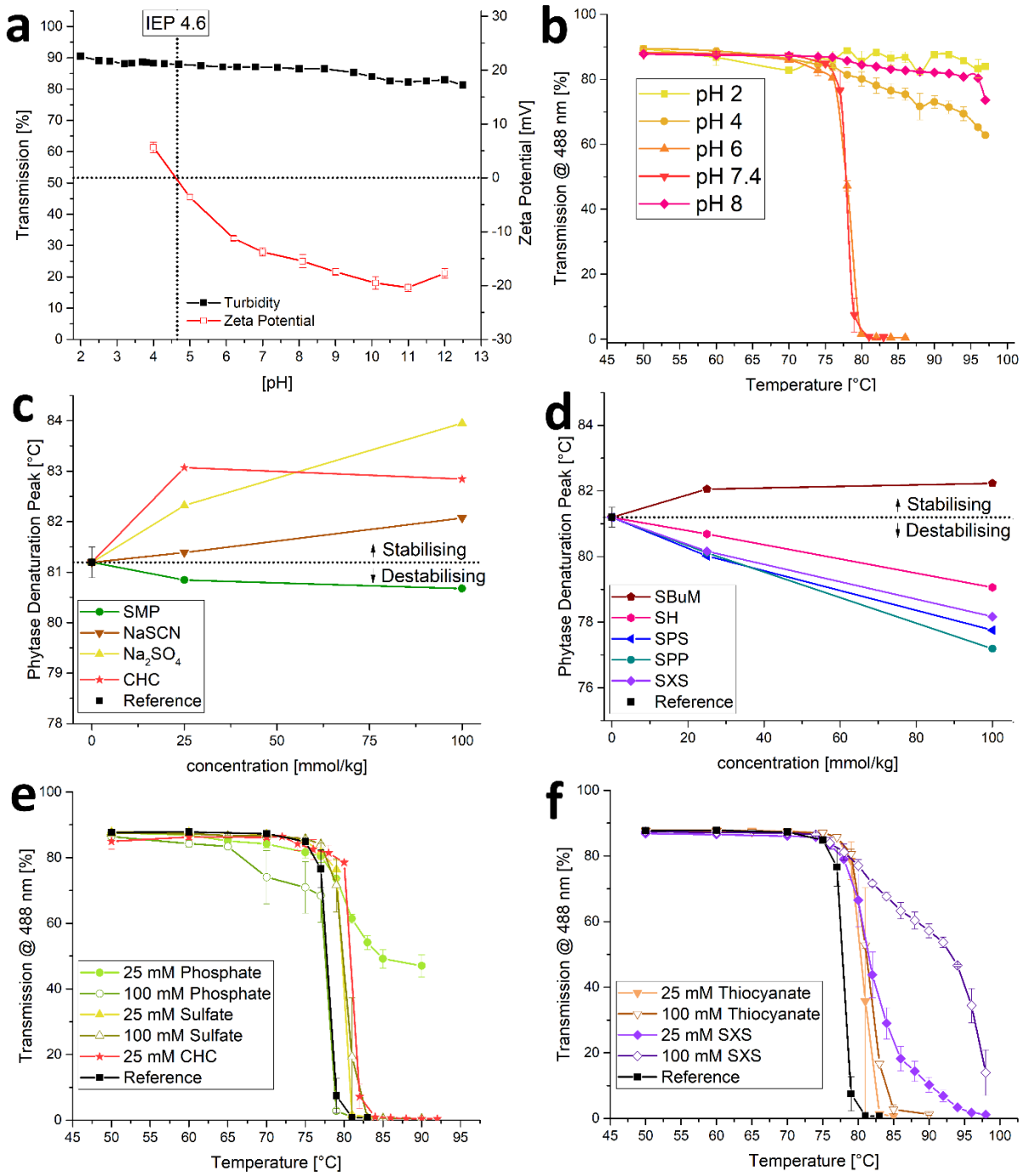

Figure 51 Effect of anionic additives on phytase stability. **a:** transmission and Zeta potential as a function of pH for phytase. Error bars mean ±SD (N=3). **b:** Phytase aggregation as a function of pH. Error bars mean ±SD (N=2). **c & d:** phytase denaturation temperatures measured by DSC for ionic (**c**) and hydrotropic (**d**) additives. Error bars for reference (buffer only) mean ±SD (N=3). **e & f:** Phytase aggregation with salting-out (**e**) and salting-in (**f**) compounds in 50 mM TRIS (pH 7.4). Error bars mean ±SD (N=2).

The phytase used in this study has an IEP of 4.6, but unlike lysozyme or protease, the colloidal stability is not compromised at zero surface charge as can be seen in Figure 51 a. On the contrary, thermal aggregation measurements have shown that the stability is actually the lowest at moderate pH (6-7.4), when the surface charge is relatively high at -15 to -20 mV. Low (<4) and high pH (>8) appear to prevent the formation of turbid aggregates (see Figure 51 b) during heating. This might also be related to a pH effect on the formation of homogeneous protein filaments (via crosslinking), that can lead to transparent gels as was observed for egg white (cf. also Figure 10 a).[91,92] A calorimetric study on the structural stability of phytase at physiological pH revealed a positive effect of inorganic salts (including the chaotropic thiocyanate), marked by an increase in denaturation temperature (see Figure 51 c). The degree of stabilization appears to follow a direct Hofmeister trend, which can be expected, given the negative surface charge of the protein. An exception to this is inorganic (ortho-) phosphate, which lowers the denaturation temperature. This could be related to a specific binding of phosphate to the protein, as phytase is designed to cleave phosphate esters and will have specific binding pockets for these moieties.[100] The results are also reminiscent of the data gathered for BSA, which also experienced less stabilization with phosphates (cf Figure 11 b). For amphiphilic structures, those that feature hydrotropic behaviour will reduce the stability of the enzyme, as they solubilize hydrophobic parts of the protein and facilitate the unfolding of the peptide chain (Figure 51 d; see also chapter 2). SPP, which is not hydrotropically active, but actually exhibits salting-out properties also destabilizes phytase due to its phosphate headgroup similar to what was seen for inorganic phosphate. On the contrary, the kosmotropic SBuM will increase the denaturation temperature, although to a lesser extent compared to the more strongly salting-out Na_2SO_4 or CHC. It was reported in the past that the long-term storage stability of phytase can be severely compromised by the presence of trace minerals (e.g. copper, iron and zinc salts).[231] This is in line with the expected destabilizing effect of such kosmotropic cations on the negatively charged phytase. As specific ion effects of various species in solution are additive by approximation (cf. Figure 9 b), stabilizing salts could compensate for destabilizing trace minerals inherent in phytase stock solutions.[87,135] Preventing thermal aggregation is equally important to an improved protein stability since it is typically irreversible leading to a total loss of protein function even after the

thermal stress is relieved. Concerning phytase, it becomes apparent that thermal aggregation very closely follows denaturation (Onset denaturation: 76.2 ±0.5°C; Onset aggregation: 76.6 ±5.8°C). This is also true for the addition of kosmotropic (Na_2SO_4 & CHC) or chaotropic (thiocyanate) salts. Here, a stabilization against denaturation (see Figure 51 c) will lead to a corresponding upshift of the aggregation point (see Figure 51 e & f). An exception to this is inorganic phosphate, which at high concentration (100 mM) will lead to an earlier onset of aggregation, in line with the observed destabilizing effect on the functional stability. Interestingly, moderate concentrations of phosphate (25 mM) will lead to reduced overall turbidity. The same was observed for the phosphonate sodium etidronate (HEDP; data not shown). Lastly, the hydrotrope SXS will lead to a reduced aggregation due to the solubilization of the peptide chains, which is in direct competition with hydrophobic intermolecular protein-protein contacts, an effect that was also apparent for CCEW and BSA (cf. chapter 1: Figure 10 h & Figure 12 e & f).

6.4 Conclusion

The activity and stability of proteins and functional enzymes in solution is the result of a variety of different effects. While simple models such as conalbumin and ovalbumin might follow classical Hofmeister lines (see chapter 1), lysozyme will already adhere to inversed or mixed orderings and savinase, lastly, appears to follow no transparent logic at all when it comes to the boosting of activity by ionic additives. Moreover, buffer effects and highly specific additive-protein interactions (as was observed for phytase with phosphates) complicate a comprehensive understanding further. It emerges, however, that the surface charge (dictated by the pH and IEP) has a profound effect over the way ionic additives influence protein stability and activity. Broadly speaking, negative surface charges (e.g. Conalbumin, Ovalbumin, Phytase) align with direct Hofmeister series (including larger ionic molecules), while positively charged proteins (Lysozyme, Protease (bovine pancr.), Savinase) will face a more diverse ion-ordering as various processes start to counter-balance each other. Additionally, surface active molecules with ionic headgroups play a special role. While they genuinely threaten protein activity and stability due to chemical denaturation (e.g. in detergent applications), they can actually contribute to enzyme activity via their headgroup ionicity (e.g. protease), in some cases to the structural stability due to hydrophobic interactions (e.g. BSA) or by preventing irreversible aggregation (e.g. lysozyme). Hence, it remains difficult to derive general rules for designing optimal ionic protein-additives. Nevertheless, this work summarizes the most important issues and highlights key aspects of protein-additive interactions. In a future work then, more emphasis can be given to finding the optimal parameters for a specific protein or functional enzyme.

CHAPTER 7: EPILOGUE

7.1 Concluding remarks

The quest for protein stability brought into being a variety of chapters concerned with different aspects of the same topic. Here, chapters 1-4 present a thought process, as one concept led to the next, manifesting in chapters with discrete questions arranged by a logical continuum. Chapters 5 and 6, then, feature very application-orientated problems that are connected with protein stability in a broader sense.

The general idea of protein stability and the effect of (an)ionic additives were explored in chapter 1, giving a brief experimental reiteration of the well-known Hofmeister effects. For simple proteins such as conalbumin, the results conform to specific ion theory with anionic kosmotropes being stabilizers and chaotropes being destabilisers. Extending the investigations to BSA, however, brought forward grave exceptions to this rule: specific interactions with hydrophobic compounds (or phosphates) easily overruled Hofmeister effects, drawing a much more complex picture for both, the functional and colloidal stability of proteins.

Chapter 2 then, sought to differentiate the effects of surface activity and ionicity for amphiphilic molecules. It was found that a fine balance between the two aspects is responsible for the macroscopic effect on various systems, including the stability of proteins in solution. This gave rise to a qualitative, yet comprehensive ordering of amphiphilic compounds according to their headgroup ionicity and tail-hydrophobicity into salting-in or salting-out domains. As such, it became apparent that amphiphilic molecules that *look* surface-active might actually exhibit a converse behaviour due to overwhelming specific ion effects.

This became relevant in chapter 3, when a proposed hydrotropism for ATP was examined. It was found that despite its amphiphilic nature, ATP cannot solubilise hydrophobic compounds and is not surface active at all (no reduction in surface tension). This heavily kosmotropic character transcends into protein science, where ATP increases the stability of conalbumin akin to inorganic triphosphate. Additionally, ATP is known to stabilise intrinsically disordered peptides, which are otherwise very aggregation-prone. This was found to be a consequence of the adenine

moiety and not in fact related to a surface-active behaviour. It also shed light on a highly specific stabilisation mechanism that did not rely on modulating peptide hydration as was the case for specific ion effects.

This path was explored further in chapter 4, where a collection of phosphorylated resveratrol derivatives was examined for its protein stabilising properties. It was found that it could prevent the aggregation of Aß42 and insulin into amyloid-type fibres in-vitro. A similar anti-aggregation property was also observed in-vivo, using a drosophila-based animal model for Alzheimer´s disease. Here, it was found that nutritional supplementation with PR led to changes in the pathological features and significantly improved locomotion.

In chapter 5 then, the focus is shifted to a completely different mode of protein stabilisation. Here, the colloidal stability of proteinaceous particles in automatic dishwasher applications was examined. The goal was to replace HEDP, a small and highly charged molecule that prevents spotting on tableware caused by the adsorption of protein particles. Using model systems, it was found that CHC, a small and similarly charged molecule, can assume the same role. The root cause appeared to be a screening of surface charges due to hard ions, which could be reinstated by the use of these highly charged molecules. This chapter then is also an example of DLVO theory dominating the (colloidal) stability of proteins as opposed to specific ion effects.

The last chapter is concerned with the stability and activity of functional enzymes. This section features the most eclectic and elusive modes of protein stabilisation: salinity, Hofmeister effects, specific protein interactions, DLVO theory and surface-activity are frequently intertwined, making a unified concept difficult to realise. Nevertheless, some general trends in the framework of specific ion effects were found for lysozyme and bovine protease. Savinase and phytase, on the other hand, exhibited a much more fragmented set of rules that remained difficult to pin down.

In conclusion, the wide-ranging results presented in this work account for the breadth of protein stabilisation by use of anionic additives and the possible applications therewithin.

7.2 Outlook

Expectedly, this work raised at least as many questions as it set out to answer.

The qualitative ordering of amphiphilic molecules into salting-in and salting-out domains raises the question of a possibility for quantitative ordering. In a future work, semi-empirical studies might be able to allow for the creation of a HLB-type system. In this way, the identity and number of the headgroups will combine with certain tail-characteristics (length, number of chains, structural motifs, electron-withdrawing groups, etc) to yield a defined place in the 2-dimensional matrix presented in this work.

The role of ATP besides its function as an energy currency is far from clear. While its importance for maintaining intracellular protein-homeostasis appears now to be beyond doubt, its assumed role in pathological diseases such as Alzheimer´s still raises many questions.

Similarly, the results for PR presented in this work are only a small piece of the puzzle. Further investigations are necessary to reveal the intrinsic effects of individual PR derivatives and to identify the physiologically (most) active form. Furthermore, the precise mode of action remains elusive and will require a tremendous amount of work. Lastly, Alzheimer´s animal models as used in this work are obviously incomplete in recreating the entire scope of the actual disease. Therefore, further studies are required to gauge a possible application in the medical field.

As environmental regulations will tighten further, automatic dishwasher formulations incorporating HEDP are bound to be taken off the market. Therefore, suitable applications, such as the CHC identified in this work, will see a renewed interest. For this, real life application testing, including parametrisation (e.g. concentration ranges), will be the next logical steps.

Finally, the effect of ionic additives on the stability and activity of functional enzymes left plenty of questions unanswered. Here, individual problems (such as the stability of x protein in y conditions) will remain subject to empirical experimentation, subtly guided by the concepts presented in this and similar publications.

REFERENCES

1. Osborne TB. The vegetable proteins. Longmans, Green, and Co.; 1909.
2. Wieland T. The History of Peptide Chemistry. *In: Peptides.,* Academic Press; 1995. p. 2.
3. Sumner JB. The Isolation and Crystallization of the Enzyme Urease. *J Biol Chem.,* 1926, *69*(*2*):435–41.
4. The Nobel Prize in Chemistry 1946 [Internet]. 2021. Available from: https://www.nobelprize.org/prizes/chemistry/1946/summary/
5. Kunz W, Henle J, Ninham BW. "Zur Lehre von der Wirkung der Salze" (about the science of the effect of salts): Franz Hofmeister's historical papers. *Curr Opin Colloid Interface Sci.,* 2004, *9*(*1–2*):19–37.
6. Gibb BC. Hofmeister's curse. *Nat Chem.,* 2019, *11*(*11*):963–5.
7. Pauli W, Handovsky H. Untersuchungen über physikalische Zustandsänderungen der Kolloide. *Beiträge zur Chem Physiol und Pathol.,* 1908, *11*:415.
8. Johnson KA, Goody RS. The original Michaelis constant: Translation of the 1913 Michaelis-Menten Paper. *Biochemistry.,* 2011, *50*(*39*):8264–9.
9. The Nobel Prize in Chemistry 1962 [Internet]. 2021. Available from: https://www.nobelprize.org/prizes/chemistry/1962/summary/
10. Lumry R, Eyring H. Conformation changes of proteins. *J Phys Chem.,* 1954, *58*(*2*):110–20.
11. Tanford C, Swanson SA, Shore WS. Hydrogen Ion Equilibria of Bovine Serum Albumin. *J Am Chem Soc.,* 1955, *77*(*24*):6414–21.
12. Tanford C, Kirkwood JG. Theory of Protein Titration Curves. I. General Equations for Impenetrable Spheres. *J Am Chem Soc.,* 1957, *79*(*20*):5333–9.
13. von Hippel PH, Schleich T. Ion Effects on the Solution Structure of Biological Macromolecules. *Acc Chem Res.,* 1969, *2*(*9*):257–65.
14. Von Hippel PH, Wong KY. Neutral salts: The generality of their effects on the stability of macromolecular conformations. *Science.,* 1964, *145*(*3632*):577–80.

15. von Hippel PH, Wong K-Y. the Conformational of Globular. *October.,* 1965, *210*(*10*).

16. Arakawa T, Timasheff SN. Mechanism of Protein Salting In and Salting Out by Divalent Cation Salts: Balance between Hydration and Salt Binding. *Biochemistry.,* 1984, *23*(*25*):5912–23.

17. Arakawa T, Timasheff SN. Preferential Interactions of Proteins with Salts in Concentrated Solutions. *Biochemistry.,* 1982, *21*(*25*):6545–52.

18. Arakawa T, Timasheff SN. Preferential interactions of proteins with solvent components in aqueous amino acid solutions. *Arch Biochem Biophys.,* 1983, *224*(*1*):169–77.

19. Arakawa T, Timasheff SN. Mechanism of Polyethylene glycol) Interaction with Proteins. *Biochemistry.,* 1985, *24*(*24*):6756–62.

20. Sheikh S, Safia, Haque E, Mir SS. Neurodegenerative Diseases: Multifactorial Conformational Diseases and Their Therapeutic Interventions. *J Neurodegener Dis.,* 2013, *2013*:1–8.

21. Soto C, Pritzkow S. Protein misfolding, aggregation, and conformational strains in neurodegenerative diseases. *Nat Neurosci.,* 2018, *21*(*10*):1332–40.

22. Lashuel HA. Rethinking protein aggregation and drug discovery in neurodegenerative diseases: Why we need to embrace complexity? *Curr Opin Chem Biol.,* 2021, *64*:67–75.

23. Carrell RW, Lomas DA. Conformational disease. *Lancet.,* 1997, *350*(*9071*):134–8.

24. Collins KD. Why continuum electrostatics theories cannot explain biological structure, polyelectrolytes or ionic strength effects in ion-protein interactions. *Biophys Chem.,* 2012, *167*:43–59.

25. Zhang Y, Cremer PS. Chemistry of hofmeister anions and osmolytes. *Annu Rev Phys Chem.,* 2010, *61*:63–83.

26. Okur HI, Hladílková J, Rembert KB, Cho Y, Heyda J, Dzubiella J, et al. Beyond the Hofmeister Series: Ion-Specific Effects on Proteins and Their Biological Functions. *J Phys Chem B.,* 2017, *121*(*9*):1997–2014.

27. Jungwirth P, Cremer PS. Beyond hofmeister. *Nat Chem.,* 2014, *6*(*4*):261–3.

28. Hofmeister F. Arbeiten aus dem pharmakologisehen Institut der deutschen Universität zu Prag. 12. Zur Lehre von der Wirkung der Salze. Dritte Mittheilung. *Arch Exp Pathol Pharmakol.,* 1888, *25*:1–30.

29. Collins KD. Ions from the Hofmeister series and osmolytes: Effects on proteins in solution and in the crystallization process. *Methods.,* 2004, *34*(*3*):300–11.

30. Nucci N V., Vanderkooi JM. Effects of salts of the Hofmeister series on the hydrogen bond network of water. *J Mol Liq.,* 2008, *143*(*2–3*):160–70.

31. Schwierz N, Horinek D, Sivan U, Netz RR. Reversed Hofmeister series—The rule rather than the exception. *Curr Opin Colloid Interface Sci.,* 2016, *23*:10–8.

32. Cacace MG, Landau EM, Ramsden JJ. The Hofmeister series: Salt and solvent effects on interfacial phenomena. *Q Rev Biophys.,* 1997, *30*(*3*):241–77.

33. Tobias DJ, Hemminger JC. Getting specific about specific Ion Effects. *Science.,* 2008, *319*:1197–8.

34. Collins KD. The behavior of ions in water is controlled by their water affinity. *Q Rev Biophys.,* 2019, *52*:e11.

35. Pegram LM, Record MT. Hofmeister salt effects on surface tension arise from partitioning of anions and cations between bulk water and the air-water interface. *J Phys Chem B.,* 2007, *111*(*19*):5411–7.

36. Zhang Y, Cremer PS. Interactions between macromolecules and ions: the Hofmeister series. *Curr Opin Chem Biol.,* 2006, *10*(*6*):658–63.

37. Lo Nostro P, Ninham BW. Hofmeister phenomena: An update on ion specificity in biology. *Chem Rev.,* 2012, *112*(*4*):2286–322.

38. Tadeo X, Pons M, Millet O. Influence of the Hofmeister anions on protein stability as studied by thermal denaturation and chemical shift perturbation. *Biochemistry.,* 2007, *46*(*3*):917–23.

39. Haynes CA, Norde W. Globular proteins at solid/liquid interfaces. *Colloids Surfaces B Biointerfaces.,* 1994, *2*(*6*):517–66.

40. Assaf KI, Nau WM. The Chaotropic Effect as an Assembly Motif in Chemistry. *Angew Chemie - Int Ed.,* 2018, *57*(*43*):13968–81.

41. Hohenschutz M, Grillo I, Diat O, Bauduin P. How Nano-Ions Act Like Ionic Surfactants. *Angew Chemie.,* 2020, *132*(*21*):8161–5.

42. Neuberg C. Hydrotropische Erscheinungen. *Biochem Z.,* 1916, *76*(*1*):107–8.

43. Mehringer J, Kunz W. Carl Neuberg's hydrotropic appearances (1916). *Adv Colloid Interface Sci.,* 2021, *294*:102476.

44. Kunz W, Holmberg K, Zemb T. Hydrotropes. *Curr Opin Colloid Interface Sci.,* 2016, *22*:99–107.

45. Bauduin P, Renoncourt A, Kopf A, Touraud D, Kunz W. Unified concept of solubilization in water by hydrotropes and cosolvents. *Langmuir.,* 2005, *21*(*15*):6769–75.

46. Horváth-Szabó G, Yin Q, Friberg SE. The hydrotrope action of sodium xylenesulfonate on the solubility of lecithin. *J Colloid Interface Sci.,* 2001, *236*(*1*):52–9.

47. Dhapte V, Mehta P. Advances in hydrotropic solutions: An updated review. *St Petersbg Polytech Univ J Phys Math.,* 2015, *1*(*4*):424–35.

48. Friberg SE, Chiu M. Hydrotropes. *J Dispers Sci Technol.,* 1988, *9*:443–57.

49. Hopkins Hatzopoulos M, Eastoe J, Dowding PJ, Rogers SE, Heenan R, Dyer R. Are hydrotropes distinct from surfactants? *Langmuir.,* 2011, *27*(*20*):12346–53.

50. Hopkins Hatzopoulos M, Eastoe J, Dowding PJ, Grillo I, Demé B, Rogers SE, et al. Effects of structure variation on solution properties of hydrotropes: Phenyl versus cyclohexyl chain tips. *Langmuir.,* 2012, *28*(*25*):9332–40.

51. Devendra LP, Gaikar VG. Is sodium cinnamate a photoswitchable hydrotrope? *J Mol Liq.,* 2012, *165*:71–7.

52. Molinier V, Aubry JM. Sugar-based hydrotropes: Preparation, properties and applications. *In: Carbohydrate Chemistry.,* 2014. p. 51–72.

53. Makowski L, Rodi DJ, Mandava S, Minh DDL, Gore DB, Fischetti RF. Molecular Crowding

Inhibits Intramolecular Breathing Motions in Proteins. *J Mol Biol.,* 2008, *375*(*2*):529–46.

54. Gao M, Held C, Patra S, Arns L, Sadowski G, Winter R. Crowders and Cosolvents—Major Contributors to the Cellular Milieu and Efficient Means to Counteract Environmental Stresses. *ChemPhysChem.,* 2017, *18*(*21*):2951–72.

55. Davis CM, Gruebele M, Sukenik S. How does solvation in the cell affect protein folding and binding? *Curr Opin Struct Biol.,* 2018, *48*:23–9.

56. Gertsch J. The Metabolic Plant Feedback Hypothesis: How Plant Secondary Metabolites Nonspecifically Impact Human Health. *Planta Med.,* 2016, *82*(*11–12*):920–9.

57. Alberts B, Johnson A, Lewis J, Morgan D, Raff M, Roberts K, et al. Molecular Biology of the Cell. 6. New York: Garland Science; 2015.

58. Gallivan JP, Dougherty DA. A computational study of cation-π interactions vs salt bridges in aqueous media: Implications for protein engineering. *J Am Chem Soc.,* 2000, *122*(*5*):870–4.

59. Strop P, Mayo SL. Contribution of surface salt bridges to protein stability. *Biochemistry.,* 2000, *39*(*6*):1251–5.

60. Kumar S, Nussinov R. Salt bridge stability in monomeric proteins. *J Mol Biol.,* 1999, *293*(*5*):1241–55.

61. Dyson HJ, Wright PE, Scheraga HA. The role of hydrophobic interactions in initiation and propagation of protein folding. *Proc Natl Acad Sci U S A.,* 2006, *103*(*35*):13057–61.

62. Gromiha MM, Selvaraj S. Inter-residue interactions in protein folding and stability. *Prog Biophys Mol Biol.,* 2004, *86*(*2*):235–77.

63. Atkins PW, de Paula J. Physikalische Chemie. Wiley-VCH; 2013. 706 p.

64. Khoury GA, Baliban RC, Floudas CA. Proteome-wide post-translational modification statistics: Frequency analysis and curation of the swiss-prot database. *Sci Rep.,* 2011, *1*:1–5.

65. Jahn TR, Radford SE. The Yin and Yang of protein folding. *FEBS J.,* 2005, *272*(*23*):5962–70.

66. Silva JL, Vieira TCRG, Gomes MPB, Ano Bom AP, Lima LMTR, Freitas MS, et al. Ligand binding and hydration in protein misfolding: Insights from studies of prion and p53 tumor suppressor proteins. *Acc Chem Res.,* 2010, *43*(*2*):271–9.

67. Teilum K, Olsen JG, Kragelund BB. Protein stability, flexibility and function. *Biochim Biophys Acta - Proteins Proteomics.,* 2011, *1814*(*8*):969–76.

68. Kossiakoff AA. Protein dynamics investigated by neutron diffraction. *Methods Enzymol.,* 1986, *131*:433–47.

69. Gomes CM. Protein Misfolding in Disease and Small Molecule Therapies. *Curr Top Med Chem.,* 2013, *12*:2460–9.

70. Muntau AC, Leandro J, Staudigl M, Mayer F, Gersting SW. Innovative strategies to treat protein misfolding in inborn errors of metabolism: Pharmacological chaperones and proteostasis regulators. *J Inherit Metab Dis.,* 2014, *37*(*4*):505–23.

71. Wang W, Nema S, Teagarden D. Protein aggregation-Pathways and influencing factors. *Int J Pharm.,* 2010, *390*(*2*):89–99.

72. Hamada H, Arakawa T, Shiraki K. Effect of Additives on Protein Aggregation. *Curr Pharm Biotechnol.,* 2009, *10*(*4*):400–7.

73. Leontidis E. Chaotropic salts interacting with soft matter: Beyond the lyotropic series. *Curr Opin Colloid Interface Sci.,* 2016, *23*:100–9.

74. Molina-Bolívar JA, Galisteo-González F, Hidalgo-Álvarez R. Cluster morphology of protein-coated polymer colloids. *J Colloid Interface Sci.,* 1998, *208*(*2*):445–54.

75. Unterhaslberger G, Schmitt C, Shojaei-Rami S, Sanchez C. Chapter 12. β-Lactoglobulin Aggregates from Heating with Charged Cosolutes: Formation, Characterization and Foaming. *In: Food Colloids: Self-Assembly and Material Science.,* RSC Publishing; 2007. p. 177–94.

76. Chi EY, Krishnan S, Randolph TW, Carpenter JF. Physical stability of proteins in aqueous solution: Mechanism and driving forces in nonnative protein aggregation. *Pharm Res.,* 2003, *20*(*9*):1325–36.

77. Matsuoka T, Hamada H, Matsumoto K, Shiraki K. Indispensable structure of solution additives to prevent inactivation of lysozyme for heating and refolding. *Biotechnol Prog.,* 2009, *25*(*5*):1515–24.

78. Ma C-Y, Harwalkar VR. Thermal Coagulation of Oat Globulin. *Cereal Chem.,* 1987, *64*(*4*):212–8.

79. Tomita S, Yoshikawa H, Shiraki K. Arginine controls heat-induced cluster-cluster aggregation of lysozyme at around the isoelectric point. *Biopolymers.,* 2011, *95*(*10*):695–701.

80. Hamada H, Takahashi R, Noguchi T, Shiraki K. Differences in the effects of solution additives on heat- and refolding-induced aggregation. *Biotechnol Prog.,* 2008, *24*(*2*):436–43.

81. Shimada K, Matsushita S. Effects of Salts and Denaturants on Thermocoagulation of Proteins. *J Agric Food Chem.,* 1981, *29*(*1*):15–20.

82. Patel A, Malinovska L, Saha S, Wang J, Alberti S, Krishnan Y, et al. ATP as a biological hydrotrope. *Science.,* 2017, *356*:753–6.

83. Sridharan S, Kurzawa N, Werner T, Günthner I, Helm D, Huber W, et al. Proteome-wide solubility and thermal stability profiling reveals distinct regulatory roles for ATP. *Nat Commun.,* 2019, *10*(*1*):1–13.

84. Donovan JW, Mapes CJ, Davis JG, Garibaldi JA. A differential scanning calorimetric study of the stability of egg white to heat denaturation. *J Sci Food Agric.,* 1975, *26*(*1*):73–83.

85. Ferreira M, Hofer C, Raemy A. A calorimetric study of egg white proteins. *J Therm Anal.,* 1997, *48*(*3*):683–90.

86. Lund H, Kaasgaard SG, Skagerlind P, Jorgensen L, Jorgensen CI, Van De Weert M. Correlation between enzyme activity and stability of a protease, an alpha-amylase and a lipase in a simplified liquid laundry detergent system, determined by differential scanning calorimetry. *J Surfactants Deterg.,* 2012, *15*(*1*):9–21.

87. Levitsky VY, Panova AA, Mozhaev V V. Correlation of high-temperature stability of α-

chymotrypsin with 'salting-in' properties of solution. *Eur J Biochem.,* 1994, *219*(*1–2*):231–6.

88. Yamasaki M, Yano H, Aoki K. Differential scanning calorimetric studies on bovine serum albumin: II. Effects of neutral salts and urea. *Int J Biol Macromol.,* 1991, *13*:321–8.

89. Rezaei-Ghaleh N, Ramshini H, Ebrahim-Habibi A, Moosavi-Movahedi AA, Nemat-Gorgani M. Thermal aggregation of α-chymotrypsin: Role of hydrophobic and electrostatic interactions. *Biophys Chem.,* 2008, *132*(*1*):23–32.

90. Righetti PG, Tudor G, Ek K. Isoelectric points and molecular weights of proteins. A new table. *J Chromatogr.,* 1981, *220*:115–94.

91. Kitabatake N, Shimizu A, Doi E. Preparation of Heat-induced Transparent Gels from Egg White by the Control of pH and Ionic Strength of the Medium. *J Food Sci.,* 1988, *53*(*4*):1091–5.

92. Handa A, Takahashi K, Kuroda N, Froning GW. Heat-induced egg white gels as affected by pH. *J Food Sci.,* 1998, *63*(*3*):403–7.

93. Markossian KA, Yudin IK, Kurganov BI. Mechanism of suppression of protein aggregation by α-crystallin. *Int J Mol Sci.,* 2009, *10*(*3*):1314–45.

94. Iwashita K, Inoue N, Handa A, Shiraki K. Thermal Aggregation of Hen Egg White Proteins in the Presence of Salts. *Protein J.,* 2015, *34*(*3*):212–9.

95. Barone G, Giancola C, Verdoliva A. DSC studies on the denaturation and aggregation of serum albumins. *Thermochim Acta.,* 1992, *199*:197–205.

96. Kelley D, McClements DJ. Interactions of bovine serum albumin with ionic surfactants in aqueous solutions. *Food Hydrocoll.,* 2003, *17*(*1*):73–85.

97. Avdulov NA, Chochina S V., Daragan VA, Schroeder F, Mayo KH, Wood WG. Direct binding of ethanol to bovine serum albumin: A fluorescent and 13C NMR multiplet relaxation study. *Biochemistry.,* 1996, *35*(*1*):340–7.

98. Celej MS, Montich GG, Fidelio GD. Protein stability induced by ligand binding correlates with changes in protein flexibility. *Protein Sci.,* 2003, *12*(*7*):1496–506.

99. Shimada K, Matsushita S. Thermal coagulation of bovine serum albumin. *Agric Biol Chem.,* 1981, *45*(*9*):1945–52.

100. Waldron TT, Modestou M, Murphy KP. Anion binding to a protein-protein complex lacks dependence on net charge. *Protein Sci.,* 2003, *12*(*4*):871–4.

101. Vlachy N, Jagoda-Cwiklik B, Vácha R, Touraud D, Jungwirth P, Kunz W. Hofmeister series and specific interactions of charged headgroups with aqueous ions. *Adv Colloid Interface Sci.,* 2009, *146*:42–7.

102. Kou R, Zhang J, Wang T, Liu G. Interactions between Polyelectrolyte Brushes and Hofmeister Ions: Chaotropes versus Kosmotropes. *Langmuir.,* 2015, *31*(*38*):10461–8.

103. Nan YQ, Xu HM, Yang N, Liu Q, Jia YF, Hao LS. Role of matching water affinities between oppositely charged headgroups in the rheological properties of aqueous mixed cationic/anionic surfactant systems. *Colloids Surfaces A Physicochem Eng Asp.,* 2015, *482*:125–37.

104. Giedyk M, Narobe R, Weiß S, Touraud D, Kunz W, König B. Photocatalytic activation of alkyl chlorides by assembly-promoted single electron transfer in microheterogeneous solutions. *Nat Catal.,* 2020, *3*(*1*):40–7.

105. Yadav SK, Kumar S. Counterion-specific clouding in aqueous anionic surfactant: a case of Hofmeister-like series. *Colloid Polym Sci.,* 2017, *295*(*5*):869–76.

106. Kunz W. Specific ion effects in colloidal and biological systems. *Curr Opin Colloid Interface Sci.,* 2010, *15*:34–9.

107. Cevc G, Seddon JM, Marsh D. The mechanism of regulation of membrane phase behaviour, structure and interactions by lipid headgroups and electrolyte solution. *Faraday Discuss Chem Soc.,* 1986, *81*:179–89.

108. Zangi R, Berne BJ. Aggregation and dispersion of small hydrophobic particles in aqueous electrolyte solutions. *J Phys Chem B.,* 2006, *110*(*45*):22736–41.

109. Hammer J, Haftka JJ-H, Scherpenisse P, Hermens JLM, de Voogt P. Investigating hydrophilic and electrostatic properties of surfactants using retention on two mixed-

mode liquid chromatographic columns. *J Chromatogr A.,* 2018, *1571*:185–92.

110. Shao Q, Jiang S. Influence of charged groups on the properties of zwitterionic moieties: A molecular simulation study. *J Phys Chem B.,* 2014, *118*(*27*):7630–7.

111. Sultana N, Ismail K. Specific ion effects of chloride vis-à-vis acetate, propionate and butyrate counterions on the cetylpyridinium headgroup at the micelle-solution and air-solution interfaces. *J Mol Liq.,* 2016, *213*:145–52.

112. Tracy DJ, Reierson RL. Commercial synthesis of monoalkyl phosphates. *J Surfactants Deterg.,* 2002, *5*(*2*):169–72.

113. Grundl G, Müller M, Touraud D, Kunz W. Salting-out and salting-in effects of organic compounds and applications of the salting-out effect of Pentasodium phytate in different extraction processes. *J Mol Liq.,* 2017, *236*:368–75.

114. Bauduin P, Wattebled L, Schrödle S, Touraud D, Kunz W. Temperature dependence of industrial propylene glycol alkyl ether/water mixtures. *J Mol Liq.,* 2004, *115*(*1*):23–8.

115. COSMOlogic GmbH & Co. KG - a Dassault Systèmes company. COSMOtherm, Release 19 ©. 2019.

116. Eckert F, Klamt A. Fast solvent screening via quantum chemistry: COSMO-RS approach. *AIChE J.,* 2002, *48*(*2*):369–85.

117. Klamt A. Conductor-like Screening Model for Real Solvents: A New Approach to the Quantitative Calculation of Solvation Phenomena. *J Phys Chem.,* 1995, *99*(*7*):2224–35.

118. Klamt A, Volker J, Bürger T, Lohrenz JCW. Refinement and Parametrization of COSMO-RS. *J Phys Chem A.,* 1998, *102*(*26*):5074–85.

119. Bauduin P, Wattebled L, Touraud D, Kunz W. Hofmeister ion effects on the phase diagrams of water-propylene glycol propyl ethers. *Z Phys Chem.,* 2004, *218*(*6*):631–41.

120. Zhang Y, Furyk S, Sagle LB, Cho Y, Bergbreiter DE, Cremer PS. Effects of hofmeister anions on the LCST of PNIPAM as a function of molecular weight. *J Phys Chem C.,* 2007, *111*(*25*):8916–24.

121. Zhao H. Are ionic liquids kosmotropic or chaotropic? An evaluation of available

thermodynamic parameters for quantifying the ion kosmotropicity of ionic liquids. *J Chem Technol Biotechnol.,* 2006, *81*(*6*):877–91.

122. Roy S, Javid N, Frederix PWJM, Lamprou DA, Urquhart AJ, Hunt NT, et al. Dramatic specific-ion effect in supramolecular hydrogels. *Chem - A Eur J.,* 2012, *18*(*37*):11723–31.

123. Klevens HB. Critical micelle concentrations as determined by refraction. *J Phys Colloid Chem.,* 1948, *52*(*1*):130–48.

124. Cosgrove T, editor. Colloid Science: Principles, Methods and Applications. Blackwell Publishing Ltd.; 2005.

125. Mazzini V, Craig VSJ. What is the fundamental ion-specific series for anions and cations? Ion specificity in standard partial molar volumes of electrolytes and electrostriction in water and non-aqueous solvents. *Chem Sci.,* 2017, *8*(*10*):7052–65.

126. Cox M, Nelson D. Lehninger, Principles of Biochemistry. New York: Freeman & Co.; 2004. 254 p.

127. Asthagiri D, Schure MR, Lenhoff AM. Calculation of hydration effects in the binding of anionic ligands to basic proteins. *J Phys Chem B.,* 2000, *104*(*36*):8753–61.

128. Maltsev AS, Grishaev A, Bax A. Monomeric α-synuclein binds congo red micelles in a disordered manner. *Biochemistry.,* 2012, *51*(*2*):631–42.

129. DePhillips P, Lenhoff AM. Determinants of protein retention characteristics on cation-exchange adsorbents. *J Chromatogr A.,* 2001, *933*:57–72.

130. Roberts JM, Diaz AR, Fortin DT, Friedle JM, Piper SD. Influence of the Hofmeister series on the retention of amines in reversed-phase liquid chromatography. *Anal Chem.,* 2002, *74*(*19*):4927–32.

131. Siew DCW, Cooney RP, Taylor MJ, Wiggins PM. Vibrational spectroscopic studies of aqueous dextran sulphate. *J Raman Spectrosc.,* 1994, *25*(*7–8*):727–33.

132. Rao A, Gebauer D, Cölfen H. Modulating nucleation by kosmotropes and chaotropes: Testing the waters. *Crystals.,* 2017, *7*(*10*):302–17.

133. Rao A, Berg JK, Kellermeier M, Gebauer D. Sweet on biomineralization: effects of

carbohydrates on the early stages of calcium carbonate crystallization. *Eur J Mineral.,* 2014, *26*(*4*):537–52.

134. Busby TF, Atha DH, Inghamg KC. Thermal Denaturation of Antithrombin III. *J Biol Chem.,* 1981, *256*(*23*):12140–7.

135. Collins KIMD, Washabaugh MW. The Hofmeister effect and the behaviour of water at interfaces. *Quartely Rev Biophys.,* 1985, *4*:323–422.

136. Mandl I, Grauer A, Neuberg C. Solubilization of insoluble matter in nature I. The part played by salts of adenosinetriphosphate. *Biochim Biophys Acta.,* 1952, *8*:654–63.

137. Mandl I, Neuberg C. Solubilization, Migration, and Utilization of Insoluble Matter in Nature. *In: Advances in Enzymology and Related Areas of Molecular Biology.,* John Wiley & Sons; 1956. p. 135–58.

138. Zhao H, Olubajo O, Song Z, Sims AL, Person TE, Lawal RA, et al. Effect of kosmotropicity of ionic liquids on the enzyme stability in aqueous solutions. *Bioorg Chem.,* 2006, *34*(*1*):15–25.

139. Silva C, Martins M, Jing S, Fu J, Cavaco-Paulo A. Practical insights on enzyme stabilization. *Crit Rev Biotechnol.,* 2018, *38*(*3*):335–50.

140. Clinic S, Jolla LA, Hatefi Y, Hanstein WG. Solubilization of Particulate Proteins and. *Proc Natl Acad Sci U S A.,* 1969, :1129–36.

141. Mandl I, Grauer A, Neuberg C. Solubilization of Insoluble Matter in Nature II: The part played by salts of orgamic and inorganic acids occuring in nature. *Biochim Biophys Acta.,* 1953, *10*:540–69.

142. McKee RH. Use of Hydrotropic Solutions in Industry. *Ind Eng Chem.,* 1946, *38*(*4*):382–4.

143. Bauduin P, Renoncourt A, Kopf A, Touraud D, Kunz W. Unified concept of solubilization in water by hydrotropes and cosolvents. *Langmuir.,* 2005, *21*(*15*):6769–75.

144. Buchecker T, Krickl S, Winkler R, Grillo I, Bauduin P, Touraud D, et al. The impact of the structuring of hydrotropes in water on the mesoscale solubilisation of a third hydrophobic component. *Phys Chem Chem Phys.,* 2017, *19*(*3*):1806–16.

145. Diat O, Klossek ML, Touraud D, Deme B, Grillo I, Kunz W, et al. Octanol-rich and water-rich domains in dynamic equilibrium in the pre-ouzo region of ternary systems containing a hydrotrope. *J Appl Crystallogr.,* 2013, *46*(*6*):1665–9.

146. Klaus A, Tiddy GJT, Rachel R, Trinh AP, Maurer E, Touraud D, et al. Hydrotrope-induced inversion of salt effects on the cloud point of an extended surfactant. *Langmuir.,* 2011, *27*(*8*):4403–11.

147. Vraneš M, Panić J, Tot A, Gadžurić S, Podlipnik Č, Bešter-Rogač M. How the presence of ATP affect caffeine hydration and self-aggregation? *J Mol Liq.,* 2020, *318*:113885.

148. Greiner J V, Glonek T. Hydrotropic Function of ATP in the Crystalline Lens. *Exp Eye Res.,* 2019, :107862.

149. Komsa-Penkova R, Koynova R, Kostov G, Tenchov BG. Thermal stability of calf skin collagen type I in salt solutions. *Biochim Biophys Acta.,* 1996, *1297*:171–81.

150. Li-Chan ECY, Ma CY. Thermal analysis of flaxseed (Linum usitatissimum) proteins by differential scanning calorimetry. *Food Chem.,* 2002, *77*(*4*):495–502.

151. Ellepola SW, Ma CY. Thermal properties of globulin from rice (Oryza sativa) seeds. *Food Res Int.,* 2006, *39*(*3*):257–64.

152. Pegram LM, Record MT. Quantifying the Roles of Water and Solutes (Denaturants, Osmolytes, and Hofmeister Salts) in Protein and Model Processes Using the Solute Partitioning Mode. *In: Shriver JW, editor. Protein Structure, Stability, and Interactions.,* Humana Press; 2009. p. 179–93.

153. Sathe SK, Mason AC, Weaver CM. Thermal Aggregation of Soybean (Glycine max L.) Sulfur-rich Protein. *J Food Sci.,* 1989, *54*(*2*):319–23.

154. Curtis RA, Prausnitz JM, Blanch HW. Protein-protein and protein-salt interactions in aqueous protein solutions containing concentrated electrolytes. *Biotechnol Bioeng.,* 1998, *57*(*1*):11–21.

155. Fink AL. The aggregation and fibrillation of α-synuclein. *Acc Chem Res.,* 2006, *39*(*9*):628–34.

156. Toyama BH, Weissman JS. Amyloid Structure: Conformational Diversity and Consequences. *Annu Rev Biochem.,* 2011, *80*(*1*):557–85.

157. Murray IVJ, Coskuner O. Adenosine triphosphate (ATP) reduces amyloid-β protein misfolding in vitro. *J Alzheimers Dis.,* 2014, *41*(*2*):561–74.

158. Klement K, Wieligmann K, Meinhardt J, Hortschansky P, Richter W, Fändrich M. Effect of Different Salt Ions on the Propensity of Aggregation and on the Structure of Alzheimer's Aβ(1-40) Amyloid Fibrils. *J Mol Biol.,* 2007, *373*(*5*):1321–33.

159. Shabestari MH, Meeuwenoord NJ, Filippov D V., Huber M. Interaction of the amyloid β peptide with sodium dodecyl sulfate as a membrane-mimicking detergent. *J Biol Phys.,* 2016, *42*(*3*):299–315.

160. Streets AM, Sourigues Y, Kopito RR, Melki R, Quake SR. Simultaneous Measurement of Amyloid Fibril Formation by Dynamic Light Scattering and Fluorescence Reveals Complex Aggregation Kinetics. *PLoS One.,* 2013, *8*(*1*):1–10.

161. Kurisaki I, Tanaka S. ATP Converts Aß42 Oligomer into Off-pathway Species by Making Contact with Its Backbone Atoms Using Hydrophobic Adenosine. *J Phys Chem B.,* 2019, *123*(*46*):9922–33.

162. Gazit E. A possible role for π-stacking in the self-assembly of amyloid fibrils. *FASEB J.,* 2002, *16*(*1*):77–83.

163. Porat Y, Abramowitz A, Gazit E. Inhibition of amyloid fibril formation by polyphenols: Structural similarity and aromatic interactions as a common inhibition mechanism. *Chem Biol Drug Des.,* 2006, *67*(*1*):27–37.

164. Ramshini H, Ebrahim-Habibi A, Aryanejad S, Rad A. Effect of cinnamomum verum extract on the amyloid formation of hen egg-white lysozyme and study of its possible role in Alzheimer's disease. *Basic Clin Neurosci.,* 2015, *6*(*1*):29–37.

165. Pal S, Paul S. ATP Controls the Aggregation of Aβ16-22 Peptides. *J Phys Chem B.,* 2019, *124*:210–23.

166. Kurzawa N. Computational methods for thermal stability proteomics. Ruperto Carola

University Heidelberg; 2021.

167. Hartl FU, Bracher A, Hayer-Hartl M. Molecular chaperones in protein folding and proteostasis. *Nature.,* 2011, *475*:324–32.

168. Cohen FE, Kelly JW. Therapeutic approaches to protein-misfolding diseases. *Nature.,* 2003, *426*:905–9.

169. Avila-Vazquez MF, Altamirano-Bustamante NF, Altamirano-Bustamante MM. Amyloid biomarkers in conformational diseases at face value: A systematic review. *Molecules.,* 2018, *23*(*1*):1–29.

170. Singh AP, Singh R, Verma SS, Rai V, Kaschula CH, Maiti P, et al. Health benefits of resveratrol: Evidence from clinical studies. *Med Res Rev.,* 2019, *39*(*5*):1851–91.

171. Caruso F, Tanski J, Villegas-Estrada A, Rossi M. Structural basis for antioxidant activity of trans-resveratrol: Ab initio calculations and crystal and molecular structure. *J Agric Food Chem.,* 2004, *52*(*24*):7279–85.

172. Mikstacka R, Rimando AM, Ignatowicz E. Antioxidant effect of trans-Resveratrol, pterostilbene, quercetin and their combinations in human erythrocytes In vitro. *Plant Foods Hum Nutr.,* 2010, *65*(*1*):57–63.

173. Hu Y, Rahlfs S, Mersch-Sundermann V, Becker K. Resveratrol modulates mRNA transcripts of genes related to redox metabolism and cell proliferation in non-small-cell lung carcinoma cells. *Biol Chem.,* 2007, *388*(*2*):207–19.

174. Robb EL, Page MM, Wiens BE, Stuart JA. Molecular mechanisms of oxidative stress resistance induced by resveratrol: Specific and progressive induction of MnSOD. *Biochem Biophys Res Commun.,* 2008, *367*(*2*):406–12.

175. Stefani M, Rigacci S. Protein folding and aggregation into amyloid: The interference by natural phenolic compounds. *Int J Mol Sci.,* 2013, *14*(*6*):12411–57.

176. Radovan D, Opitz N, Winter R. Fluorescence microscopy studies on islet amyloid polypeptide fibrillation at heterogeneous and cellular membrane interfaces and its inhibition by resveratrol. *FEBS Lett.,* 2009, *583*(*9*):1439–45.

177. Feng Y, Wang X ping, Yang S gao, Wang Y jiong, Zhang X, Du X ting, et al. Resveratrol inhibits beta-amyloid oligomeric cytotoxicity but does not prevent oligomer formation. *Neurotoxicology.,* 2009, *30*(*6*):986–95.

178. Jiang P, Li W, Shea JE, Mu Y. Resveratrol inhibits the formation of multiple-layered β-sheet oligomers of the human islet amyloid polypeptide segment 22-27. *Biophys J.,* 2011, *100*(*6*):1550–8.

179. Camont L, Cottart CH, Rhayem Y, Nivet-Antoine V, Djelidi R, Collin F, et al. Simple spectrophotometric assessment of the trans-/cis-resveratrol ratio in aqueous solutions. *Anal Chim Acta.,* 2009, *634*(*1*):121–8.

180. Vingtdeux V, Dreses-Werringloer U, Zhao H, Davies P, Marambaud P. Therapeutic potential of resveratrol in Alzheimer´s disease. *BMC Neurosci.,* 2008, *9*:1–5.

181. Intagliata S, Modica MN, Santagati LM, Montenegro L. Strategies to improve resveratrol systemic and topical bioavailability: An update. *Antioxidants.,* 2019, *8*(*8*):244.

182. McGuire SE, Roman G, Davis RL. Gene expression systems in Drosophila: A synthesis of time and space. *Trends Genet.,* 2004, *20*(*8*):384–91.

183. Schindelin J, Arganda-Carreras I, Frise E, Kaynig V, Longair M, Pietzsch T, et al. Fiji: An open-source platform for biological-image analysis. *Nat Methods.,* 2012, *9*(*7*):676–82.

184. Zhang G, Flach CR, Mendelsohn R. Tracking the dephosphorylation of resveratrol triphosphate in skin by confocal Raman microscopy. *J Control Release.,* 2007, *123*(*2*):141–7.

185. Declercq L, Corstjens H, van Brussel W, Schelkens G. Topical compositions containing phopshorylated polyphenols. US 8.465,973 B2, 2013.

186. Aleo D, Cardile V, Chillemi R, Granata G, Sciuto S. Chemoenzymatic Synthesis and Some Biological Properties of O-phosphoryl Derivatives of (E)-resveratrol. *Nat Prod Commun.,* 2008, *3*(*10*):1693–700.

187. Trouillas P, Sancho-García JC, De Freitas V, Gierschner J, Otyepka M, Dangles O. Stabilizing and Modulating Color by Copigmentation: Insights from Theory and Experiment. *Chem*

Rev., 2016, *116*(*9*):4937–82.

188. Heras-Roger J, Alonso-Alonso O, Gallo-Montesdeoca A, Díaz-Romero C, Darias-Martín J. Influence of copigmentation and phenolic composition on wine color. *J Food Sci Technol.,* 2016, *53*(*6*):2540–7.

189. Lucas-Abellán C, Mercader-Ros MT, Zafrilla MP, Gabaldón JA, Núñez-Delicado E. Comparative study of different methods to measure antioxidant activity of resveratrol in the presence of cyclodextrins. *Food Chem Toxicol.,* 2011, *49*(*6*):1255–60.

190. Yang I, Kim E, Kang J, Han H, Sul S, Park SB, et al. Photochemical generation of a new, highly fluorescent compound from non-fluorescent resveratrol. *Chem Commun.,* 2012, *48*(*32*):3839–41.

191. Sciacca MFM, Chillemi R, Sciuto S, Greco V, Messineo C, Kotler SA, et al. A blend of two resveratrol derivatives abolishes hIAPP amyloid growth and membrane damage. *Biochim Biophys Acta - Biomembr.,* 2018, *1860*(*9*):1793–802.

192. Jameson LP, Smith NW, Dzyuba S V. Dye-binding assays for evaluation of the effects of small molecule inhibitors on amyloid (Aβ) self-assembly. *ACS Chem Neurosci.,* 2012, *3*(*11*):807–19.

193. Nielsen L, Khurana R, Coats A, Frokjaer S, Brange J, Vyas S, et al. Effect of environmental factors on the kinetics of insulin fibril formation: Elucidation of the molecular mechanism. *Biochemistry.,* 2001, *40*(*20*):6036–46.

194. Wang SH, Dong XY, Sun Y. Effect of (-)-epigallocatechin-3-gallate on human insulin fibrillation/aggregation kinetics. *Biochem Eng J.,* 2012, *63*:38–49.

195. Giehm L, Lorenzen N, Otzen DE. Assays for α-synuclein aggregation. *Methods.,* 2011, *53*(*3*):295–305.

196. Iijima K, Liu HP, Chiang AS, Hearn SA, Konsolaki M, Zhong Y. Dissecting the pathological effects of human Aβ40 and Aβ42 in Drosophila: A potential model for Alzheimer's disease. *Proc Natl Acad Sci U S A.,* 2004, *101*(*17*):6623–8.

197. Chakraborty R, Vepuri V, Mhatre SD, Paddock BE, Miller S, Michelson SJ, et al.

Characterization of a drosophila Alzheimer's disease model: Pharmacological rescue of cognitive defects. *PLoS One.,* 2011, *6*(*6*).

198. Harada T, Kuroda R. CD measurements of β-amyloid (1-40) and (1-42) in the condensed phase. *Biopolymers.,* 2011, *95*(*2*):127–34.

199. Costa R, Speretta E, Crowther DC, Cardoso I. Testing the therapeutic potential of doxycycline in a Drosophila melanogaster model of Alzheimer disease. *J Biol Chem.,* 2011, *286*(*48*):41647–55.

200. Broersen K, Rousseau F, Schymkowitz J. The culprit behind amyloid beta peptide related neurotoxicity in Alzheimer's disease: oligomer size or conformation? *Alzheimers Res Ther.,* 2010, *2*(*4*):12.

201. Nevzglyadova O V., Mikhailova E V., Amen TR, Zenin V V., Artemov A V., Kostyleva EI, et al. Yeast red pigment modifies Amyloid beta growth in Alzheimer disease models in both Saccharomyces cerevisiae and Drosophila melanogaster. *Amyloid.,* 2015, *22*(*2*):100–11.

202. Caesar I, Jonson M, Nilsson KPR, Thor S, Hammarström P. Curcumin promotes a-beta fibrillation and reduces neurotoxicity in transgenic Drosophila. *PLoS One.,* 2012, *7*(*2*):e31424.

203. Hatami A, Albay R, Monjazeb S, Milton S, Glabe C. Monoclonal antibodies against Aβ42 fibrils distinguish multiple aggregation state polymorphisms in vitro and in Alzheimer disease brain. *J Biol Chem.,* 2014, *289*(*46*):32131–43.

204. De Groote D, Van Belleghem K, Devire J, Van Brussel W, Mukaneza A, Amininejad L. Effect of the intake of resveratrol, resveratrol phosphate, and catechin-rich grape seed extract on markers of oxidative stress and gene expression in adult obese subjects. *Ann Nutr Metab.,* 2012, *61*(*1*):15–24.

205. Sciacca MFM, Chillemi R, Sciuto S, Pappalardo M, La Rosa C, Grasso D, et al. Interactions of two O-phosphorylresveratrol derivatives with model membranes. *Arch Biochem Biophys.,* 2012, *521*(*1–2*):111–6.

206. dos Santos JL. Pan-Assay Interference Compounds (PAINS): Warning Signs in Biochemical-

Pharmacological Evaluations. *Biochem Pharmacol Open Access.,* 2015, *04*(*02*).

207. Baell JB. Feeling Nature's PAINS: Natural Products, Natural Product Drugs, and Pan Assay Interference Compounds (PAINS). *J Nat Prod.,* 2016, *79*(*3*):616–28.

208. MacAdam J, Parsons SA. Calcium carbonate scale formation and control. *Rev Environ Sci Biotechnol.,* 2004, *3*(*2*):159–69.

209. Bertleff W, Neumann P, Baur R, Kiessling D. Aspects of polymer use in detergents. *J Surfactants Deterg.,* 1998, *1*(*3*):419–24.

210. Zyzyck L, Gorlin PA, Dixit N, Lai K-Y. Liquid Automatic Dishwasher Detergents. *In: Liquid Detergents.,* 2007. p. 319–76.

211. Schindler DW. Recent advances in the understanding and management of eutrophication. *Limnol Ocean.,* 2006, *51*(*1*):356–63.

212. Shen CY. Effects on Detergent Processing . *J Am Oil Chem Soc.,* 1968, *43*:510–6.

213. Hong Y, Letzelter N, Evans JSO, Yufit DS, Steed JW. Phosphate-Free Inhibition of Calcium Carbonate Dishwasher Deposits. *Cryst Growth Des.,* 2018, *18*(*3*):1526–38.

214. Manoli F, Dalas E. The effect of sodium alginate on the crystal growth of calcium carbonate. *J Mater Sci Mater Med.,* 2002, *13*(*2*):155–8.

215. Heinzman S. Small-molecule polycarboxylate builders. *J Surfactants Deterg.,* 1998, *1*(*1*):105–8.

216. Soontravanich S, Lopez HE, Scamehorn JF, Sabatini DA, Scheuing DR. Dissolution study of salt of long chain fatty acids (Soap Scum) in surfactant solutions. Part I: Equilibrium dissolution. *J Surfactants Deterg.,* 2010, *13*(*4*):367–72.

217. Ryznar JW, Green J, Winterstein MG. Determination of the pH of Saturation of Magnesium Hydroxide. *Ind Eng Chem.,* 1946, *38*(*10*):1057–61.

218. Behrens SH, Grier DG. The charge of glass and silica surfaces. *J Chem Phys.,* 2001, *115*(*14*):6716–21.

219. Dougherty GM, Rose KA, Tok JBH, Pannu SS, Chuang FYS, Sha MY, et al. The zeta potential

of surface-functionalized metallic nanorod particles in aqueous solution. *Electrophoresis.,* 2008, *29*(*5*):1131–9.

220. Johnson LN. The structure and function of lysozyme. *Sci Prog.,* 1966, *54*(*215*):367–85.

221. Jain S, Ahluwalia JC. Differential scanning calorimetric studies on the effect of ammonium and tetraalkylammonium halides on the stability of lysozyme. *Biophys Chem.,* 1996, *59*:171–7.

222. Hirano A, Hamada H, Okubo T, Noguchi T, Higashibata H, Shiraki K. Correlation between thermal aggregation and stability of lysozyme with salts described by molar surface tension increment: An exceptional propensity of ammonium salts as aggregation suppressor. *Protein J.,* 2007, *26*(*6*):423–33.

223. Kudou M, Shiraki K, Fujiwara S, Imanaka T, Takagi M. Prevention of thermal inactivation and aggregation of lysozyme by polyamines. *Eur J Biochem.,* 2003, *270*(*22*):4547–54.

224. Bosshard HR, Marti DN, Jelesarov I. Protein stabilization by salt bridges: Concepts, experimental approaches and clarification of some misunderstandings. *J Mol Recognit.,* 2004, *17*(*1*):1–16.

225. Elcock AH. The stability of salt bridges at high temperatures: Implications for hyperthermophilic proteins. *J Mol Biol.,* 1998, *284*(*2*):489–502.

226. Dušeková E, Garajová K, Yavaşer R, Varhač R, Sedlák E. Hofmeister effect on catalytic properties of chymotrypsin is substrate-dependent. *Biophys Chem.,* 2018, *243*:8–16.

227. Endo A, Kurinomaru T, Shiraki K. Hyperactivation of α-chymotrypsin by the Hofmeister effect. *J Mol Catal B Enzym.,* 2016, *133*:S432–8.

228. Endo A, Kurinomaru T, Shiraki K. Hyperactivation of serine proteases by the Hofmeister effect. *Mol Catal.,* 2018, *455*:32–7.

229. Maste MCL, Rinia HA, Brands CMJ, Egmond MR, Norde W. Inactivation of a subtilisin in colloidal systems. *Biochim Biophys Acta (BBA)/Protein Struct Mol.,* 1995, *1252*(*2*):261–8.

230. Gupta R, Beg Q, Lorenz P. Bacterial alkaline proteases: Molecular approaches and industrial applications. *Appl Microbiol Biotechnol.,* 2002, *59*(*1*):15–32.

231. De Jong JA, Derouchey JM, Tokach MD, Dritz SS, Good Band RD, Woodworth JC, et al. Stability of commercial phytase sources under different environmental conditions. *J Anim Sci.,* 2016, *94*(*10*):4259.

LIST OF PUBLICATIONS

Original research papers

Salting-in and salting-out effects of short amphiphilic molecules: a balance between specific ion effects and hydrophobicity (J. Mehringer, E. Hofmann, D. Touraud, S. Koltzenburg, M. Kellermeier and W. Kunz, *Phys. Chem. Chem. Phys.*, 2021, *23*, 1381-1391).

Hofmeister versus Neuberg: is ATP really a biological hydrotrope? (J. Mehringer, T. Do, D. Touraud, M. Hohenschutz, A. Khoshsima, D. Horinek and W. Kunz, *Cell Reports Physical Science*, 2021, *2*, 100343.).

Phosphorylated resveratrol as a protein aggregation suppressor in-vitro and in-vivo (J. Mehringer, J. Navarro, D. Touraud, S. Schneuwly and W. Kunz, *RSC Chemical Biology,* 2022)

Other

Carl Neuberg's hydrotropic appearances (1916) (J. Mehringer, W. Kunz, *Advances in Colloid and Interface Science*, 2021, 294, 102476).

LIST OF ABBREVIATIONS

Abbreviation	Meaning	Abbreviation	Meaning
ADP	adenosine diphosphate	SBP	sodium benzene phosphate
AMP	adenosine monophosphate	SBPho	sodium benzene phosphonate
ATP	adenosine triphosphate	SBSul	sodium benzene sulfonate
BSA	bovine serum albumin	SBuM	sodium butylmalonate
CCEW	crude chicken egg white	SDP	sodium diphosphate
CD	circular dichroism	SDPP	sodium diphenyl phosphate
CHC	1,2,3,4,5,6- Cyclohexane-hexacarboxylate	SDS	sodium dodecyl sulfate
DEPC	diethylpyrocarbonate	SH	sodium hexanoate
DLCA	diffusion-limited cluster aggregation	SMP	sodium monophosphate
DLS	dynamic light scattering	SPAA	sodium polyacrylic acid
DLVO	Derjaguin-Landau-Verwey-Overbeek	SPP	sodium pentyl phosphate
DPnP	glycol n-propyl ether	SPS	sodium pentyl sulfate
DSC	differential scanning calorimetry	SPSul	sodium pentyl sulfonate
HEDP	sodium etidronate	STP	sodium triphosphate
LCST	lower critical solubilization temperature	SXC	sodium xylene carboxylate
MilliQ	Milli-pore water	SXS	sodium xylene sulfonate
QCM	quartz chip microscale	Td	melting temperature
qPCR	quantitative polymerase chain reaction	TMAO	trimethylamine N-oxide
RLCA	reaction-limited cluster aggregation	TRIS	Trishydroxymethylaminomethane
SB	sodium benzoate	XPS	x-ray photoelectron spectroscopy

DECLARATION IN LIEU OF OATH

I hereby declare that I have completed the dissertation presented without the impermissible help of third parties, without the use of resources other than those indicated, and that any data and concepts stemming directly or indirectly from other sources are indicated with citations to the literature.

No further persons were involved with the creation of the contents of the dissertation presented. In particular, I have not made use of the assistance of a doctoral consultant or other person in return for payment. No-one has received payment in kind either directly or indirectly for work which is associated with the content of the dissertation submitted.

The dissertation has not been submitted in the same or similar form to another examining authority, neither in Germany nor abroad.

Regensburg, 12.10.2021

_____

Johannes Mehringer